Biochemical and immunocytochemical characterization of canine corneal cells cultured in two different media

Jamie Jolee Schorling, DVM

Thesis submitted to the faculty of the Virginia Polytechnic Institute and State University
in partial fulfillment of the requirements for the degree of

Master of Science
In
Biomedical and Veterinary Sciences

Ian P. Herring, DVM, MS, DACVO
William R. Huckle, MS, PhD
J. Phillip Pickett, DVM, DACVO
Robert B. Duncan, DVM, PhD, DACVP

April 26, 2007
Blacksburg, Virginia

Keywords: corneal culture, dog, pancytokeratin, vimentin, E-cadherin, cytokeratin 5

Biochemical and immunocytochemical characterization of canine corneal cells cultured in two different media

Jamie J. Schorling

ABSTRACT

The study purpose was to determine whether canine corneal cultures demonstrate superior growth when cultured in a fully defined epithelial selective medium, Epilife®, compared to Dulbecco's modification of Eagle's medium (DMEM) with fetal bovine serum (FBS), and to characterize cultured canine corneal cells. Superficial keratectomies were performed on three dogs. Samples were trypsinized to separate cell layers. Post-trypsinization, immunohistochemistry confirmed that epithelial cells had been released from the stroma. Both cell populations (presumed epithelial cells and stromal tissues) were cultured in DMEM with FBS or Epilife®. First passage cells were fixed for immunocytochemistry and prepared for PCR. Immunocytochemical staining for pancytokeratin, vimentin, and E-cadherin was evaluated, and immunofluorescence for zonula occludens-1 was attempted. Amplification of cytokeratin 5 (CK5) mRNA was assessed by PCR. Primary presumed epithelial cells grew faster when cultured in DMEM with FBS compared to Epilife®. Stromal tissue segments in Epilife® medium failed to adhere to culture plates, indicating that this medium may inhibit attachment and growth of non-epithelial tissues. Staining of corneal tissue segments confirmed that epithelial layers were pancytokeratin and E-cadherin positive, while stromal cells were vimentin positive. Immunocytochemistry of cultured cells revealed that epithelial cells stained positively for pancytokeratin, vimentin, and E-cadherin, while stromal cells remained only vimentin positive. Greater amplification of CK5 mRNA occurred from epithelial cells grown in Epilife® compared to epithelial cells in DMEM with FBS or the stromal cells. Based on PCR results, Epilife® medium may support retention of the epithelial characteristic of CK5 mRNA expression better than DMEM with FBS.

ACKNOWLEDGEMENTS

The author wishes to recognize the Virginia Veterinary Medical Association Memorial Fund for providing funding for the project. The author wishes to thank all the members of the graduate committee for their continued assistance throughout this project, and for their support of the author's professional career. The author would like to recognize Jill Songer, Barbara Steele, and Luther Vest for their technical assistance, Pamela Arnold for acquiring the canine specimens, Dr. Stephen Werre for statistical analysis, Dr. Willard Eyestone for the use of his laboratory microscope, and Betsy Snyder for her continued support as the Ophthalmology Service technician.

TABLE OF CONTENTS

ABSTRACT ii
ACKNOWLEDGEMENTS iii
TABLE OF CONTENTS iv
INTRODUCTION 1
Corneal Anatomy and Physiology 1
In Vitro Research 3
OBJECTIVES 4
CHAPTER I. LITERATURE REVIEW 6
In Vitro Research 6
Factors Influencing Cell Cultures 9
Characterization Techniques for Cultured Cells 12
Immunohistochemistry and Immunocytochemistry 12
PCR 15
CHAPTER II. MATERIALS AND METHODS 17
Donor Material 17
Tissue Processing into Culture 18
Passaging Cells 19
Cell Fixation Techniques 21
Immunohistochemistry and Immunocytochemistry 21
Immunofluorescence 23
RNA crude cell lysate 24
RNA isolation 24
Complementary DNA Synthesis 26
Canine CK5 Alignment Sequence 27
PCR Gel Electrophoresis 28
DNA Sequencing Preparation 29
CK5 mRNA Amplification Efficiency 30
Quantitative Real Time PCR for Amplification of CK5 mRNA 31
Statistical Methods 33
Flowchart 1 34
CHAPTER III. RESULTS 35
Immunohistochemistry of Primary Corneal Tissue Samples 35
Immunohistochemistry of Trypsinized Corneal Tissues 35
Cell Culture and Passaging 36
Immunohistochemistry and Immunocytochemistry 40
Immunofluorescence 42
RNA Concentrations and cDNA Synthesis 42
PCR Gel Electrophoresis 42
DNA Sequencing of PCR Product from Corneal Samples 43
CK5 mRNA Amplification Efficiency 43
Quantitative Real Time PCR for Amplification of CK5 mRNA 44
Statistical Analysis 47
DNA Sequencing of PCR Product from MDCK Cells 47
CHAPTER IV. DISCUSSION 84

CHAPTER V. CONCLUSIONS 90
LITERATURE CITED 92
APPENDIX 1. CK5 SEQUENCE ALIGNMENT 101
APPENDIX 2. PCR AMPLIFICATION PRODUCTS FROM CORNEAL CELLS AND MDCK CELLS 107
VITA 108

LIST OF FIGURES

Figure 1. Positive tissue controls. 49
Figure 2. Primary corneal tissue sections. 50
Figure 3. Post-trypsin corneal tissue sections. 51
Figure 4. Seventy-two hours in culture. 52
Figure 5. Seven days in culture. 53
Figure 6. Presumed epithelial cells in Epilife on day 10. 54
Figure 7. Presumed epithelial cells in DMEM on day 10. 55
Figure 8. First passage presumed epithelial cells in Epilife on day 14. 56
Figure 9. First passage presumed epithelial cells in DMEM on day 14. 57
Figure 10. Explant culture in DMEM on day 14. 58
Figure 11. Explant culture in Epilife on day 14. 59
Figure 12. Explant culture in DMEM on day 21, dog 1. 60
Figure 13. First passage explant culture in DMEM on day 21, dog 2. 61
Figure 14. Explant culture on day 27 after medium change, dog 2. 62
Figure 15. MDCK immunocytochemistry. 63
Figure 16. Presumed epithelial cells in Epilife. 64
Figure 17. Presumed epithelial cells in DMEM, dog 2 65
Figure 18. Presumed epithelial cells in DMEM, dog 1 66
Figure 19. Primary explant tissue in DMEM. 67
Figure 20. First passage explant cells in DMEM. 68
Figure 21. Primary explant tissue in Epilife. 69
Figure 22. MDCK immunofluorescence 70
Figure 23. PCR gel electrophoresis from CK5 mRNA amplification. 71

LIST OF TABLES

Table 1. Culture timeline. 72
Table 2. RNA concentrations 73
Table 3. Comparative C_T analysis concentrations. 74
Table 4. Associations between cell type with growth media and CK5 mRNA expression. 75

LIST OF CHARTS

Chart 1. CK5 mRNA PCR amplification of serial dilutions cDNA from canine corneal sample 3EE. 76
Chart 2. Amplification efficiency of CK5 mRNA from canine cornea. 77

Chart 3. CK5 mRNA PCR amplification from canine corneal samples. 78
Chart 4. Mean C_T values for CK5 mRNA amplification from canine cornea. 79
Chart 5. Dissociation curves of PCR products from canine corneal samples. 80
Chart 6. Dissociation curve of PCR product from MDCK cells 81
Chart 7. ΔC_T values from canine cornea. 82
Chart 8. Relative expression of CK5 mRNA from canine corneal samples. 83

INTRODUCTION

Corneal Anatomy and Physiology

The canine cornea comprises the anterior fourth of the fibrous tunic of the globe.[1] It provides structural support, protects the intraocular contents, assists in maintenance of surface immunity directed against invasive pathogens, serves as the major refractive surface of the eye, and maintains optical clarity via various physiological functions.[2-6] The corneal layers include the outer stratified squamous epithelium, the basement membrane of the epithelium, the corneal stroma, the basement membrane of the endothelium, known as Descemet's membrane, and the endothelium.[1] The cornea is relatively thin, non-keratinized, non-pigmented, avascular, and deturgescent, with regular arrangement of collagen fibers spanning the corneal stroma.[1] It is one of the most highly innervated structures in the body, predominantly by the ophthalmic branch of the trigeminal nerve and to a lesser degree by sympathetic neurons.[7] The central cornea is thinner than the perilimbal region, with an overall thickness ranging between 500-700µm.[8]

The anterior epithelium comprises 25-40µm of the total corneal thickness in dogs.[1] It is five to seven cell layers thick in the dog, arranged with a single row of columnar basal cells, two to three polyhedral wing cells, and two to three layers of flattened non-keratinized superficial squamous epithelial cells on the surface.[1] The corneal epithelial turnover rate is approximately seven days in the dog.[2] The two populations of mitotically active cells in the corneal epithelium are stem cells, located at the limbus, and transient amplifying cells, located among the basal cells of the epithelium.[9] While stem cells may proliferate and self-renew extensively, transient amplifying cells have reduced mitotic abilities and are incapable of self-renewal.[9] With mitosis, cellular products migrate centripetally and form the basal epithelial layer.[2,4] The basal epithelial cells undergo progressive differentiation into polyhedral cells and superficial squamous epithelial cells.[2,4]

The anatomy of the epithelium, in concert with the precorneal tear film, provides a formidable barrier against fluids and invasive pathogens.[1,3] The outer non-keratinized stratified epithelium is of surface ectoderm origin, and it is a hydrophobic and lipophilic structure laden with hemidesmosomal and desmosomal attachments between cells.[1,2,4] These attachments prevent imbibition of fluids that would otherwise result in corneal edema and decreased optical clarity.[1] Additionally, the epithelium is the most important corneal layer in determinations of ocular drug penetration.[10,11] This structural and biochemical design also prevents invasion by most organisms, and for particularly virulent pathogens, the corneal epithelium is able to express various pro-inflammatory mediators to recruit host immune activities.[3] Once the corneal epithelium is damaged, several events facilitate rapid recovery.[12] Adjacent epithelial cells migrate into the wound bed and adhere to the exposed underlying stromal surface.[4,5,12] Mitosis of corneal stem cells and transient amplifying cells, followed by differentiation of the cellular products, allows re-organization of the corneal epithelial morphology over the subsequent 6-8 weeks.[12]

Underlying the corneal epithelium is the stroma, which provides approximately 90% of the corneal thickness.[1] It is hydrophilic, avascular, and comprised of parallel bundles of collagen fibers and proteoglycans arranged in lamellar sheets, which span the entire corneal diameter.[1,13] To help maintain clarity, there are few cells present in the corneal stroma. Keratocytes, mesenchymal cells of neural crest origin, are the principle stromal cell type.[13] They are responsible for collagen and proteoglycan production, and though keratocytes are mitotically quiescent in adults, they form a network of cells through extensive dendritic processes linked by gap junctions.[13,14] Other cells within the corneal stromal include rare wandering cells, which are typically leukocytes.[1]

During episodes of stromal injury, there is recruitment of leukocytes to the site of injury and altered expression of collagens, proteoglycans, and proteolytic enzymes.[4,5,13,15] Additionally, keratocytes may become fibroblastic or myofibroblastic.[13,15] These phenotypically altered cells are better able to proliferate, migrate to the injured area, and

stimulate wound contraction, resulting in rapid repair of corneal integrity.[13,15,16] These fibroblastic cells also result in decreased corneal clarity by promoting scar formation.[13,15] However, some corneal scars clear over time, indicating that a return to the quiescent keratocyte phenotype may occur.[15]

Separated from the corneal stroma by Descemet's membrane is the endothelium.[1] As a single cell layer, the corneal endothelium contributes insignificantly to the measured thickness of a healthy cornea.[1] However, the relative deturgescence of the cornea is actively maintained by Na^+-K^+ ATPase channels in the endothelial cells, which pump water out of the cornea and into the anterior chamber.[1,8,17] Tight junctions between endothelial cells also act as barriers to the influx of fluid.[1] Once destroyed, endothelial cells in adult mammals have virtually no regenerative abilities; however, cells may expand and migrate across adjacent endothelial defects.[5,17]

In Vitro Research

Given the unique anatomy and physiology of the cornea, the importance of *in vitro* research of this tissue cannot be ignored. While canine corneal *in vitro* research is in its relative infancy, human and laboratory *in vitro* corneal studies have continued to gain importance over the decades.[10,18-22] Despite unquestionable limitations, *in vitro* cultures of cells provide a controlled environment with identifiable variables and potentially repeatable results, permit advancements in the understanding of molecular biology for various physiologic and pathologic events, allow for evaluation of drug metabolism, permeability, and toxicity, and minimize the use of live and dead animal models.[10,11] Additionally, recent sophisticated *in vitro* investigations are developing cultured transplant materials for certain organs, including the cornea.[9,18,23] While *in vivo* investigations are ultimately necessary, precedent *in vitro* investigations may greatly improve the efficiency and margin of safety for *in vivo* work.[10,11]

While *in vitro* studies are clearly beneficial, the limited ability of a laboratory setting to mimic a natural physiologic environment is probably the greatest shortcoming of *in vitro*

investigations.[10,24] Use of the appropriate cell type, sampling and processing techniques, culture conditions, and substrate characteristics must be accomplished for optimal *in vitro* results.[10,24] Selection of the appropriate cell type is important because cellular activities, interactions, and responses to drugs and injuries vary considerably, depending on the cellular origin.[10,13,17,25-27] Within an organ system or given cell type, there is also considerable *in vitro* variation among species, indicating that a culture model of one cell type from one species may not be adequate for others.[6,11,13,14,16,19,28-34] Additional features of *in vitro* studies that require careful scrutiny include sampling and processing techniques, which aim to maximize numbers of primary viable cells of interest, while minimizing potential contaminating cell types.[13,27,34-38] Culture conditions, including culture medium and incubation parameters, are also of the utmost importance in propagation of the primary cells of interest.[10,27,39-41] Determining the necessary medium components for optimal cell growth is a challenge for *in vitro* investigations. While the use of serum, which contains unknown components, has long been included in the medium for *in vitro* studies, more recent investigations are attempting to eliminate serum from the culture medium.[24,40-43] Ideally, fully defined media for optimal growth of various cell types will be established.[39,42] Substrate characteristics have also been recognized as important contributing factors to successful *in vitro* investigations.[10,24,35,40,41] Variations in substrate qualities have resulted in changes in cellular growth characteristics in different media, altered cell alignment behaviors, and differences in cell-to-substrate adhesion properties.[10,24,35,40,41]

OBJECTIVES

In efforts to accomplish an optimal *in vitro* environment for corneal studies, extensive research has been performed in several species.[6,9,13,14,16,19,23,24,29,32,44-46] However, only limited work has been accomplished in canine corneal culture systems.[30,31,47,48] There are few studies in which the epithelial layers have been cultured, and there are no studies in which growth characteristics of corneal stromal cells have been demonstrated.[30,31,47,48] The biochemical and immunocytochemical characterization of these cells has thus been poorly documented.[30,47] Though two *in vitro* studies have evaluated the morphologic and

migration characteristics of canine corneal epithelial cells in response to exposure to various antibiotics and anti-inflammatory agents,[30,47] most of the information on corneal epithelial penetration and ocular toxicity has been extrapolated to dogs from studies in other species.[10,14,45,49-51] Studies have been performed *in vivo* in canine colonies prior to determining safety and efficacy *in vitro*.[52-58] By overlooking the potential benefits of corneal cultures, the risks and costs of *in vivo* studies are greatly increased.[10,11]

Given the relatively common presentation of corneal disease in dogs and the frequency with which topical ophthalmic medications are administered to the canine eye,[5,59,60] gaining a better understanding of the canine corneal characteristics *in vitro* will lead to improved ophthalmic therapeutics in this species. An *in vitro* investigation characterizing canine corneal epithelial and stromal cells will provide the groundwork for future development of standardized culture techniques for canine corneal epithelial cells and stromal cells, as well as encourage studies of ocular toxicity and pharmacokinetics. The goals of this project were to culture canine corneal epithelial cells and stromal cells in two different media and to determine whether either medium was superior in promoting cell attachment, growth, and expression of appropriate biochemical and immunocytochemical cellular characteristics. Specifically, these cells were grown in Epilife® medium, a fully-defined serum-free medium reported to be selective for epithelial cell growth, and Dulbecco's modification of Eagle's medium (DMEM) supplemented with fetal bovine serum (FBS). The investigators hypothesized that corneal epithelial cell proliferation would be superior in the Epilife® medium, while corneal stromal cells would preferentially thrive in DMEM with FBS. To document variations in cell morphology, growth, and biochemical and immunocytochemical characteristics, photomicrographs were taken of live cultures, immunocytochemical staining properties of the cultured canine corneal epithelial and stromal cells to antibodies against pancytokeratin, vimentin, and E-cadherin were evaluated, immunofluorescent properties of these cultured cells against zonula occludens-1 (ZO-1) were assessed, and quantitative real time reverse transcriptase polymerase chain reaction (RT-PCR) of the cultured cells for amplification of cytokeratin 5 (CK5) messenger RNA (mRNA) expression with subsequent DNA sequencing of the amplified product was performed.

CHAPTER I. LITERATURE REVIEW

In Vitro Research

In vitro investigations of the canine corneal tissues have been reported by four groups of investigators.[30,31,47,48] In the two studies by Huang *et al*., an explant technique was used, efforts to characterize the corneal cells grown in culture were not reported, and methods of ensuring minimal fibroblast contamination from the explants were not clearly indicated.[31,48] The purposes of these two studies were to understand mechanisms of bradykinin-mediated calcium signaling and characterize the bradykinin receptors present in cultured canine corneal epithelial cells. The investigations were biochemical in nature, with little emphasis on the morphologic characteristics of the cells. In the two studies performed by Hendrix *et al*., an explant technique was employed in one of the studies, and an initial cell suspension technique by chemical digestion with dispase, followed by physical removal of the epithelial cells from the underlying superficial stroma, was used for the other study.[30,47] The effects of various anti-inflammatories, antimicrobials, and preservatives on the morphologic characteristics of the cultured cells were documented using photomicrographs to assess for cell shrinkage, rounding, or death.[30,47] Additionally, the epithelial characteristics of the cultured cells were documented by immunocytochemical staining with a monoclonal antibody against multi-cytokeratin.[30,47] In these latter two studies, Madin-Darby canine kidney (MDCK) cells were used as a positive control for canine epithelial staining characteristics, and mouse 3T3 feeder cells were employed as a negative control.[30,47] However, no biochemical comparisons were made to differentiate canine corneal epithelial cells from corneal stromal cells or fibroblasts that may have been present in the *in vitro* environment. Specifically, no immunocytochemistry, PCR, or other analyses were performed to document the distinguishing characteristics of corneal epithelial cells from stromal cells.

Among other domestic species, *in vitro* corneal studies have also been reported infrequently. Sandmeyer *et al*. reported a series of investigations on cultures of feline

corneal epithelial cells in which epithelial cells were digested from the underlying stroma using dispase.[32,61,62] Morphologic characteristics were documented by photomicrographs, and the epithelial immunocytochemical features were demonstrated using antibody AE5 directed against cytokeratins 3 and 12, and antibody AE1/AE3 for recognition of cytokeratins 1, 2, 3, 4, 5, 6, 8, 10, 14, 15, 16, and 19.[32,61,62] Cells scraped from fresh corneal samples served as positive controls, and omission of the primary antibodies of interest functioned as negative controls. These analyses were performed before and after exposure of the cultured corneal epithelial cells to feline herpesvirus-1 and to certain anti-viral agents.[32,61,62] One report of cultured equine corneal epithelial cells and keratocytes by Haber *et al*. investigated the effects of various concentrations of epidermal growth factor, platelet-derived growth factor, and transforming growth factor-beta on corneal epithelial and stromal cell proliferation.[44] Epithelial cells of corneal sections were separated from underlying stroma using dispase and physical removal of the epithelial sheet, while stromal layers from other corneal sections were digested from the epithelium and endothelium utilizing trypsin.[44] Cells were distinguished by the polygonal appearance of the epithelial cells and the spindle shape of the keratocyte cells, but no biochemical or immunocytochemical analyses were performed to characterize the cell types.[44] The effect of latanoprost on culture porcine corneal stromal cells was investigated by Wu, Wang, and Hong.[14] Corneal dissection samples were digested with trypsin to separate the stromal cells from epithelium and endothelium.[14] Though morphologic descriptions and routine immunocytochemical staining characteristics were not provided, immunofluorescent staining for Type I collagen was analyzed, and various biochemical evaluations were performed to characterize the cells.[14] Rates of cellular uptake of certain amino acids, mitochondrial viability, cell migration assays, western blot for fibronectin protein, and spectrofluorophotometry for detection of intracellular calcium were performed.[14] Bovine keratocytes have also been cultured using collagenase digestion with trypsin.[15] Phase contrast photomicrographs were taken to document the cellular morphologies in media with and without serum over time, and differential expression of various soluble proteins in normal dendritic keratocytes and keratocytes made fibroblastic by serum were compared using western blot analyses.[15] Results of the study indicate that normal dendritic bovine keratocytes become fibroblastic by addition

of serum to the culture medium, and that removal of serum from the fibroblastic cell cultures allows for partial restoration of the more dendritic keratocyte phenotype.[15]

In contrast to the relatively few reports of *in vitro* corneal research in dogs and other domestic species, investigations of human and laboratory animal corneal cultures are more extensive. Morphological and cytochemical features of primary cultured corneal cells from humans and laboratory animals have been characterized thoroughly using photomicrographs, electron microscopy, immunocytochemistry including immunofluorescence, protein electrophoresis, and PCR.[11,16,33,63,64] Photomicrographs demonstrate the polygonal appearance of corneal epithelial cells in culture, as compared to the dendritic keratocytes, which may elongate and become more fibroblastic under certain culture conditions.[12,16,33,64,65] Electron microscopy provides images of cell morphologic characteristics in greater detail, including depictions of the microvilli of epithelial cells and tight junctions between cells.[11,34,66] Immunocytochemical and immunofluorescent properties of corneal cells from *in vitro* studies have been thoroughly described, including staining for cytokeratins, vimentin, cadherins, zonula occludens, pinin, p63, desmoplakin, and connexin, to list a few.[16,21,33,34,46,63,64,66-69] Protein eletrophoresis has been utilized extensively to confirm the presence of and further characterize proteins expressed in cultured corneal cells.[16,33,46,64,66] Polymerase chain reaction has provided a highly sensitive method of amplifying and identifying proteins expressed by the cultured corneal epithelial and stromal cells.[16,21,46,63,66,69] Corneal epithelial cell lines from humans, rabbits, hamsters, and rats have been immortalized to facilitate research while minimizing variation among experimental cell populations.[17,19,28,29,42,46] Functional reconstruction of cultured corneal epithelial cell sheets from limbal cell populations have also been accomplished.[9,23,34,70] Additional aspects of the *in vitro* corneal research that have been performed in humans and laboratory species will be emphasized in the following sections based on investigations conducted during the current research project.

Factors Influencing Cell Cultures

Numerous factors, including cell isolation techniques and culture medium qualities, may affect cell growth, morphology, differentiation, and ability to express various proteins. Cultures may be established by explantation, whereby cells migrate from the tissue of origin onto the culture substrate, or cell suspension, in which intercellular collagens are digested, and cells are suspended in the culture medium.[34,37,71] Though explantation cultures of corneal tissues have been employed with considerable success,[22,33,40,67,68] there is some debate as to whether cell explants or cell suspensions are more appropriate for corneal cultures.[35,37] Koizumi *et al*. reported that the cell suspension culture technique for human corneal limbal epithelial cells was superior to explant-cultured cells.[37] This determination was based on decreased intercellular spaces between cells in the initially suspended cultures as compared to the explant cultures.[37] The authors theorized that the use of cell suspension technique allowed better clonal expansion of individual limbal stem cells than the explant technique. Results of a study by Zhang *et al*. were in agreement with the Koizumi *et al*. research, reporting that cell suspension cultures had greater content of stem cells and less fibroblast contamination.[35] Huang *et al*. utilized cellular explantation for their *in vitro* canine corneal research.[31,48] In two separate investigations, Hendrix *et al*. used cell suspension and explantation techniques for cultures of canine corneal epithelial cells; however, the products resulting from these techniques were not compared.[30,47]

When cell suspension cultures are initiated, cellular digestion is required to separate and isolate cells.[13,30,32,34,35,37,70,71] Digestion techniques that have been evaluated for corneal tissues include mechanical and chemical separation of tissues.[13,30,32,34,35,37,70,71] A combination of techniques are often utilized to minimize cell damage and improve isolation of the cell type of interest.[13,30,32,35] Collagenases such as dispase and trypsin digest proteins that maintain intercellular adhesions.[37,38,71] Zito-Abbad *et al*. compared corneal epithelial cell growth after digestion with dispase or trypsin and found that for cells treated with trypsin, there was decreased cell growth after two and three weeks in culture.[34] Cell digestion with dispase often requires longer incubation times than trypsin

to successfully separate corneal cells.[13,35,71] In the study by Zito-Abbad *et al*., cells were incubated with either enzymatic agent for one hour, which may have been longer than necessary for trypsin.[34] It is also possible that factors other than the digestion agents affected the cells, since the differences in cell growth were not observed for two weeks.[34] Additionally, since trypsin is routinely used to subculture cells as they approach confluence, it is unlikely to be cytotoxic when exposure time and concentration is limited.[30,32,38,47] While Hendrix *et al*. used dispase for initial digestion of tissues in their cell suspension cultures, Huang *et al*. and Hendrix *et al*. subcultured their canine corneal cells using trypsin when the cultures approached confluence.[30,31,47,48]

In addition to deciding between a cell suspension or explantation technique, and applying digestion agents if needed, researchers must also identify the appropriate cell culture medium and additives. Identification of ideal culture media for various cell types is gaining importance for *in vitro* research. Serum has historically been used as an important additive to basal media for support of cell growth and longevity *in vitro*.[22,24,40,43] However, the components of serum are not fully defined and composition may vary due to its biological origin.[13,22,24,39,40,43] Serum also induces alterations in cellular behaviors and morphologies.[13,24,39,40,43] Corneal epithelial cells respond differently to changes in substrate topography when cultured in serum-free medium as compared to serum-containing medium.[24] Keratocytes lose their dendritic morphology and become fibroblastic when cultured in the presence of serum.[13] Additionally, some of the physiologic properties of the dendritic keratocytes, such as production of keratan sulfate proteoglycan production are diminished when serum is present.[13] Corneal endothelial cell cultures are reportedly of higher quality when cultured in serum-free conditions, with improved cell survival and cell membrane integrity.[39] In corneal organ culture systems, endothelial cell viability was superior when serum-free medium was used instead of serum-containing medium.[43] In addition to serum, the effects of numerous other compounds on corneal cell cultures have been investigated. Fibronectin, substance P, and insulin-like growth factor are examples of compounds that promote cellular growth *in vitro*.[50,51] The neurotrophic influences of trigeminal and sympathetic neurons also improve proliferation and possibly differentiation of corneal epithelial cells in culture.[49,72]

In contrast, calcitonin gene-related peptide, corticotrophin-releasing hormone, dilute alcohol, various anti-glaucoma agents, and high extracellular calcium levels inhibit corneal cell growth *in vitro*.[36,45,49,69,73,74] Reduction of pinin levels and lipopolysaccharide challenge alter expression of junctional proteins in cultured cells,[69,75] and exposure of cells in culture to various inflammatory agents increases expression of numerous cytokines.[3,21] These reports demonstrate the importance of the culture medium qualities on cell growth, proliferation, and longevity *in vitro*.

Though the effects of serum and other supplements on corneal cell growth in culture have been investigated, there is still considerable debate on which basal media and supplements are ideal for corneal cultures.[24,39,76] Dulbecco's modification of Eagle's medium (DMEM) is a commonly used culture medium which is not selective for epithelial cells and is often supplemented with fetal bovine serum (FBS).[38,40,77,78] Another commonly used non-selective culture medium is a 1:1 mixture of DMEM with Ham's F12 (DMEM/F12).[24,32,47,76] In contrast, Epilife® is a fully defined serum-free culture medium with defined supplements, used for selective expansion of epithelial cell cultures.[24,70,77,79,80] Epilife® and DMEM with FBS have been used sequentially in numerous investigations to alter the human corneal culture environment.[40,77-79] Barnard *et al*. compared *in vitro* human corneal growth in Epilife® and DMEM/F12, and Teixeira *et al*. determined in two separate studies that these two media have differing effects on human corneal epithelial cellular alignment, depending on substrate characteristics.[24,76,79] However, no studies directly comparing the effects of DMEM with 10% FBS and Epilife® on human corneal cell cultures were identified by a literature search.

In dogs, Epilife® culture medium has been used by Song *et al*. for development and characterization of a canine oral mucosa equivalent.[27] In their study, no comparison was made to assess whether the effects of Epilife® differed from other culture media.[27] No additional references for Epilife® use in canine *in vitro* research were identified. Previous investigators of canine corneal cultures utilized DMEM/F12 as their sole culture medium, and to date, there have been no publications documenting the effects of different culture media on canine corneal cell growth *in vitro*.[30,31,47,48]

Characterization Techniques for Cultured Cells

Immunohistochemistry and Immunocytochemistry

Immunohistochemistry and immunocytochemistry are techniques of cell characterization, which may be applied to tissue sections (immunohistochemistry) or individual cells (immunocytochemistry). Direct or indirect detection methods may be employed. With direct detection systems, the primary antibody directed against the antigen of interest is applied to the cells or tissue, and this primary antibody is labeled with an enzyme or fluorophore that permits visualization of cells with positive staining characteristics. With indirect detection techniques, the primary antibody is applied to the cells or tissue, and the antibody binds to the cellular antigen of interest if it is expressed. A secondary antibody is then applied to detect the initial antibody-antigen complex, and this secondary antibody is enzyme-labeled. Routine immunocytochemical stains are enzyme-mediated with either horseradish peroxidase or alkaline phosphatase. Immunofluorescence, on the other hand, utilizes a molecule that fluoresces under ultraviolet light attached to the antibody for detection.[81]

Cytokeratins

Keratins are a family of proteins that form tonofilaments, a class of intermediate filaments, which contribute to the cytoskeleton of epithelial cells in vertebrates, including corneal epithelial cells.[6,33,82,83] The 54 known human keratins range between 40 and 67 kilodaltons, and they can be divided into two subclasses based on their charge characteristics and amino acid sequences.[6,82,83] Type I keratins are acidic and include K9-K23, while type II keratins are basic and include K1-K8.[6,82,83] One member of each family is required to form a heterodimeric double-stranded coil, and these keratin pairs are typically co-expressed according to tissue specificity and differentiation.[6,82] Keratins 5 and 14 are expressed in the basal cells of all stratified epithelia, and K3 and K12 are expressed in the differentiated superficial epithelium of the cornea in most species.[6,82]

According to research by Chaloin-Dufau *et al*., K3 may be present in only small amounts in the corneal tissue of dogs and humans, and it is not detectable in mice.[82] The authors speculated that in these species, acidic keratin K12 may interact with basic keratin K5 to form the heterodimeric coiled intermediate filament structure.[82] Lu *et al*. demonstrated that keratin 5 knockout mice reveal plasticity of keratin expression by up-regulating keratin 4 in the corneal epithelium.[6] Many researchers utilize monoclonal antibodies AE1, AE3, and AE5 when assessing immunocytochemical staining characteristics of corneal epithelial cells.[25,26,32,68,70,83,84] Antibody AE1 recognizes acidic keratins 10, 14, 15, 16, and 19, AE3 binds basic keratins 1, 2, 3, 4, 5, 6, and 8, and AE5 adheres to keratins 3 and 12.[32,84] Antibodies AE1 and AE3 are routinely combined to provide for broad recognition of epithelial cell types, and this combination of two monoclonal antibodies is referred to as multicytokeratin or pancytokeratin.[26,32,68,70,84]

Cultured canine corneal epithelial cells stain with multicytokeratin according to Hendrix *et al*.[47] Chaloin-Dufau *et al*. determined that monoclonal antibody AE5 stains canine corneal tissue sections.[82] Additional canine tissues in which cytokeratin staining has been investigated include renal tubular epithelial cells from the MDCK cell line, epithelial and myoepithelial cells of mammary tumors, and normal and neoplastic prostatic tissues.[25,26,85,86]

Vimentin

Vimentin is another intermediate filament, but in contrast to the keratin intermediate filaments, vimentin is usually associated with cells of mesenchymal origin.[13,33,70,84] Cells such as corneal stromal keratocytes, fibroblasts, and myofibroblasts are of mesenchymal cell origin, and thus express vimentin.[13,70] Although vimentin is generally not expressed in epithelial cells *in vivo*,[13,25,84] there are sporadic reports of cell types which co-express vimentin and cytokeratins *in vivo*.[87-89] In contrast, vimentin expression is frequently up-regulated by epithelial cells, including rabbit corneal epithelial cells, *in vitro*.[33,34,67,70,84,85] Authors have provided speculations to explain why cultured epithelial cells express vimentin. SundarRaj *et al*. discussed that vimentin expression is associated with changes

in cellular shape, which includes activities such as cellular proliferation, migration, and differentiation.[33] Since vimentin expression *in vitro* decreases as cell density and desmosomal attachments increase, and since keratin filaments terminate at desmosomes, the authors theorized that vimentin replaces cytokeratin filaments temporarily in phases of rapid cellular migration where few desmosomal attachments exist.[33] Zito-Abbad *et al*. demonstrated that vimentin expression in their cultured limbal cells occurred most frequently in poorly differentiated cells.[34] Grieco *et al*. agreed that vimentin expression represented poorly differentiated cells in neoplastic prostatic tissues, and they also theorized that vimentin expression increased in non-neoplastic exfoliated epithelial cells due to their independent existence and loss of cell-to-cell contact.[25]

Vimentin expression in canine corneal tissues has not been previously investigated. Madin-Darby canine kidney cells have been shown to co-express cytokeratins and vimentin.[85,86] Neoplastic canine prostatic epithelial cells also co-express these two intermediate filaments.[25]

E-Cadherin

E-cadherin is a member of the cadherin superfamily, comprised of calcium-dependent cell-cell adhesion proteins expressed by cells of epithelial origin.[90,91] The adherens junctions formed by E-cadherin play important roles in the development of epithelial tissues and the polarization of apical/basal cellular orientations.[90] E-cadherin also participates in cell signaling events that affect cell differentiation, proliferation, migration, and survival.[90-92] Because of calcium dependence, a reversible decrease in cadherin expression is observed when cells are cultured in low calcium concentrations.[93] Pinin, substance P, and certain matrix metalloproteinases (matrilysin and stromelysin) also play regulatory roles in the expression of E-cadherin in epithelial cells.[75,91,94] Numerous studies have demonstrated the presence of E-cadherin in epithelial junctions of rabbit and human corneal epithelial cells.[40,66,75,94] The junctional protein is expressed in the basal and suprabasal corneal epithelial cells *in vitro* and *in vivo*, but reports vary as to

whether the stain accumulation occurs diffusely throughout the cytoplasm or whether it is restricted to the cell membrane and junctional regions.[40,66,75,94]

E-cadherin expression has not been determined for canine corneal epithelial cells. Madin-Darby canine kidney cells react positively to E-cadherin staining, with variable stain uptake throughout the cellular cytoplasm or along cellular junctions.[85,90,91,93]

Zonula Occludens-1

Tight junctions, or zonula occludens, are expressed just below the apical surface of most epithelial cells and provide the main barrier to passive movement of fluids, electrolytes, large molecules, and cells.[69] Tight junctions are especially important in the corneal epithelium, as they play an important role in the maintenance of the relatively dehydrated state of the cornea, which is essential for corneal clarity.[1,2,4,69] Zonula occludens-1, ZO-2, and ZO-3 are members of the membrane-associated guanylate kinase homologue (MAGUK) family.[69,95,96] In the cornea, ZO-1 is present in the superficial, wing, and basal cells of the epithelium of humans, rabbits, and rats.[46,69,75,95,96] Cellular staining distribution tends to be restricted to the cell-cell borders, where tight junctions are located, and ZO-1 is expressed both *in vitro* and *in vivo*.[69]

Expression of ZO-1 has not been evaluated in canine corneal tissues, though MDCK cells have been confirmed to express ZO-1.[85] Stain uptake in the MDCK cells was restricted to the cell periphery, where tight junctions are established.[85]

PCR

Polymerase chain reaction is a technique of amplification of selected portions of DNA, performed by repeated melting of the DNA double-helix, followed by replication of selected regions by extension of a chosen primer. Theoretically, the amplification process is exponential, allowing for quantitative detection of the protein of interest. However, since all cells of a host contain the same DNA, amplification of a DNA-based target via

PCR is possible even if that particular cell type does not actually express the corresponding mRNA *in vivo*. Reverse transcriptase polymerase chain reaction provides a method of determining whether the gene of interest is actively expressed by the cells of interest. RNA is isolated from lysed cells, with subsequent complementary DNA (cDNA) synthesis. Polymerase chain reaction is then performed on the cDNA sample, allowing for indirect detection of the mRNA of interest, with the assurance that the cells sampled naturally express that gene.[97]

Cytokeratin 5

Cytokeratin 5 is a 58 kilodalton protein found in basal epithelial cells of various tissues.[6,26,46,82,86,98] Lack of CK5 results in fragile epidermal structures with poor attachments to the dermis due to absence of the necessary keratin intermediate filaments.[6] Expression of CK5 has been confirmed in the corneal tissues of humans, mice, and dogs, and Lu *et al*. reported successful PCR amplification of CK5 from corneal epithelial cells.[6,46,82] Additional canine tissues that express CK5 include MDCK cells and mixed tumors of the canine mammary gland.[26,86]

CHAPTER II. MATERIALS AND METHODS

The study was conducted with approval from the Virginia Tech Animal Care and Use Committee.

For a flowchart illustration of the methods described here, the reader is referred to Flowchart 1 at the end of the section.

Donor Material

Corneal tissue was acquired from three young male dogs (labels: 1, 2, 3) euthanized for reasons unrelated to the study. Within 20 minutes of euthanasia, a 2.5% methylcellulose-containing eye lubricant (Gonak®, Akorn, Inc., Buffalo Grove, IL) was applied liberally to the corneal surfaces to prevent desiccation. Diffuse and slit beam biomicroscopy were performed to evaluate for corneal, adnexal, or anterior segment pathology. None of the sampled eyes had evidence of ophthalmic disease. Within 3 hours of euthanasia, corneal samples were obtained. The animals were positioned in dorsal recumbency under an operating microscope (Weck Operating Microscope, J. K. Hoppl Corporation, Long Island, NY), and the eyes were aseptically prepared by flushing with 1:50 dilute povidone iodine in eye irrigating solution to decrease microbial flora. Using aseptic technique, a #6400 Beaver® blade (BD Ophthalmic Systems, Waltham, MA) was used to groove the corneal tissue into quadrants, and superficial keratectomies were performed. All superficial corneal tissue inside of the limbus was removed from both eyes. One triangular quadrant from each dog was placed directly into 10% neutral buffered formalin on a sponge for subsequent histopathology, with the epithelial surface up and the stromal surface in contact with the sponge (1a, 2a, 3a). The remaining corneal tissue from each dog was placed into a refrigerated transport medium consisting of 15ml Hank's balanced salt solution (HBSS; Invitrogen Corporation, Carlsbad, CA) with 0.1% bovine serum albumin (BSA; Mediatech, Inc., Herndon, VA), 0.025ml Hepes buffered solution (BioWhittaker, Inc., Walkersville, MD) per 1ml HBSS, 2.5ug 250ug/ml fungizone (Sigma-Aldrich Corporation, St. Louis, MO) per 1ml HBSS, and 0.05mg 10mg/ml

gentamicin (Invitrogen Corporation, Carlsbad, CA) per 1ml HBSS. Samples from each dog were maintained separately and refrigerated until further processing.

To provide a positive control comparison for canine epithelial cells, Madin-Darby canine kidney cells (MDCK; American Type Culture Collection, Manassas, VA) were purchased and maintained in culture in minimum essential medium Eagle (MEM; Mediatech, Inc., Herndon, VA), with 1.0mM sodium pyruvate and 0.1mM nonessential amino acids added as supplements.

Tissue Processing into Culture

The transport medium was aspirated, and the tissues were washed twice with Dulbecco's phosphate-buffered saline (DPBS; Mediatech, Inc., VA) to decrease the amount of serum albumin present from the transport medium. A 1:1 volume of 0.05% trypsin/0.53mM ethylenediaminetetraacetic acid (trypsin/EDTA; Invitrogen Corporation, Carlsbad, CA) was added to the tissue samples and incubated at 37º Celsius (C) for 30 minutes.

To inactivate the trypsin/EDTA, 10ml of DMEM (Mediatech, Inc. Herndon, VA) with 4.5 g/L glucose, L-glutamine, and sodium pyruvate, supplemented with 10% FBS by volume and 50µg/ml gentamicin were added to each sample. The supernate, presumed to contain a predominance of epithelial cells in suspension, was aspirated and dispensed into separate tubes for each dog. The remaining tissues were washed twice with DMEM, and the supernate was aspirated and added to the tubes containing the suspended cells. These trypsinized cells were centrifuged at 150 x g for 10 minutes, and the supernate was then aspirated and discarded. Cells were resuspended in 10ml DMEM, and samples from each dog were divided into two separate tubes. Both tubes from each dog were then spun again at 150 x g for 10 minutes. Supernates were again aspirated and discarded. One pellet was then resuspended in 10ml DMEM with 10% FBS and 50ug/ml gentamicin (1ED, 2ED, 3ED), and the other was suspended in 10ml Epilife® medium (Cascade Biologics, Inc., Portland, OR) with human corneal growth supplement (HCGS; Cascade Biologics, Inc., Portland, OR) and 50µg/ml gentamicin added (1EE, 2EE, 3EE). The HCGS contains

undisclosed quantities of bovine pituitary extract, bovine insulin, hydrocortisone, bovine transferrin, and mouse epidermal growth factor. Cells in each medium were plated onto 10cm culture dishes and incubated at 37ºC, 5% CO_2.

To the remaining tissue pieces from the initial trypsin/EDTA step, one tissue quadrant from each dog was placed into formalin on a sponge for post-trypsinization histopathological evaluation (1b, 2b, 3b). The remaining corneal tissues were processed and cultured using a cell explant technique. They were cut into small pieces using fine corneal scissors and forceps. With tissue from each dog processed separately, small pieces of presumed corneal stromal tissues were distributed evenly into 10ml DMEM with FBS (labels: 1SD, 2SD, 3SD) or 10ml Epilife® (1SE, 2SE, 3SE) in 10cm culture dishes. Cultures were incubated at 37ºC, 5% CO_2.

Cultures were monitored for growth and attachment every 24 hours, utilizing an inverted microscope (Nikon TMS, Nikon Corporation, Japan). Every 72-96 hours, cells were fed by changing the culture medium. Photomicrographs were intermittently taken using an inverted phase contrast Olympus CKX41 microscope (Olympus America, Inc., Center Valley, PA) with an Infinity 3 digital camera (Lumenera Scientific, Ontario, Canada).

Passaging Cells

The cultures from the initially suspended cells (1ED, 2ED, 3ED, 1EE, 2EE, 3EE) became adherent and approached confluence more quickly than the explanting cultures from the tissue pieces (1SD, 2SD, 3SD, 1SE, 2SE, 3SE). Once cells reached approximately 80% confluence, passaging was performed. After aspirating the medium and washing cells with DPBS, 2ml trypsin/EDTA was added to the culture dishes. Cultures with trypsin/EDTA were maintained at room temperature for approximately 20 minutes. Once cells were released from the dishes, as determined by evaluation with the inverted microscope, 10ml DMEM with FBS was added to inactivate the trypsin/EDTA. Thereafter, corneal cells were spun at 150 x g for 10 minutes, the supernate was aspirated and discarded, and cells were resuspended in 10ml DMEM with FBS or Epilife®.

First passage cells from DMEM cultures (1ED, 2ED, 3ED, 1SD, 2SD, 3SD) were proportionately distributed into two 6cm culture dishes, two 35mm glass bottom culture dishes, and five single well chamber slides (Lab-Tek Chamber Slide System, Nalge Nunc International, Rochester, NY), based on the surface areas of each culture container. First passage cells from 1EE, 2EE, and 3EE cultures were distributed proportionately among one 6cm dish, 2 glass bottom slides, and 5 chamber slides. One 6cm dish was omitted from the Epilife® (1EE, 2EE, 3EE) cultures, as the cellular density was lower than that in the corresponding DMEM cultures. Final volumes were 5ml medium in each 6cm dish, and 2.5ml medium in the chamber slides and glass bottom dishes. Cells were then returned to the incubator, at 37ºC, 5% CO_2. Cells were monitored every 12-24 hours, and further processing was performed once the cells reached 75-90% confluence or earlier.

For the cultures in the 6cm dishes in DMEM medium (1ED, 2ED, 3ED, 1SD, 2SD, 3SD), RNA crude cell lysate was performed on cells in one of the dishes, in preparation for PCR. To the other 6cm culture dishes in DMEM with FBS, the medium was aspirated and replaced with Epilife® (1ED→E, 2ED→E, 3ED→E, 1SD→E, 2SD→E, 3SD→E). After 92 hours, RNA crude cell lysate was performed on this altered group of cultures. As the 6cm presumed epithelial cultures in Epilife® approached confluence (1EE, 2EE, 3EE), RNA crude cell lysate was performed.

Passaging and sub-culturing was not possible for the tissue pieces cultured in Epilife® (1SE, 2SE, 3SE), as the pieces of tissue failed to adhere, and cells did not explant onto the surfaces of the initial 10cm culture dishes. On the same day as the corresponding cultures from the tissue pieces in DMEM with FBS (1SD, 2SD, 3SD) were processed, the medium on the Epilife® cultures (1SE, 2SE, 3SE) was changed to DMEM with FBS (1SE→D, 2SE→D, and 3SE→D). Cultures were monitored for several days for tissue attachment and cell explantation, but further investigations of these altered cultures were not pursued.

MDCK cells were maintained in a T_{75} flask with 10ml MDCK medium, as described earlier. Cells were monitored every 24-48 hours, and medium was changed every 72 hours. Once the culture reached approximately 85-95% confluence, cells were passaged by trypsinization. The procedure was similar to that described previously, with the exception that MDCK medium, not DMEM, was used to quench the trypsin/EDTA for the MDCK cells. Passaging of these cells was typically performed at a 1:20 dilution, and cells tended to approach confluence within 72-100 hours of passaging.

Cell Fixation Techniques

First passage cells in the single well chamber slides were fixed using a cold methanol: acetone fixation technique. After aspirating the medium from the chamber wells, the wells were manually removed, and the gasket seals were removed using a metal spatula. The slides were then washed twice in DPBS, and placed into cold 1:1 methanol: acetone in a -20ºC freezer for 10 minutes. Slides were then washed three additional times in DPBS. Cells were stored in DPBS containing 0.1% BSA and 0.1% sodium azide and refrigerated until immunocytochemical staining 12-48 hours later.

First passage cells in the 35mm glass bottom culture dishes were fixed when they reached 75-90% confluence in the glass bottom region of the dish. After the medium was aspirated, cultures were washed twice with DPBS. Cold methanol fixation was performed by adding methanol to the cultures, then placing the dishes in the -20ºC freezer for 10 minutes. Fixed cells were washed twice with DPBS, and then refrigerated for storage in DPBS with 0.1% BSA and 0.1% sodium azide.

Immunohistochemistry and Immunocytochemistry

Corneal tissue sections obtained before and after trypsin/EDTA (1a, 2a, 3a, 1b, 2b, 3b) were fixed in 10% neutral buffered formalin for 24 hours. Tissue processing and dehydration were performed with sequential 70%, 80%, 95%, and 100% blended alcohols (Richard-Allan Scientific, Kalamazoo, MI) using a Sakura-Finetek VIP V Tissue

Processor (Torrance, CA). Tissues were cleared in xylene (Fischer Scientific, Pittsburgh, PA), infiltrated with paraplast paraffin (McCormick Scientific, St. Louis, MO), and embedded in EM 400 embedding medium (Surgipath Medical Industries, Richmond, IL). Tissues were sectioned at 5µm, and five sections of each tissue block were made. Routine hematoxylin and eosin phloxine (H&E) staining (Richard-Allan Scientific, Kalamazoo, MI) was performed using a Leica Autostainer XL (Wetzlar, Germany) on one slide from each tissue, with subsequent application of mounting medium (Richard-Allan Scientific, Kalamazoo, MI) and a coverslip.

For the remaining four slides for each tissue section, a Benchmark XT® automated stainer (Ventana Medical Systems, Tucson, AZ) was utilized for immunohistochemical staining with rabbit anti-cow polyclonal antibody to pancytokeratin (reference # ZO622, lot # 0073C, Dako, Carpinteria, CA) at a dilution of 1:1000, vimentin antibody clone V9 (reference # 790-2917, lot # 513349, Ventana Medical Systems, Tucson, AZ), and E-cadherin antibody clone ECH-6 (reference # 760-2830, lot # 12056, Ventana Medical Systems, Tucson, AZ). Positive tissue controls were used to ascertain that the stain and technique were working properly. These positive tissue controls were canine skin for pancytokeratin, canine tonsil and lymph node for vimentin, and canine pancreas for E-cadherin. Negative controls were established by omitting primary antibodies from the staining protocol.

The Benchmark XT® Protocol #4 was used for pancytokeratin, Protocol #26 was used for vimentin, and Protocol #16 was used for E-cadherin. Though specific details of proprietary reagents were not available from Ventana, the general staining technique for pancytokeratin commenced with cyclic heating of the slides to 75-76ºC, application of EZPrep, and incubation. The slides were then rinsed with a Reaction Buffer, followed by incubation with PROTEASE 1, and then the pancytokeratin antibody was applied to the samples. Blockers A and B were then sequentially applied and incubated. After rinsing again with the Reaction Buffer, ENH BIOT Ig/VR and ENH SA-AP/VR were added, followed by applications of ENH ENHANCER/VR and ENH NAPHTHOL, and lastly by incubation with ENH FAST RED A and ENH FAST RED B. The staining protocol for

vimentin differed in that Cell Conditioner #1 was applied instead of EZPrep and PROTEASE 1. For E-cadherin, EZPrep was applied initially, PROTEASE 1 was not utilized, and Cell Conditioner #1 was applied prior to antibody incubation.

After cold methanol: acetone fixation described previously, five chamber slides from each dog and culture category (1ED, 2ED, 3ED, 1EE, 2EE, 3EE, 1SD, 2SD, 3SD) were submitted for immunocytochemistry. For the post-trypsin tissue sections from all three dogs cultured in Epilife® medium (1SE, 2SE, 3SE), the tissue sections did not adhere and no cells explanted in the primary culture, so passaging into chamber slides was not feasible. Routine hematoxylin and eosin staining was performed on one slide from 1ED, 2ED, 3ED, 1EE, 2EE, 3EE, 1SD, 2SD, 3SD. Using the automated Ventana stainer, the remaining four slides were stained with pancytokeratin, vimentin, E-cadherin, and a negative control. Positive tissue controls, MDCK cells, and corneal sections were used to ascertain that the stains and techniques were working properly. The protocols used were similar to those used for the formalin fixed paraffin-embedded tissues described previously, however, no deparaffinizing steps were required for the culture samples.

Representative photographs were taken of the stained slides using a Nikon Eclipse E600 microscope (Nikon Corporation, Japan) with a Nikon DXM1200 digital camera (Nikon Corporation, Japan) using Nikon ACT-1 version 2.63 software (Nikon Corporation, Japan) to allow for assessments of the staining characteristics of various antibodies on the different cell types from Epilife® and DMEM with FBS culture conditions.

Immunofluorescence

Immunofluorescence was performed on the fixed cells from the 35mm glass bottom dishes. After aspirating the 0.1% BSA/DPBS in which the fixed cells had been stored, the cells were washed twice with DPBS. Fluorescein isothiocyanate (FITC)-conjugated mouse-anti-ZO-1 antibody (Invitrogen Corporation, Carlsbad, CA) was used for immunofluorescent detection. The stock solution was diluted from 500µg/ml to 10µg/ml in 0.5% BSA/DPBS, and cells were incubated for one hour at room temperature in

darkness with 80µl diluted antibody. FITC- conjugated mouse IgG1 (Product Code: MG101; Caltag Laboratories, Burlingame, CA) was used as a negative control, with the same concentration and incubation as that used for the ZO-1 antibody. After one hour of exposure, cells were washed twice with 0.5% BSA/DPBS, and a nuclear staining reagent was applied to the cells. A Zeiss Axiovert 100M confocal microscope (Cark Zeiss, Inc., Thornwood, NY) with argon (458, 488, 514nm) and enterprise (351, 364nm) lasers was used to visualize the fluorescence. Representative photographs were taken using Carl Zeiss Laser Scanning Systems LSM 510 imaging software (Carl Zeiss, Inc., Thornwood, NY).

RNA crude cell lysate

In preparation for PCR, RNA crude cell lysates were prepared using the 6cm dishes for each culture, with the exceptions of 1SE, 2SE, and 3SE. Culture medium was aspirated, and 600µl RNA lysis buffer (QIAGEN Inc., Valencia, CA) containing 1% β-mercaptoethanol was added to solubilize cells. The viscous fluid was carefully scraped from the culture dish, aspirated, and dispensed into a QIA shredder (QIAGEN Inc., Valencia, CA). After centrifuging for 2 minutes to homogenize the samples, forceps were used to carefully replace the cap, and the samples were labeled and frozen at -20ºC.

RNA isolation

Total RNA isolation was performed as described in the RNeasy Minikit (QIAGEN Inc., Valencia, CA) and quantified using ultraviolet light at 260nm. During processing, care was taken to minimize exposure of the samples to other sources of RNA. RNA crude cell lysate samples were retrieved from -20ºC, and the caps were carefully removed with forceps. To each sample, 600µl 70% ethanol was added to the samples and mixed well. Approximately one half, or 600µl, of the mixture was then dispensed into tubes provided in the RNeasy kit, in which a silica gel membrane traps RNA. Samples were spun for 15 seconds at ≥8000 x g, and flow-thru was aspirated and discarded. The remaining 600µl from the initial ethanol mixture was added to the tube with the filter, the sample was spun

again for 15 seconds at ≥8000 x g. The flow-thru was again aspirated and discarded. To each tube, 350µl Buffer RW 1, provided in the RNeasy kit, was added. Tubes were again spun for 15 seconds at ≥8000 x g, and the flow-thru was aspirated and discarded. A mixture containing 70µl Buffer RDD, provided in the kit, and 10µl DNase was dispensed directly onto the silica gel membrane and allowed to sit for 15 minutes. Another 350µl Buffer RW 1 was added to the samples, which were then spun for 15 seconds at ≥8000 x g. Flow-thru and collection tubes were then discarded. The membranous upper portions of the tubes were moved to additional tubes provided in the kit. To each sample, 500µl Buffer RPE, provided in the kit, was added, and samples were spun for 15 seconds at ≥8000 x g. Flow-thru was aspirated and discarded, and another 500µl Buffer RPE was added. Samples were spun for 2 minutes at ≥8000 x g, and flow-thru was again discarded. The upper portions of the tubes were again moved to labeled 1.5ml vials provided in the kit, and samples were eluted with 40µl RNase-free water, provided in the kit, dispensed directly onto the white silica gel membrane. Samples were centrifuged for one minute at ≥8000 x g. This RNA elution step was repeated, and the upper silica gel membrane was then discarded.

To fresh labeled 1.5ml tubes, 5µl RNA elutant was added along with 500µl distilled water, providing a 101-fold dilution. Ultraviolet absorption for 260nm and 280nm for each sample were evaluated after ensuring proper analyzer function by testing with distilled water. The concentration of RNA in the samples was then determined using the following formula:

$$[\text{RNA}] = A_{260} \times 40\mu\text{g/ml} \times \text{dilution factor}$$

[RNA] is the concentration of RNA in µg/ml.
A_{260} is the absorption of 260nm ultraviolet light.
40µg/ml is the extinction coefficient constant associated with RNA.
Dilution factor is the dilution of the RNA elutant in distilled water, or 101, for these samples.

After determining the RNA concentration in each sample, further calculations were performed to determine how much of each RNA elutant sample to add to distilled water to reach a total volume of 8µl while maintaining an RNA concentration of 1µg. This partially accounted for differing original concentrations of RNA, and allowed for comparable cDNA products and PCR results in subsequent steps. However, for the following samples, the RNA concentrations were less than 1µl/µg, so the maximum volume of RNA (8µl) was used with no distilled water: 1EE, 2EE, 3EE, 1ED, 3ED, 1EDE, 2EDE, 3EDE.

Complementary DNA Synthesis

Synthesis of complementary DNA (cDNA) from the isolated total RNA was performed as described in the SuperScript First-Strand Synthesis System for RT-PCR User Manual, page 7 (Invitrogen Corporation, Carlsbad, CA). Complementary DNA was synthesized from 1EE, 2EE, 3EE, 1ED, 2ED, 3ED, 1SD, 2SD, 3SD, 1ED→E, 2ED→E, 3ED→E, 1SD→E, 2SD→E, 3SD→E, and MDCK RNA isolates. Negative controls for cDNA synthesis were established for 3EE, 2SD, and MDCK RNA isolates by omitting the reverse transcriptase (no-RT). RNA/primer mixtures were prepared as follows:

≤1µg total RNA
1µl 10mM dNTP mix
1µl random hexamers (50ng/µl)
10µl DEPC-treated water

After 5 minutes of incubation at 65ºC, the samples were placed on ice for 2 minutes. A reaction mixture was prepared:

2µl 10X RT buffer
4µl 25mM $MgCl_2$
2µl 0.1M DTT
1µl RNaseOUT Recombinant Ribonuclease Inhibitor

Each RNA/primer mixture was combined with 9µl of the reaction mixture and incubated at 25ºC for 2 minutes. One microliter (50 units) of SuperScript II RT was added to each tube, except for the three negative controls, 3EE, 2SD, and MDCK, for which there was no-RT. After mixing, the samples were incubated at 25ºC for 10 minutes, then 42ºC for 50 minutes, followed by 70ºC for 15 minutes. Samples were then chilled on ice until 1µl of RNase H was added to each tube, followed by 20 minutes of incubation at 37ºC. Samples were then frozen at -20ºC until further processing.

Canine CK5 Alignment Sequence

The NCBI genetic analysis program BLAST (http://www.ncbi.nlm.nih.gov/BLAST/) was used to retrieve individual canine CK5 cDNA sequences. The sequence alignment for canine CK5 with highlighted regions of the forward and reverse primers is shown in Appendix 1.

The primer sequences designed for the study were derived from the region of greatest homology among the known canine CK5 sequences (100% identical in 18 of 20 reported sequences, including transcript variants 1-4 and 7-20). The identifications of the 18 matching sequences are as follows:

XM_844906	XM_855259	XM_855231
XM_855192	XM_855152	XM_563648
XM_855095	XM_855053	XM_855013
XM_854983	XM_854944	XM_854908
XM_854866	XM_854833	XM_854800
XM_854761	XM_854659	XM_854630

Two additional 100% matches, identified as XM_855364 and XM_844915, were reported to encode for variants of CK6a instead of CK5. The predicted amplified CK5 product of 189 bp bridged an exon-exon boundary, with matched forward and reverse

primer melting temperatures of 59ºC. Melting temperature for the entire CK5 sequence was 83ºC. The primer sequences for CK5 were as follows:

Canine CK5-79F

5′-GAGCGCGAGCAGATCAAGA (sense)

Canine CK5-267R

5′-CAGCTGTCTCCTGAGGTTGTTG (anti-sense)

PCR Gel Electrophoresis

To verify that the CK5 primers amplify the desired target sequence, conventional PCR using a Hybaid PCR Sprint Thermal Cycler (Mandel Scientific Company, Inc., Guelph, Ontario, Canada) was run with both the forward and reverse primers on 3EE, 2SD, and MDCK cDNA. The following components for each sample were mixed for conventional PCR:

9µl	H_2O
0.5µl	CK5 forward primer
0.5µl	CK5 reverse primer
10µl	2X Taq Master mix
2µl	cDNA template or negative control

The forward and reverse primers were diluted from 10µM to 0.25µM, and the Taq Master mix was diluted from 2X to 1X. For each sample, 22µl was the total volume for PCR.

The following 30 temperature cycles were used for the analysis:

1 cycle	94ºC	2 minutes
	55ºC	1 minute
	72ºC	2 minutes
28 cycles	94ºC	1 minute
	55ºC	1 minute
	72ºC	2 minutes
1 cycle	94ºC	1 minute
	55ºC	1 minute
	72ºC	10 minutes

A 2% agarose PCR gel containing 1X TBE (0.89M Tris base, 0.89M boric acid, 20mM EDTA) buffer was formulated. Molecular size markers were a combination of bacteriophage restriction enzyme digests LAMDA DNA *Hin*d III Digest (New England Biolabs, Inc., Ipswich MA) and ΦX174 DNA *Hae* III Digest (New England Biolabs, Inc., Ipswich, MA). After separation of DNA fragments by electrophoresis at 100V on a Horizon 58 Life Technologies Electrophoresis Apparatus (Invitrogen Corporation, Carlsbad, CA), the gel was stained with 1µg/ml ethidium bromide for 40 minutes. An ultraviolet light was used to visualize the stained bands, and the gel was photographed using a Polaroid Electrophoresis Photo-documentation camera (FB-PDC-34; Fisher Scientific, Pittsburgh, PA). After comparing the migration of PCR-amplified products to that of the reference markers, the bands of interest were cut from the gel to allow direct DNA sequencing of the products for 3EE, 2SD, and MDCK.

DNA Sequencing Preparation

The Qiaex Gel Extraction Protocol on pages 12-13 of the Qiaex II Handbook, February 1999 (Qiagen, Inc., Valencia, CA) was followed to extract DNA from the gels. The bands were weighed and a 3x volume of dissolving buffer was added to each gel. After vortexing, 10µl Qiaex II was added to each sample, and they were incubated for 10

minutes at 50ºC to solubilize the agarose and bind DNA. After centrifuging for 30 seconds, the supernate was aspirated and discarded. The pellets were washed with 500µl Buffer QX1 to remove agarose contaminants, vortexed, and centrifuged. The supernate was aspirated and discarded. The pellets were then washed with 500µl Buffer PE to remove salt contaminants, vortexed, and centrifuged. The supernate was aspirated and discarded. Samples were air dried for approximately 20 minutes, and 20µl water was added. The samples were vortexed and incubated at room temperature for 5 minutes to elute DNA. After centrifuging, the supernates, containing eluted DNA, were aspirated and placed into clean tubes.

Forward and reverse CK5 primers were also prepared for sequencing by diluting them from 10µM to 5µM in water. DNA sequencing was performed on 3EE, 2SD, and MDCK cDNA, and the forward and reverse CK5 primers at the VBI Core Laboratory Services DNA Sequencing Lab at the Virginia Polytechnic Institute and State University in Blacksburg, VA.

CK5 mRNA Amplification Efficiency

Amplification efficiency of PCR for CK5 mRNA was evaluated using serial dilutions (10^5-fold range) of cDNA from 3EE cells. One additional sample contained no template as a negative control. Three replicates were made for each sample, and for each replicate set of 3, the following mixture was created:

42µl	2X	SybrGreen Taq Master mix
42µl	2X	Primer mix
3µl		3EE cDNA dilution (or no template control)

SybrGreen Taq Master mix (Applied Biosystems, Foster City, CA) is a commercially available mixture that contains SybrGreen, which fluoresces when it attaches to double-stranded PCR product. Sense and anti-sense primer stock solutions were 10µM, and these were diluted to 0.3µM for the final concentrations. No probe was included in the primer

mix, and adequate water was added to the primer mixture to obtain the final volume of 42µl. For each replicate, the final volume for PCR was 25µl.

The efficiency of amplification using the designed CK5 forward and reverse primers for the serial dilutions of 3EE cDNA was determined by calculating the slope of the line created by plotting the threshold cycle against the cDNA dilution. The resultant value was compared to the known ideal standard slope of -3.2, which serves as an indicator of efficiency of amplification.

Quantitative Real Time PCR for Amplification of CK5 mRNA

The preparatory mixture for PCR of the canine corneal samples for CK5 mRNA consisted following combinations:

42µl	2X	Taq Master Mix
42µl	2X	Primer mix
3µl		cDNA template, no-RT, no cDNA

SybrGreen Taq Master mix was used to provide a detection method, and CK5 primer and final stock solutions were the same as those for the PCR performed on the serial dilutions of 3EE cDNA, as previously described. Each replicate contained 25µl as the final volume for PCR.

PCR was also performed on the cDNA samples to amplify the endogenous positive control, 18S ribosomal RNA (rRNA). For each replicate set, the following mixture was created:

42µl	2X	Taq Master mix
42µl	2X	Primer/Probe mix
1µl		cDNA template, no-RT, no cDNA

The Taq Master mix for this amplification process did not contain SybrGreen. The sense and anti-sense primer stock solutions were 10μM, and they were diluted to 0.05μM for the final concentrations. The TaqMan® Ribosomal RNA Control Reagents (VIC Probe; Applied Biosystems, Foster City, CA) original stock solution was 40μM, diluted to 0.2μm for the final concentration. The remainder of the 42μl of primer/probe mix was water. In contrast to the fluorescent detection method of SybrGreen, the fluorescing agent for 18S rRNA is attached to the probe in an inactive state. During the cycles of PCR, the fluorescing agent is detected once it becomes liberated from the probe during the amplification process. Each replicate contained 25μl as the final volume for PCR.

PCR amplification of CK5 mRNA and 18S rRNA were performed on the following cDNA samples:

1EE	1ED	1SD	1ED→E	1SD→E
2EE	2ED	2SD	2ED→E	2SD→E
3EE	3ED	3SD	3ED→E	3SD→E
MDCK	3EE no-RT	2SD no-RT	MDCK no-RT	no cDNA

An ABI Prism 7700 Sequence Detector (Applied Biosystems, Foster City, CA) performed the quantitative real time PCR amplification. The following temperature cycle was applied:

1 cycle	50ºC	2 minutes
1 cycle	95ºC	10 minutes
40 cycles	95ºC	15 seconds
40 cycles	60ºC	1 minute

Sequence Detection System (SDS 1.9.1) software (Applied Biosystems, Foster City, CA), using the QPCR protocol for SybrGreen was used for CK5 analyses. Analysis of data included retrieval of raw data, adjustment of the threshold cycle (C_T) line above the noise level, post-run dissociation curve assessment, and comparative C_T analysis. The C_T line

was set at a level above noise, in the region of early exponential amplification of the products. Post-run dissociation curves were analyzed on the products of the serial dilutions for amplification efficiency, the corneal samples, and MDCK cells. The melting temperature of the amplified product was determined by maintaining the samples at 50ºC for 15 seconds, then increasing the temperature over 10 minutes to 90ºC, and then maintaining the 90ºC heat for fifteen seconds. The resultant dissociation curves were compared to the known melting temperatures of CK5, reported to be 83ºC.

Statistical Methods

A comparative C_T analysis method was used to allow calculation of relative ratios of CK5 mRNA expression, using the following formula:

$$\Delta C_T \text{ (target)} = C_T \text{ (target)} - C_T \text{ (18S rRNA endogenous control)}$$

The C_T of the endogenous control, 18S rRNA, was subtracted from the C_T of each of the target corneal samples, yielding a value for ΔC_T. The mean ΔC_T of corneal samples 1EE, 2EE, and 3EE were compared to the mean ΔC_T for 1ED, 2ED, and 3ED, and the mean ΔC_T for 1SD, 2SD, and 3SD. Data were analyzed using the Relative Expression Software Tool (REST).[99,100] REST generates the relative gene expression ratios according to the Pfaffl method, and provides a 95% bootstrap confidence interval for the ratios, as well as a P-value.[99,100] The level of significance was set at α=0.05.

Flowchart 1

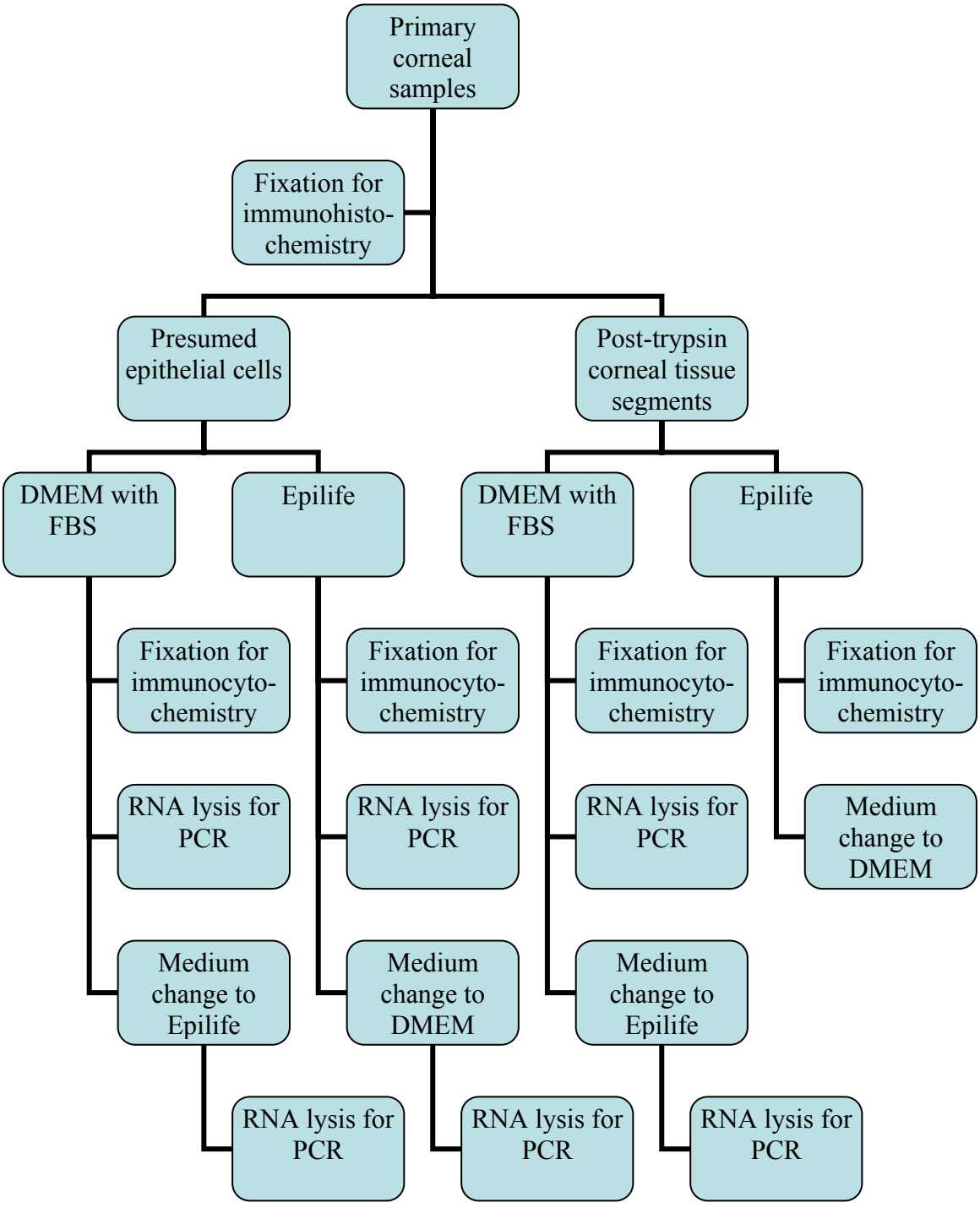
Primary corneal samples
Fixation for immunohisto-chemistry
Presumed epithelial cells
Post-trypsin corneal tissue segments
DMEM with FBS
Epilife
DMEM with FBS
Epilife
Fixation for immunocyto-chemistry
Fixation for immunocyto-chemistry
Fixation for immunocyto-chemistry
Fixation for immunocyto-chemistry
RNA lysis for PCR
RNA lysis for PCR
RNA lysis for PCR
Medium change to DMEM
Medium change to Epilife
Medium change to DMEM
Medium change to Epilife
RNA lysis for PCR
RNA lysis for PCR
RNA lysis for PCR

CHAPTER III. RESULTS

All figures, tables, and charts are provided at the end of the section.

Immunohistochemistry of Primary Corneal Tissue Samples

Routine H&E staining was performed on one slide from each corneal tissue section to assess general tissue architecture features. The positive tissue control for pancytokeratin was canine skin, for vimentin was canine tonsil, and for E-cadherin was canine pancreas (Figure 1); these tissues were used to ascertain proper staining technique. Staining characteristics of the primary canine corneal tissue specimens from the three dogs were similar, and representative images from dog 2, including a negative control, are shown in Figure 2. Pancytokeratin staining of all primary canine corneal tissue sections was densely positive throughout the stratified epithelial cell layers and negative in the stromal cell layers. Vimentin staining was negative in the corneal epithelial cells and positive in the stromal cell layers of all tissue samples. E-cadherin staining was positive in the epithelial cell layers, with increased stain accumulation near the periphery of the cells, and negative in the stromal cells.

Immunohistochemistry of Trypsinized Corneal Tissues

In preliminary studies of enzymatic digestion to separate the epithelial and stromal cells from the initial corneal tissue sections, use of trypsin appeared superior to dispase/collagenase (Roche Molecular Biochemicals, Mannheim, Germany), based on the larger size of the cell pellet that was observed after trypsinization. After trypsinization of the primary corneal tissue sections, H&E staining of tissue sections from each dog demonstrated that the epithelial cells had been released and stromal tissue remained (Figure 3). Staining was negative throughout the stromal tissue layers for pancytokeratin, positive for vimentin, and negative for E-cadherin (Figure 3). The only cells which stained positively for pancytokeratin and E-cadherin in the post-trypsinized samples were

rare residual epithelial cells that were detached from the underlying stroma. Immunohistochemical staining demonstrated the trypsinization was successful in releasing the majority of epithelial cells from the underlying stromal tissues.

Cell Culture and Passaging

Table 1 depicts the dog number (1, 2, 3), treatment group (presumed epithelial or explant, Epilife or DMEM), days to attachment, days to passage, and days in culture prior to fixation for each analysis.

Within 24 hours of tissue acquisition and commencement of cell cultures, the initially suspended cells, presumed to be predominantly epithelial cell types, from all three dogs demonstrated large numbers of round suspended cells, and moderate numbers of adherent round and fusiform individual or clumped cells in both culture media. The explant cultures, established using the pieces of corneal tissue post-trypsinization, represented mostly stromal cells. After 24 hours in culture, no tissue pieces were adherent to the culture plates, there were rare suspended round cells and rare attached round and fusiform cells. After 48 and 72 hours, there were increasing numbers of attached cells recognized in the presumed epithelial cultures, regardless of the medium type or dog. In addition to the round and fusiform cell shapes, adherent polyhedral cells were recognized in these cultures from all three dogs. Little change was observed in the explant cultures, as the tissue pieces were not adherent to the culture plates in either culture medium. During the active phases of culturing, pictures were intermittently taken to demonstrate the appearances of the two cell types growing in the two different media. Cells from the presumed epithelial and explant cultures in both media for dog 3 were photographed after 72 hours in culture (Figure 4).

After 6 days in culture, discrepancies in cell growth were noted among the cultures from the different dogs. For dog 3, there was moderate cellular attachment of round, polyhedral, and fusiform cells in the presumed epithelial cultures, and the cell numbers subjectively appeared equal in Epilife and DMEM. For dogs 1 and 2, there was better

individual cellular attachment in the presumed epithelial culture in Epilife, as compared to dog 3, and cell morphology was a mixture of round, fusiform, and polyhedral. Presumed epithelial cultures in DMEM for dogs 1 and 2 demonstrated a more extensive meshwork of interconnected fusiform to stellate cells mixed with round and polyhedral cells. In the explant culture in DMEM for dog 3, there was one tissue piece adherent to the plate. There were two adherent tissue pieces in the DMEM medium for both dogs 1 and 2. There were no adherent tissue pieces in any of the Epilife cultures.

One week after culture commencement, primary cells cultured from dog 2 approached confluence faster than cells cultured from dogs 1 and 3, regardless of medium or cell type. For dog 2, 20-25% of the cells were attached in the presumed epithelial cultures in Epilife. Adherent round, polyhedral, and fusiform cells covered approximately 15-20% of the plates for the presumed epithelial cultures in Epilife from dogs 1 and 3. The presumed epithelial culture in DMEM medium for dog 2 approached confluence with webs of interconnecting cells, as well as fusiform and polyhedral cells observed, and these cells were passaged (P1). For dogs 1 and 3, there were more attached, interconnected, and branching cells in the presumed epithelial cultures in DMEM than in Epilife. The explant cultures in DMEM for all three dogs demonstrated 2-3 well attached tissue pieces with tightly packed, narrow, fusiform cells explanting onto the plates. The explant cultures in Epilife for all three dogs failed to show any well attached tissue pieces, and only rare stellate cells were observed to adhere to the plates. Photographs were taken of dog 2 to demonstrate the varied cell growth and morphologies in Epilife and DMEM (Figure 5).

For the subsequent two days, progressive cell growth was observed in all cultures except the explant cultures in Epilife for all three dogs. On day 10, confluence of the presumed epithelial cultures in Epilife for all three dogs was 50-60%, demonstrating a combination of polyhedral, spindle, and round cells (Figure 6). Primary presumed epithelial cultures in DMEM for dogs 1 and 3 demonstrated 70% plate coverage with polyhedral, fusiform, and round cells, and these cultures were passaged. First passage presumed epithelial cultures from dog 2 in DMEM approached confluence (Figure 7) and were fixed for immunocytochemistry and immunofluorescence and processed for RNA crude cell lysate.

For one 60mm culture of P1 cells from dog 2 in DMEM, the medium was changed from DMEM to Epilife. Tissue pieces in DMEM for all three dogs were attached and cells were explanting well, with tightly packed narrow fusiform cells mixed with regions of polyhedral cells. No tissue pieces were adherent in the Epilife cultures.

On day 11, the primary presumed epithelial cells in Epilife for all three dogs were approximately 70% confluent, and they were passaged. The recently passaged cells from dogs 1 and 3 in DMEM were becoming adherent to the culture plates and chamber slides. The 60mm culture dish from dog 2, in which the medium had been changed from DMEM to Epilife on day 10, remained at approximately 80% confluence. Explant cultures of the tissue pieces were left undisturbed.

After 14 days in culture, P1 cells in chamber slides from the presumed epithelial cultures in Epilife from all 3 dogs approached confluence and were fixed for immunocytochemistry. These P1 presumed epithelial Epilife cultures in the glass bottom dishes were approximately 30% confluent. Based on preliminary studies in which epithelial cell growth was limited beyond 2 weeks, the decision was made to fix the cells for immunofluorescence. This same group of Epilife cultures of P1 presumed epithelial cells from all three dogs in the 60mm dishes were approximately 50% confluent (Figure 8), and RNA crude cell lysate was performed. First passage cultures of the presumed epithelial cultures in chamber slides from dogs 1 and 3 in DMEM were approximately 30% confluent, and the cells were fixed for immunocytochemistry. First passage cultures in glass bottom dishes for dogs 1 and 3 in DMEM were 50-60% confluent, and cells were fixed for immunofluorescence. The P1 presumed epithelial cultures from dogs 1 and 3 in DMEM in 60mm dishes were 70-80% confluent (Figure 9), and RNA lysis was performed on one of the dishes from each dog. The medium in the second 60mm dish from dogs 1 and 3 was changed from DMEM to Epilife. RNA lysis was performed on the P1 60mm culture from dog 2, in which the medium had been changed from DMEM to Epilife four days previously. At the time of this RNA crude cell lysate, approximately 30% cellular confluence of predominantly polyhedral cells were observed. The explant culture for dog 2 in DMEM demonstrated 40% plate coverage (Figure 10), while the

explant cultures for dogs 1 and 3 in DMEM demonstrated 20% plate coverage. No tissue pieces in Epilife were adherent for any of the dogs (Figure 11).

On culture day 15, P1 presumed epithelial cells from dogs 1 and 3, in which the medium was changed from DMEM to Epilife on day 14, demonstrated 70% confluence for dog 1 and 85% confluence for dog 3. On day 17, these percentages decreased to 50% and 75 %, respectively. RNA lysis was performed on these cells on day 18, four days after the medium was changed, which was similar to the procedure followed for dog 2. By day 18, the culture for dog 1 was only 30% confluent, and for dog 3 was 50% confluent. During this time, the tissue cultures in DMEM continued to explant. For dog 2, approximately 65% confluence was observed by day 18, and 25% confluence was seen in the cultures for dogs 1 and 3. Explant cultures in Epilife failed to adhere to the plates.

After 19 days in culture, the primary explant culture in DMEM for dog 2 was 75% confluent, and the cells were passaged after removing the tissue pieces and submitting them for immunohistochemistry. The explant culture in Epilife for dog 2 showed no adherent tissues or explanting cells. Two tissue pieces from the Epilife culture were submitted for immunohistochemistry, and the culture medium was changed from Epilife to DMEM.

By day 21, primary explant cultures in DMEM from dogs 1 and 3 were approximately 25-30% confluent (Figure 12), and the decision was made to passage the cells. Prior to passaging the explanting cells from each of these cultures, the tissue pieces were extracted and submitted for immunohistochemistry. No improvement was seen in the explant cultures in Epilife for dogs 1 and 3, and the medium was changed to DMEM after submitting two pieces of tissue from each dog for immunohistochemistry. First passage cells of the explant cultures in DMEM from dog 2 were nearly confluent in the chamber slides, 60mm dishes (Figure 13), and glass bottom dishes, and these cells were fixed for further processing. In one of the 60mm dishes, the medium was changed from DMEM to Epilife, and the culture was maintained. Figures 12 and 13 demonstrated the variety of cell morphologies observed in the explant cultures.

On day 22, first passage explant cultures from dogs 1 and 3 were nearly confluent in the chamber slides, 60mm dishes, and glass bottom dishes, and the cells were fixed for further processing. For one 60mm dish from each dog, the medium was changed from DMEM to Epilife, similar to the procedure followed for dog 2. No tissues were adherent for the primary explant cultures in which Epilife medium was replaced with DMEM.

On day 25, RNA crude cell lysate was performed on the 60mm dish from dog 2, in which the DMEM medium had been replaced with Epilife four days previously. At the time of lysis, cells were 80% confluent. On day 26, RNA crude cell lysate was performed on the remaining 60mm dishes from dogs 1 and 3, in which the medium had been changed from DMEM to Epilife on day 22. At the time of lysis, cultures from both dogs were approximately 80% confluent. No tissues in the explant cultures in which the medium had been changed from Epilife to DMEM became adherent to the plates.

On day 27, for the culture in which Epilife had been replaced with DMEM on day 19 for dog 2, one piece of corneal tissue was adherent, and fusiform and stellate cells were explanting onto the surface of the culture plate (Figure 14). No adherent tissue pieces were observed in the similar cultures from dogs 1 and 3. These final three cultures were not evaluated further.

Immunohistochemistry and Immunocytochemistry

To provide a control for culture, fixation, and staining techniques, MDCK cells were cultured and processed for H&E, pancytokeratin, vimentin, and E-cadherin staining characteristics, and a negative control (Figure 15). This cell line stains positively for pancytokeratin, vimentin, and E-cadherin. The negative control for these cells was provided by omitting the primary antibody from the staining protocol.

Images of the immunocytochemical staining characteristics for P1 presumed epithelial cells and explant cultures from each dog in both Epilife and DMEM were photographed.

For the presumed epithelial cells in Epilife, cell densities appeared greatest from dog 2. Figure 16 depicts H&E staining, positive pancytokeratin, vimentin, and E-cadherin staining, and a negative control for dog 2. For the presumed epithelial cells in Epilife from dogs 1 and 3, cell densities were lower than for dog 2, but immunocytochemical staining qualities were similar.

Cellular density also appeared higher from dog 2 for first passage presumed epithelial cells in DMEM. At the time these cells from dog 2 were fixed and processed, they approached confluence. Figure 17 shows the H&E staining, as well as positive pancytokeratin, vimentin, and E-cadherin staining, and a negative control. The chamber slides for P1 presumed epithelial cultures in DMEM from dogs 1 and 3 were fixed and processed at the same time, and they were approximately 30% confluent. Immunocytochemical staining of the slides from dogs 1 and 3 demonstrated very few cells, indicating a potential flaw in the fixation or processing steps for these slides. Regardless, cells stained as expected, and Figure 18 shows staining with H&E, pancytokeratin, vimentin, E-cadherin, and a negative control for dog 1.

Prior to passaging primary explant cultures in DMEM, the pieces of tissue were removed, fixed, and stained immunohistochemically. Staining characteristics were similar for all three dogs. Figure 19 demonstrates H&E, negative pancytokeratin, positive vimentin, and negative E-cadherin staining, as well as a negative control from dog 3.

First passage explant cells from DMEM revealed similar staining characteristics for all three dogs (Figure 20). Staining for pancytokeratin and E-cadherin was negative, except for rare cells which were presumed to be epithelial cell contaminants of the stromal cultures. Vimentin staining was consistently positive among the explanted cells.

Primary explant tissue pieces in Epilife failed to adhere to the culture plates. Tissues were fixed and stained immunohistochemically, with all three dogs demonstrating similar staining characteristics. Figure 21 shows the appearances of H&E, pancytokeratin, vimentin, and E-cadherin staining for dog 1.

Immunofluorescence

Immunofluorescence using FITC-conjugated mouse-anti-ZO-1 antibody failed to result in fluorescence near the cell junctions. Figure 22 demonstrates the (a) nuclear staining and (b) similar nuclear fluorescence with a lack of cytoplasmic fluorescence for FITC-ZO-1 for MDCK cells. The lack of fluorescence in the cell cytoplasm, particularly near the cell junctions indicates that the immunofluorescence did not support the expected presence of ZO-1 in these cells. A similar lack of cytochemical immunofluorescence was observed in the canine corneal cells.

RNA Concentrations and cDNA Synthesis

RNA crude cell lysate was performed on the following cell cultures:

1EE	1ED	1SD	1ED→E	1SD→E
2EE	2ED	2SD	2ED→E	2SD→E
3EE	3ED	3SD	3ED→E	3SD→E
MDCK				

After isolating total RNA, the concentration of RNA in each sample was calculated, and the result was used to determine the volume of RNA used for cDNA synthesis in each sample. The results of these calculations are provided in Table 2. Total RNA recovery ranged from 1.36 to 38.48µg, and cDNA synthesis was performed using 0.13-1µg total RNA. The maximum volume (8µl) of RNA was added to the following samples: 1EE, 2EE, 3EE, 1ED, 3ED, 1EDE, 2EDE, 3EDE.

PCR Gel Electrophoresis

To analyze the PCR products, conventional PCR followed by gel electrophoresis was performed on cDNA from 3EE, 2SD, and MDCK samples. The bands from 3EE and 2SD

were similar, and their molecular weights were near 189 kilodaltons, as expected. The band produced by the MDCK product appeared to be slightly smaller. Results of DNA sequencing are reported in subsequent sections.

DNA Sequencing of PCR Product from Corneal Samples

Sequencing of DNA extracted from the bands produced by corneal samples 3EE and 2SD revealed that the amplified product sequences were 189 base pairs and matched 100% to the predicted canine CK5 sequence (see Appendix 2).

CK5 mRNA Amplification Efficiency

Using serial dilutions of cDNA from corneal sample 3EE, PCR amplification efficiency of canine CK5 mRNA was evaluated, and the plot of cycle and amplification is demonstrated in Chart 1. As expected, the negative control sample in which there was no cDNA did not demonstrate amplification of product. Approximately three cycles of amplification were required to permit detection of each sequential dilution above a designated noise threshold. Three replicates were amplified for each dilution, and the mean C_T and standard deviation (SD) are listed below:

Dilution	Mean C_T	SD
10^0	16.16	0.02
10^{-1}	19.47	0.08
10^{-2}	22.99	0.15
10^{-3}	26.75	0.14
10^{-4}	30.46	0.05
10^{-5}	34.11	0.02

By plotting the threshold cycle against the serial 3EE cDNA dilution concentration, or nanogram (ng) RNA equivalents per reaction, the slope of the line for PCR amplification efficiency of canine CK5 mRNA was calculated to be -3.61. This yielded an

amplification efficiency of 94.6%. Chart 2 demonstrates the PCR amplification efficiency of CK5 mRNA for the serial dilutions of 3EE cDNA.

Quantitative Real Time PCR for Amplification of CK5 mRNA

Amplification of CK5 mRNA was performed on each of the canine corneal samples, and Chart 3 demonstrates the plot of the cycle and amplification. Three negative controls from 3EE, 2SD, and MDCK were produced by omitting the reverse transcriptase when synthesizing cDNA. For an additional negative control, template was omitted from the sample. For the negative controls, no amplification was detected throughout the 40 cycles, except for minimal amplification from 2SD, verifying the absence of detectable CK5 signal attributable to genomic DNA carry-over.

Three replicates were amplified for each sample, and the mean C_T and SD are listed below:

Sample	Mean C_T	SD
1EE	16.43	0.06
2EE	16.18	0.03
3EE	16.19	0.02
1ED	18.29	0.07
2ED	17.13	0.05
3ED	16.87	0.06
1EDE	21.30	0.07
2EDE	17.67	0.03
3EDE	19.38	0.11
1SD	28.15	0.02
2SD	19.47	0.04
3SD	19.70	0.03
1SDE	29.31	0.14
2SDE	21.22	0.03
3SDE	23.13	0.05
MDCK	21.81	0.11
3EE no RT	40.00	0.00
2SD no RT	39.06	1.62
MDCK no RT	40.00	0.00
No Template	40.00	0.00

Chart 4 provides a graphical representation of the data shown above. These mean C_T values were used subsequently in the comparative C_T analysis.

The post-run dissociation curve for the PCR amplification products of CK5 mRNA for the 3EE efficiency sample and the routine corneal samples yielded a melting temperature of 85ºC with a single symmetric peak, shown in Chart 5. However, the melting temperatures of the MDCK samples were 80-83ºC, suggesting a qualitative difference in

the product from these samples and the corneal samples. The dissociation curve for PCR amplification product from the MDCK cells is shown in Chart 6.

PCR amplification of 18S rRNA provided an endogenous positive control for the cultured canine corneal and MDCK cells. Three negative controls from 3EE, 2SD, and MDCK were produced by omitting the reverse transcriptase when synthesizing cDNA. For an additional negative control, template was omitted from the sample. For all negative controls, no amplification was detected throughout the 40 cycles. Three replicates were amplified for each corneal sample, and the mean and SD are listed below:

Sample	Mean C_T	SD
1EE	19.24	0.10
2EE	19.08	0.07
3EE	19.50	0.14
1ED	18.50	0.07
2ED	18.39	0.04
3ED	18.45	0.05
1EDE	21.00	0.03
2EDE	18.51	0.05
3EDE	20.11	0.13
1SD	18.81	0.09
2SD	18.53	0.05
3SD	18.36	0.07
1SDE	18.62	0.06
2SDE	18.29	0.41
3SDE	18.99	0.13
MDCK	19.11	0.04
3EE no RT	40.00	0.00
2SD no RT	40.00	0.00
MDCK no RT	40.00	0.00
No Template	40.00	0.00

The mean C_T values from PCR amplification of 18S rRNA for each corneal sample were then subtracted from the mean C_T values from PCR amplification of CK5 mRNA, yielding the ΔC_T of the corneal samples with reference to CK5. Table 3 shows the calculations, and a graphical representation of the ΔC_T values from the corneal samples is shown in Chart 7.

Statistical Analysis

Table 3 shows the calculations for the comparative C_T analysis, including the mean C_T values from CK5 mRNA and 18S rRNA amplification, the ΔC_T values for each sample, and the mean ΔC_T values for selected samples. The 1EE, 2EE, and 3EE samples represented the initially suspended cells, presumed to contain predominantly epithelial cells, cultured in the Epilife medium. The 1ED, 2ED, and 3ED group represents initially suspended cells, presumed to contain predominantly epithelial cells, cultured in DMEM with FBS. The 1SD, 2SD, and 3SD samples are predominantly stromal cells cultured in DMEM with FBS. The relative ratios of CK5 mRNA expression in the target corneal samples 1EE, 2EE, and 3EE, normalized to 18S rRNA, were compared to CK5 mRNA expression in the 1ED, 2ED, 3ED group and to CK5 mRNA expression in the 1SD, 2SD, 3SD group, shown in Table 4. Chart 8 graphically demonstrates that when the mean ΔC_T of 1EE, 2EE, and 3EE was compared to the mean ΔC_T of 1ED, 2ED, and 3ED, the relative expression of CK5 mRNA in the EE group was up-regulated by a factor of 3.97. However, when the mean ΔC_T from 1EE, 2EE, and 3EE was compared to the mean ΔC_T of 1SD, 2SD, and 3SD, the results were not reliable due to a large confidence interval for the relative expression ratio.

DNA Sequencing of PCR Product from MDCK Cells

Figure 23 shows the bands produced from PCR gel electrophoresis from corneal samples 2SD and 3EE, as well as the MDCK cells. The DNA extracted from the band produced by the MDCK sample demonstrated approximately 35 mismatches when the sequence was compared to the predicted canine CK5 sequence. The sequenced product from the

MDCK sample matched 100% with the predicted canine CK8 sequence between primers. Appendix 2 shows the sequences of the products from PCR amplification of the corneal cells, matching the sequence for CK5, and the MDCK cells, matching the sequence for CK8.

Figure 1. Positive tissue controls. The positive tissue control for (a) pancytokeratin was canine skin, (b) vimentin was canine tonsil, and (c) E-cadherin was canine pancreas, demonstrating proper staining techniques. Original magnification of 20x.

a.

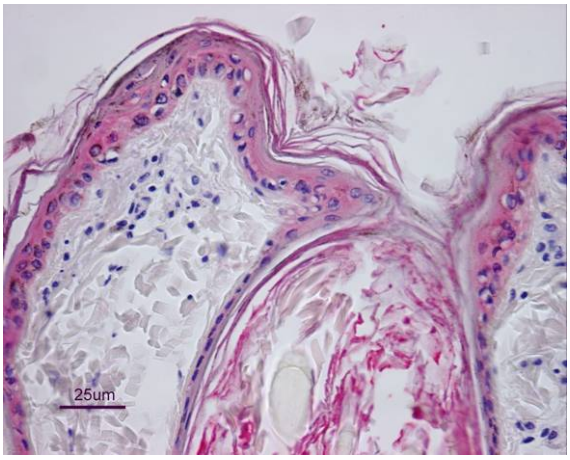

b.

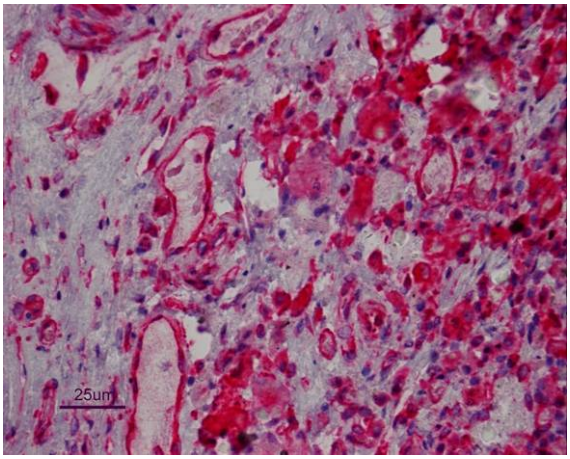

c.

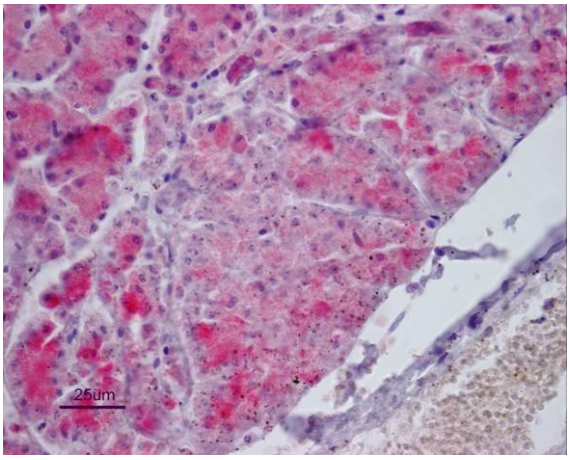

Figure 2. Primary corneal tissue sections. Representative images from dog 2 of the staining characteristics of primary canine corneal tissue sections for (a) H&E, (b) pancytokeratin, (c) vimentin, (d) E-cadherin, and (e) negative control. Original magnification of 40x.

a.

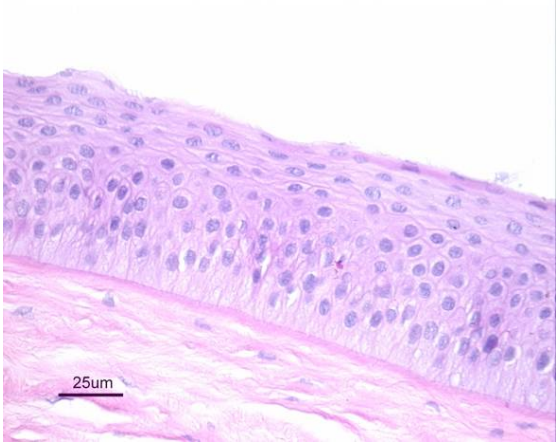

b.

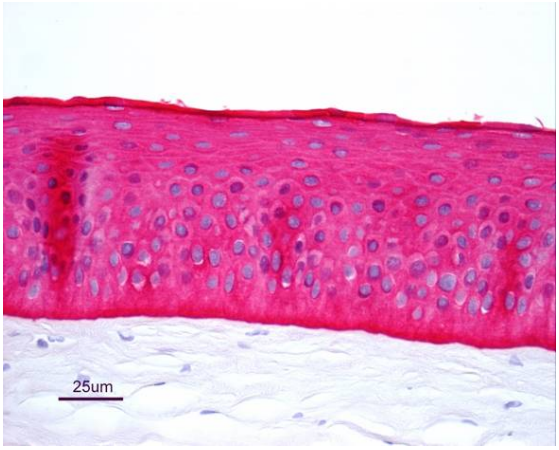

c.

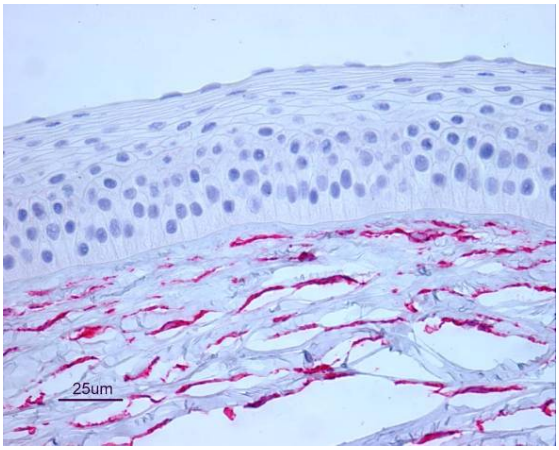

d.

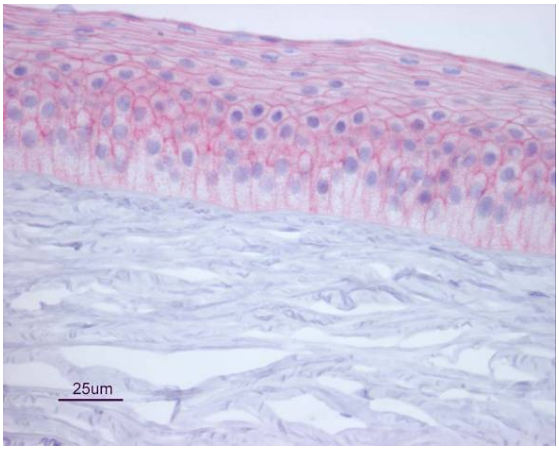

e.

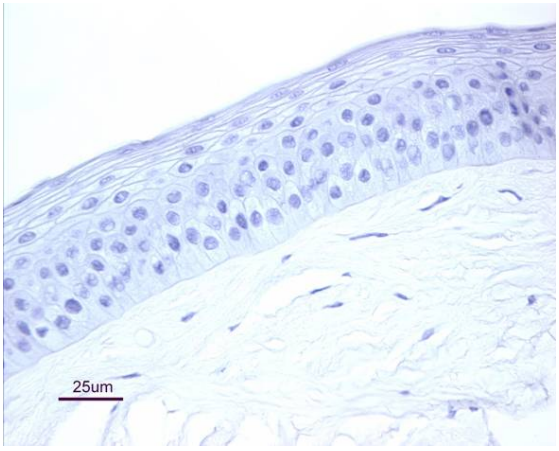

Figure 3. Post-trypsin corneal tissue sections. Representative images from dog 3 of post-trypsin canine corneal tissue samples, including (a) H&E, (b) pancytokeratin, (c) vimentin, and (d) E-cadherin. Original magnification of 40x.

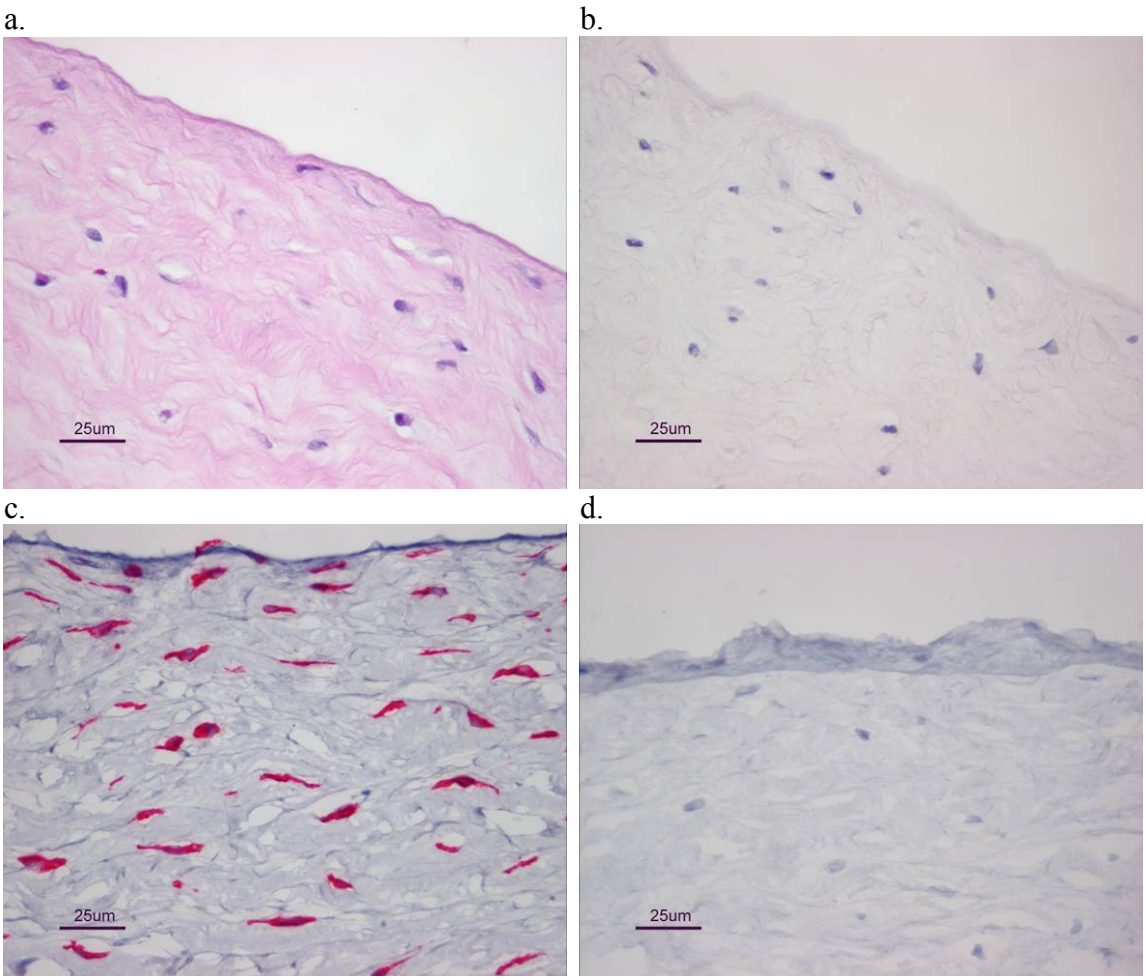

Figure 4. Seventy-two hours in culture. Appearances of cells from dog 3 after 72 hours in culture, showing (a) cultures of presumed epithelial cells in Epilife, (b) cultures of presumed epithelial cells in DMEM, (c) rare adherent cells in explant tissue cultures in Epilife, and (d) non-adherent tissue pieces in explant cultures in DMEM. All images were taken at 10x objective magnification.

a.

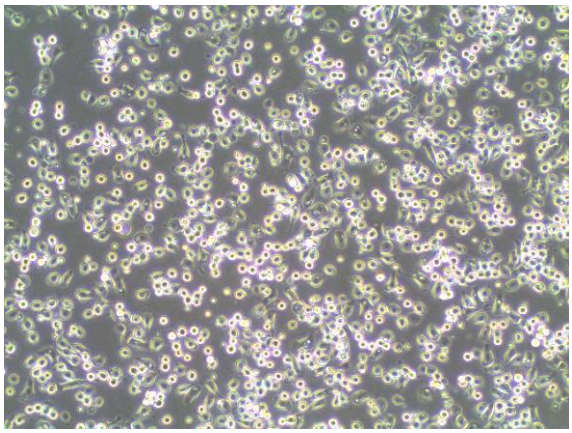

b.

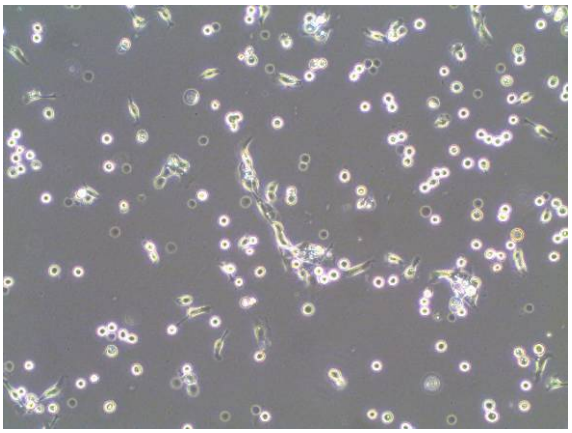

c.

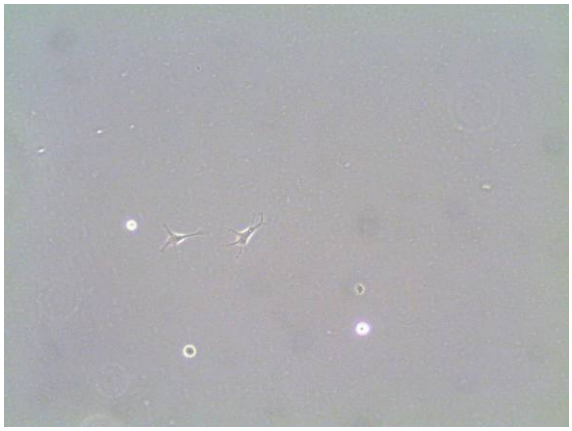

d.

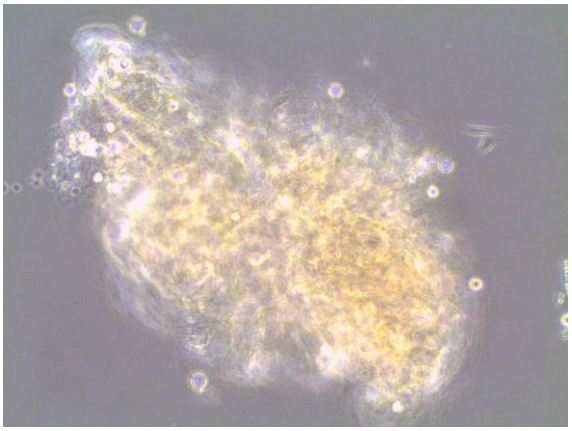

Figure 5. Seven days in culture. Cultures from dog 2 after 7 days demonstrated improving cell attachments for the presumed epithelial cultures in (a) Epilife and (b) DMEM. The explant cultures show (c) explanting cells in DMEM, and (d) rare adherent cells in Epilife. Original magnification for 5a-d was 10x.

a.

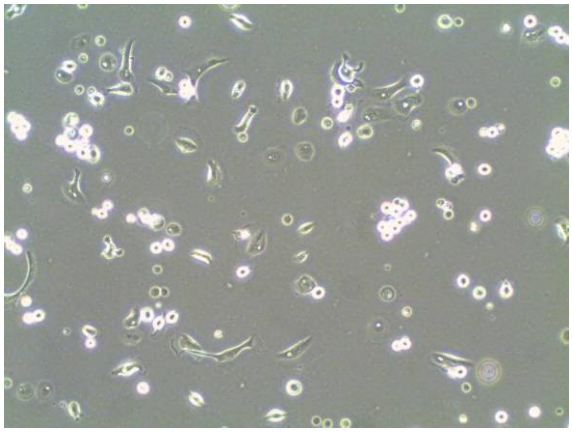

b.

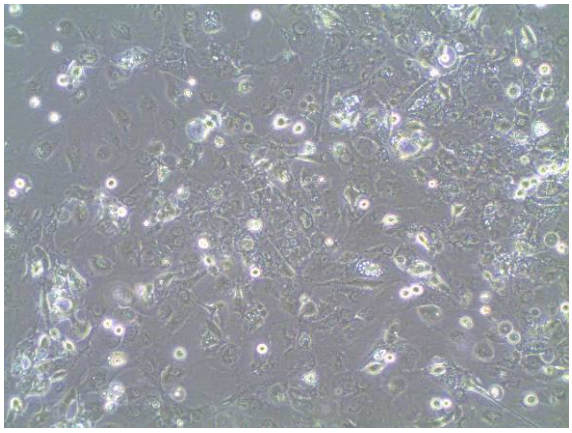

c.

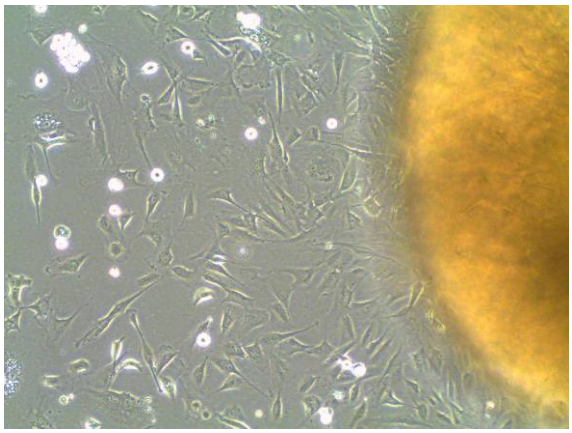

d.

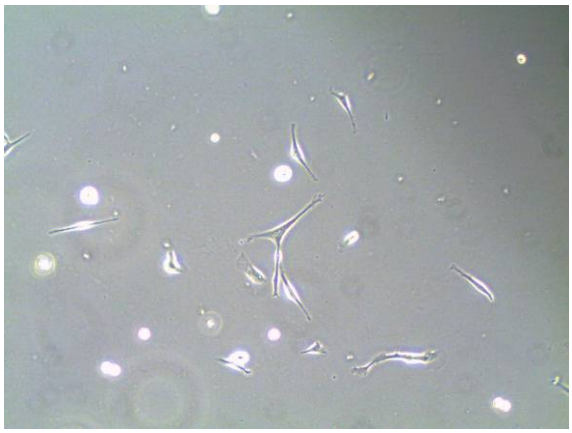

Figure 6. Presumed epithelial cells in Epilife on day 10. On day 10, primary cultures from the presumed epithelial cells of dog 3 in Epilife. The original magnification of (a) is 10x, and the original magnification of (b) is 20x.

a.

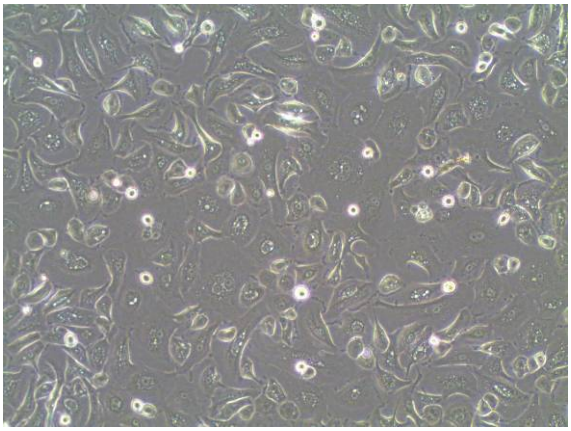

b.

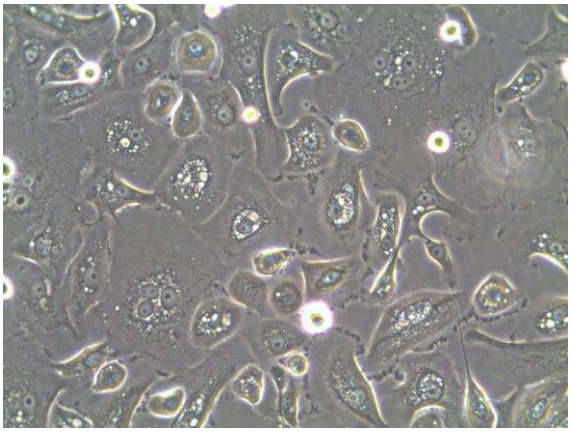

Figure 7. Presumed epithelial cells in DMEM on day 10. On day 10, passage 1 cultures from the presumed epithelial cells in DMEM from dog 2. The original magnification for (a) is 10x, and the original magnification for (b) is 20x.

a.

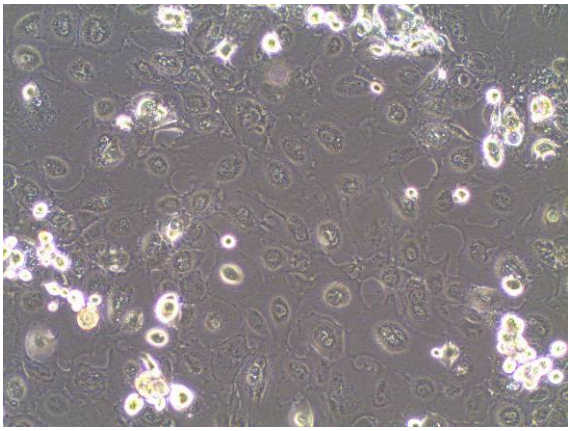

b.

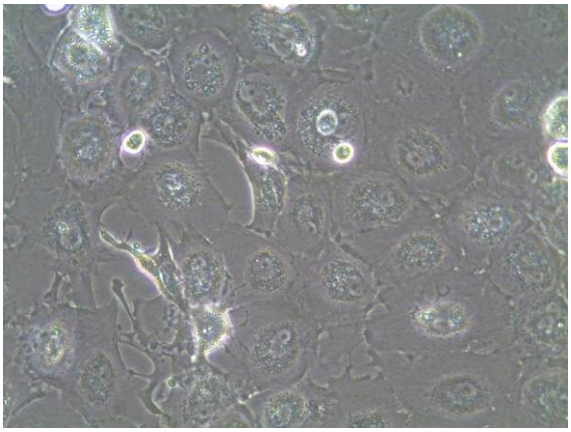

Figure 8. First passage presumed epithelial cells in Epilife on day 14. On day 14, first passage cultures from the presumed epithelial cells in Epilife from dog 3. The original magnification of (a) was 10x, and (b) was 20x.

a.

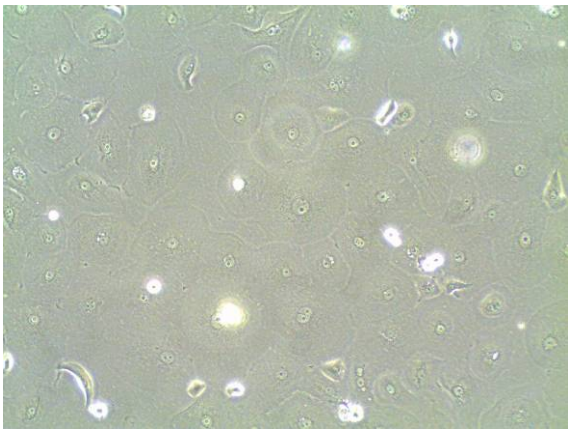

b.

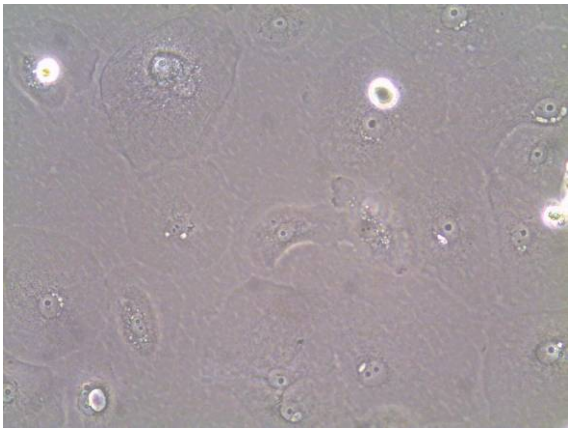

Figure 9. First passage presumed epithelial cells in DMEM on day 14. On day 14, first passage culture of the presumed epithelial cells from dog 3 in DMEM. Original magnification for (a) was 10x, and for (b) was 20x.

a.

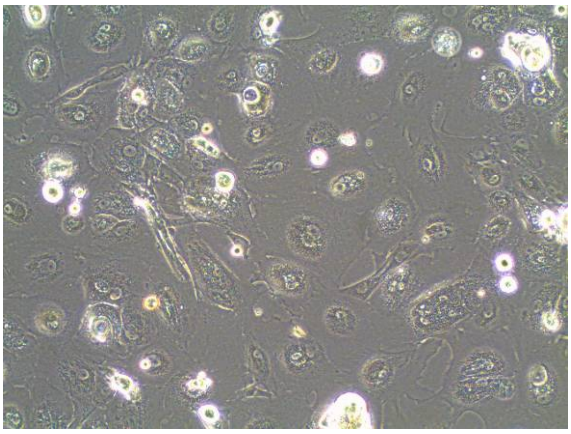

b.

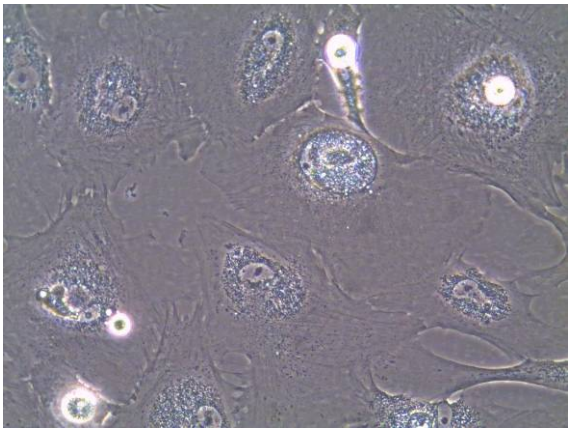

Figure 10. Explant culture in DMEM on day 14. On day 14, explant culture from dog 2 in DMEM. Original magnification of (a) was 10x, and (b) was 20x.

a.

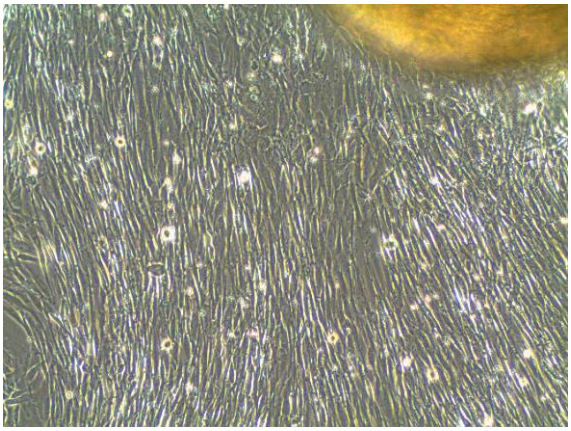

b.

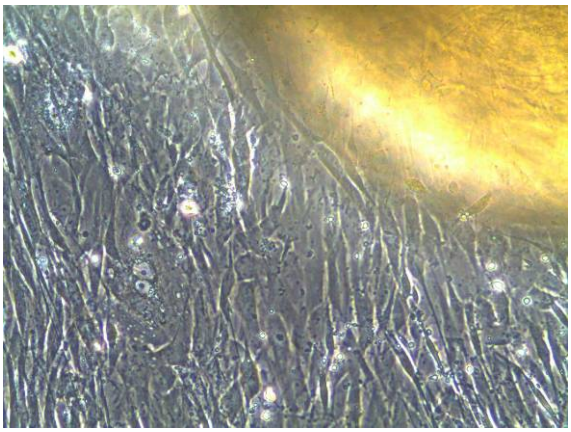

Figure 11. Explant culture in Epilife on day 14. On day 14, explant culture from dog 2 in Epilife. The edge of a floating piece of corneal tissue is imaged, and cells are not explanting from the tissue onto the culture plate.

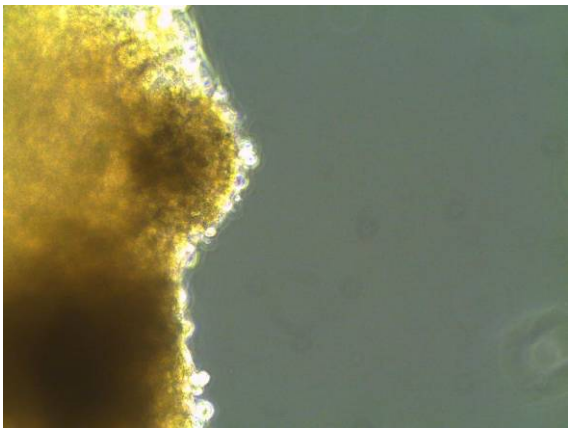

Figure 12. Explant culture in DMEM on day 21, dog 1. Day 21, primary explant cultures in DMEM from dog 1, with original magnification for (a) at 10x, and (b) at 20x.

a.

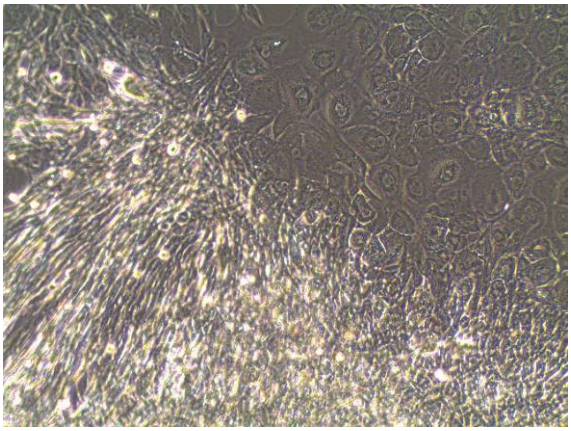

b.

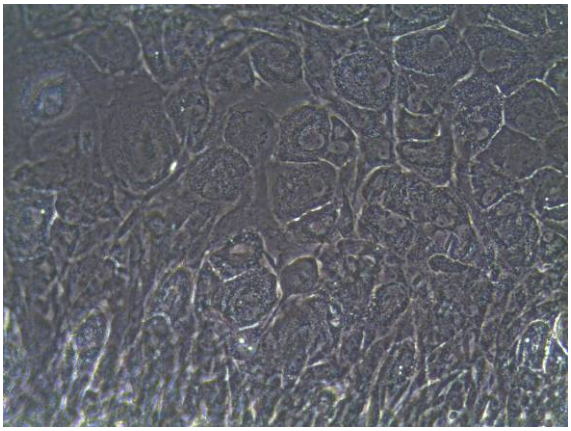

Figure 13. First passage explant culture in DMEM on day 21, dog 2. Day 21, first passage explant cultures in DMEM from dog 2, with original magnification for (a) at 10x, and (b) at 20x.

a. b.

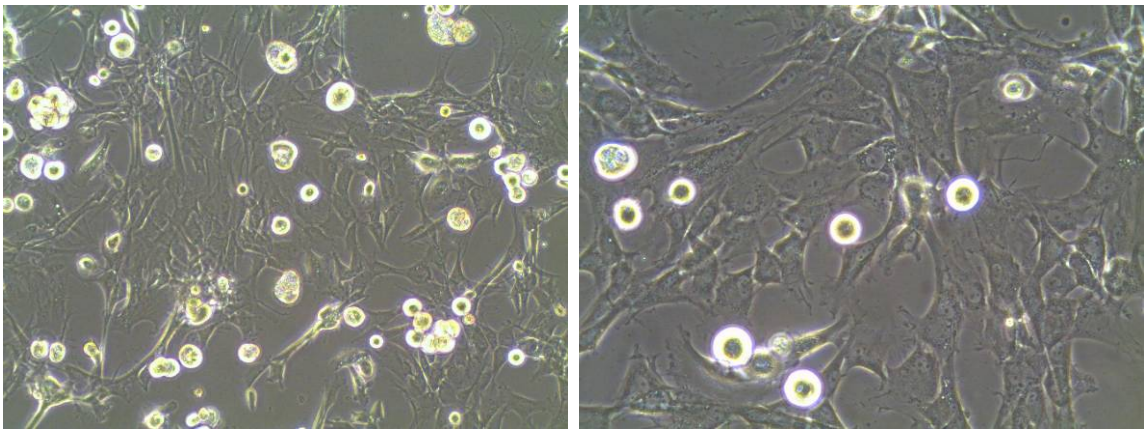

Figure 14. Explant culture on day 27 after medium change, dog 2. Day 27, explant culture dog 2, in which Epilife was replaced with DMEM 8 days previously, demonstrating an adherent piece of tissue and cells explanting onto the culture plate. Original magnification of 10x.

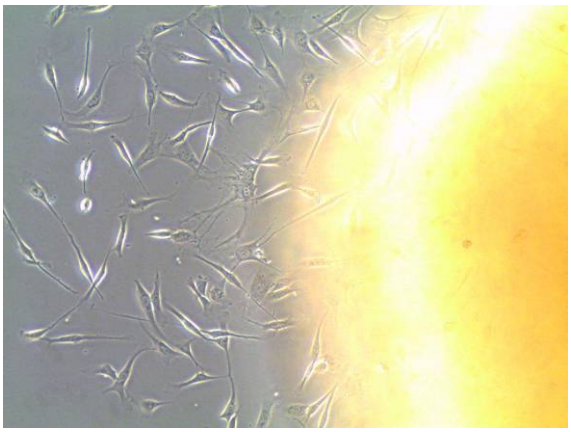

Figure 15. MDCK immunocytochemistry. MDCK cells staining characteristics for (a) H&E, (b) pancytokeratin, (c) vimentin, (d) E-cadherin, and (e) negative control. Original magnification of 40x.

a.

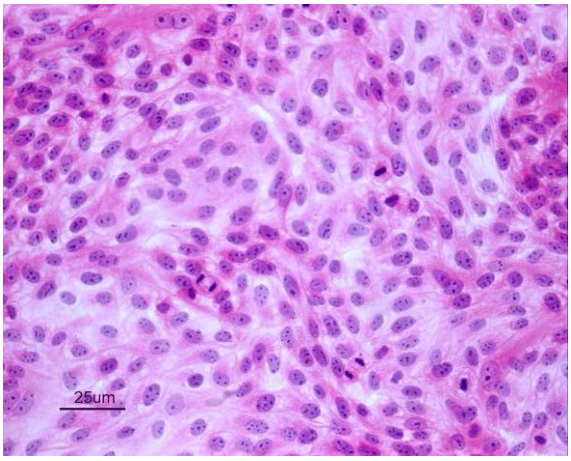

b.

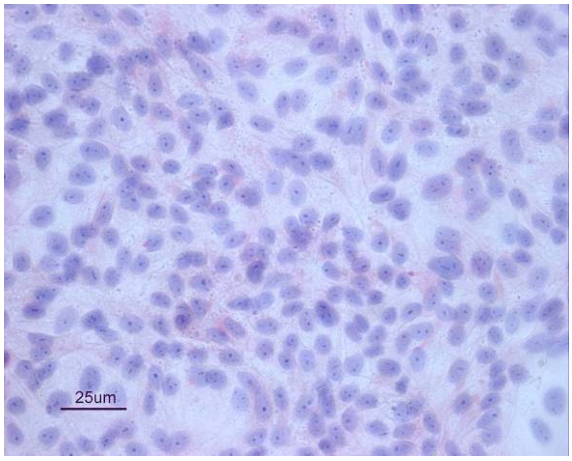

c.

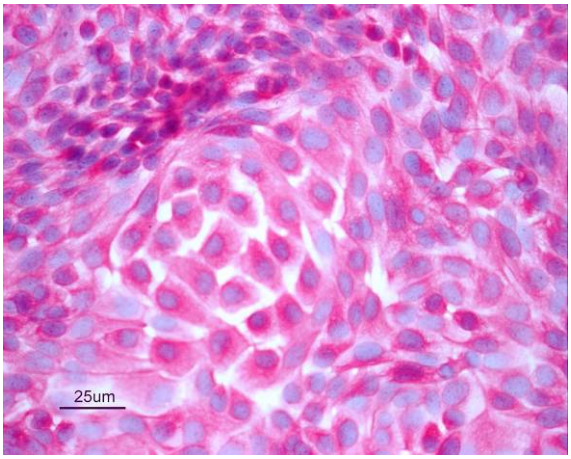

d.

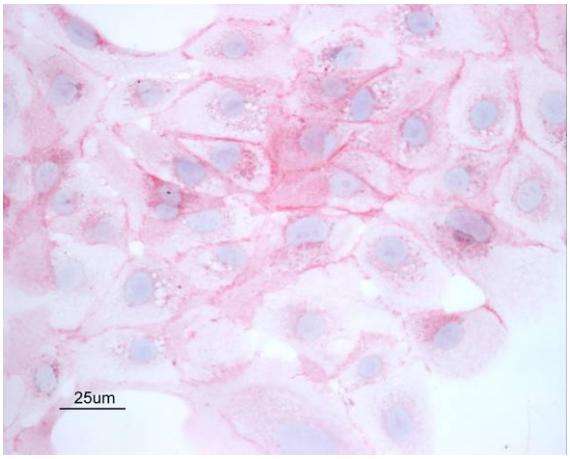

e.

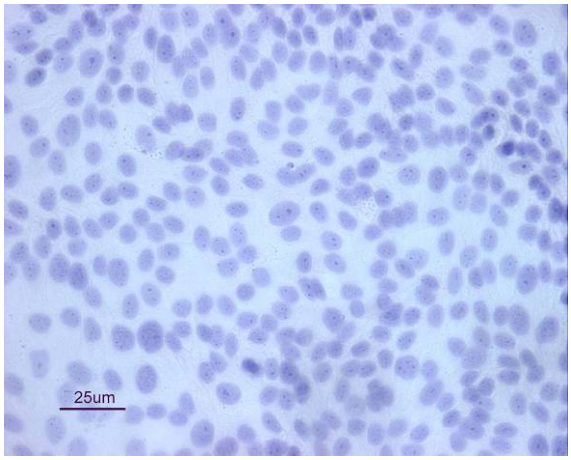

Figure 16. Presumed epithelial cells in Epilife. First passage presumed epithelial cells in Epilife from dog 2 showing staining characteristics for (a) H&E, (b) pancytokeratin, (c) vimentin, (d) E-cadherin, and (e) negative control. Original magnification of 40x.

a.

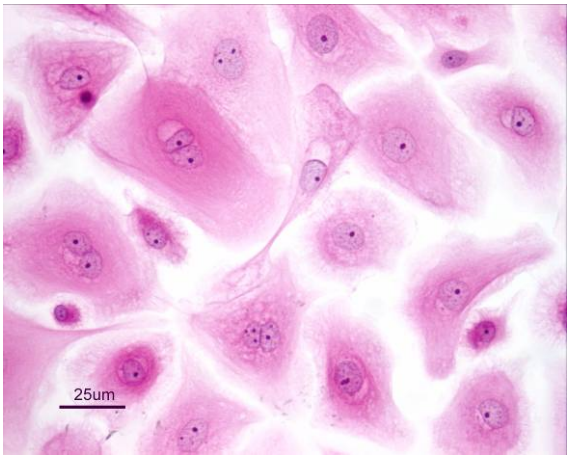

b.

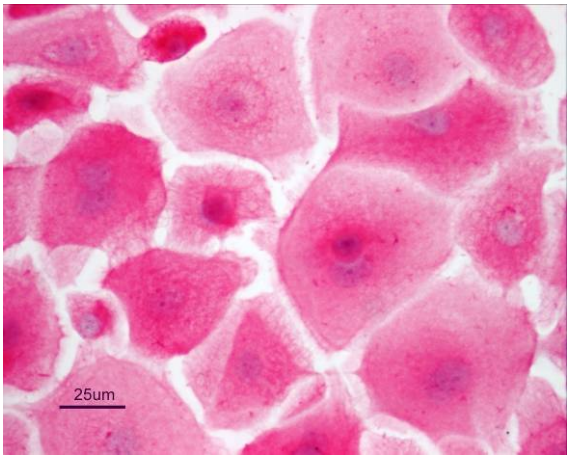

c.

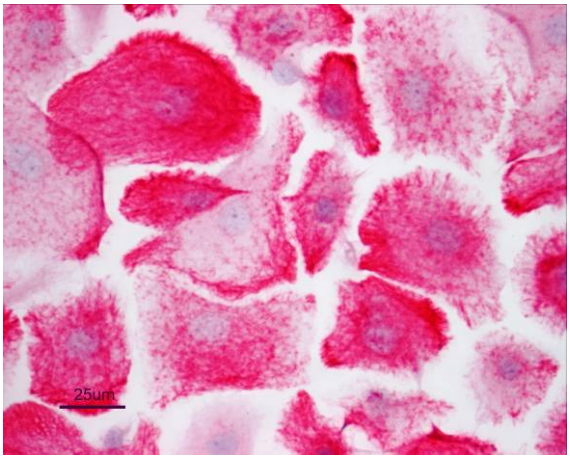

d.

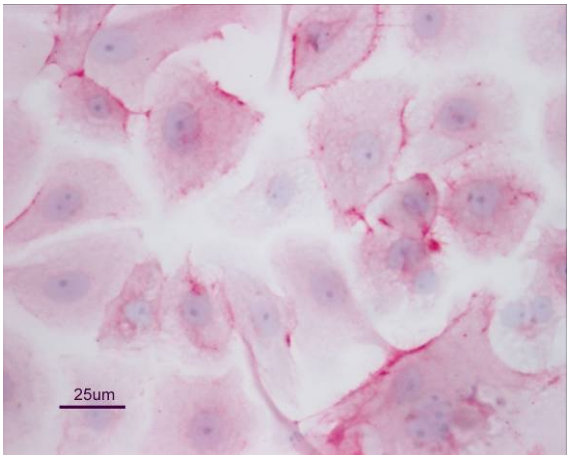

e.

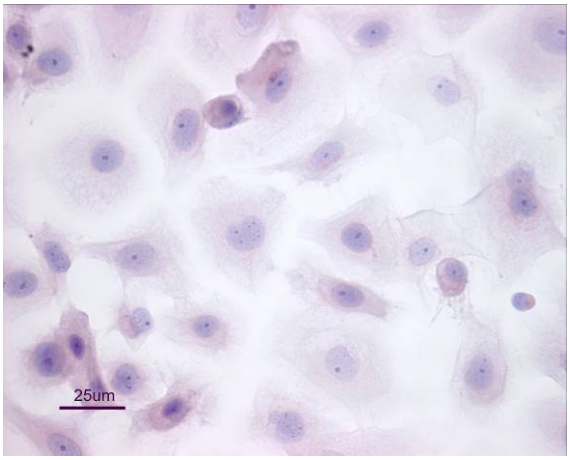

Figure 17. Presumed epithelial cells in DMEM, dog 2. First passage presumed epithelial cells in DMEM from dog 2, showing staining characteristics for (a) H&E, (b) pancytokeratin, (c) vimentin, (d) E-cadherin, and (e) negative control. Original magnification of 40x.

a.

b.

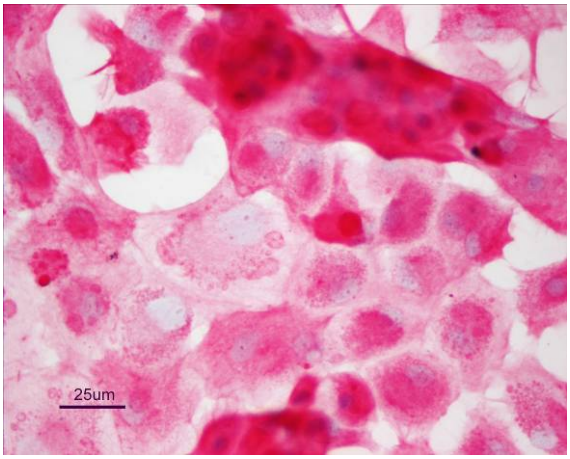

c.

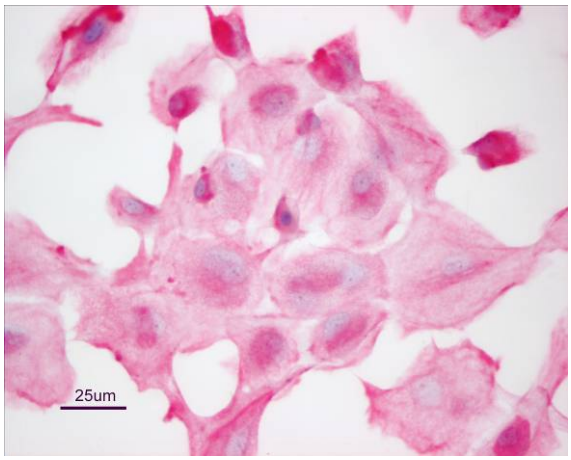

d.

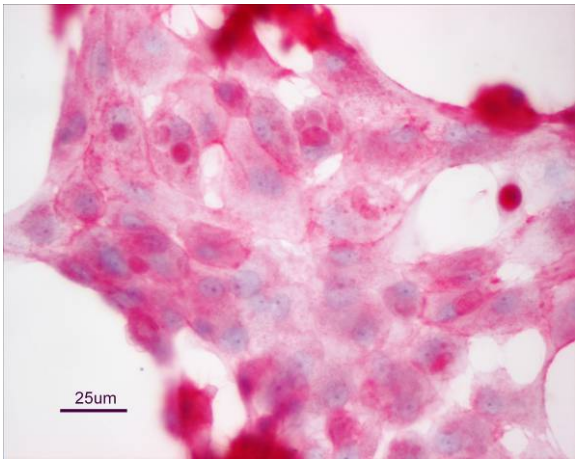

e.

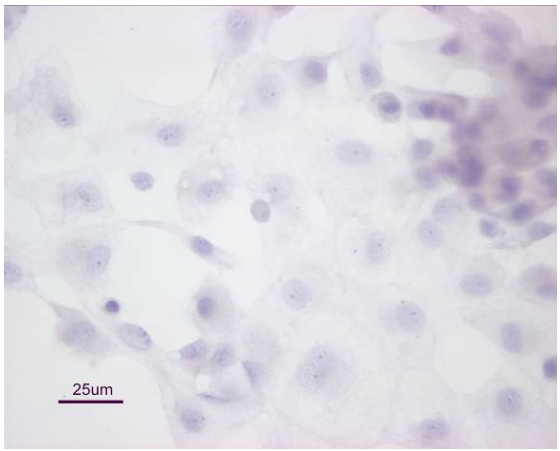

Figure 18. Presumed epithelial cells in DMEM, dog 1. First passage presumed epithelial cells in DMEM from dog 1, showing few cells on the slide, and staining characteristics for (a) H&E, (b) pancytokeratin, (c) vimentin, (d) E-cadherin, and (e) negative control. Original magnification of 40x.

a.

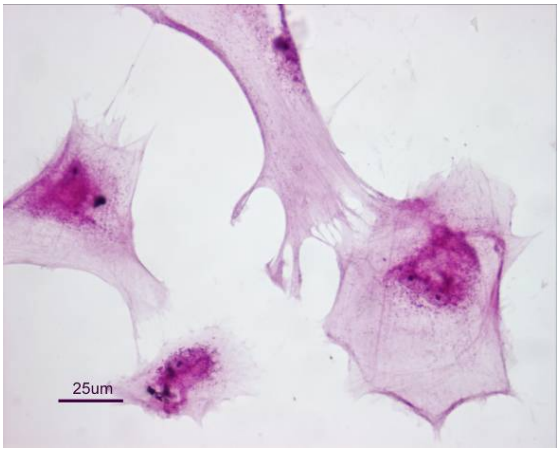

b.

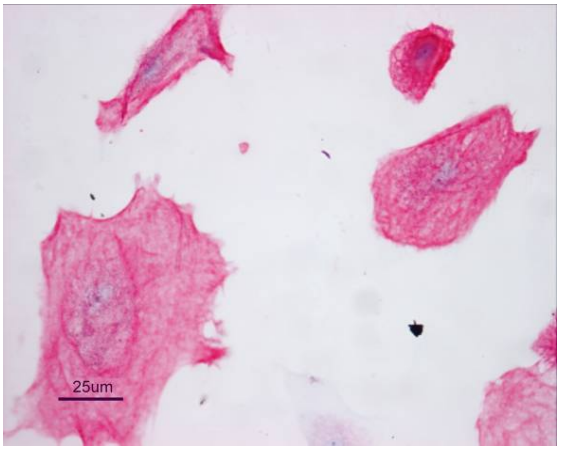

c.

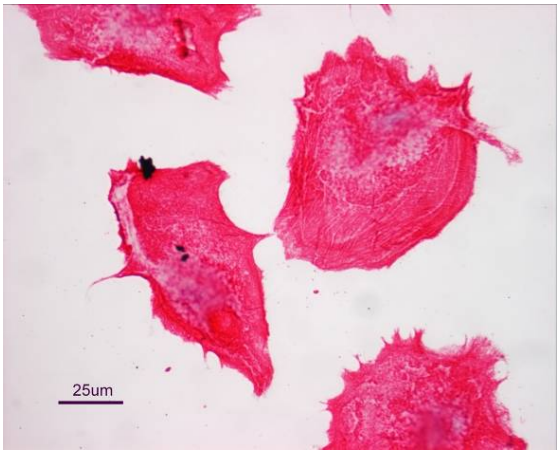

d.

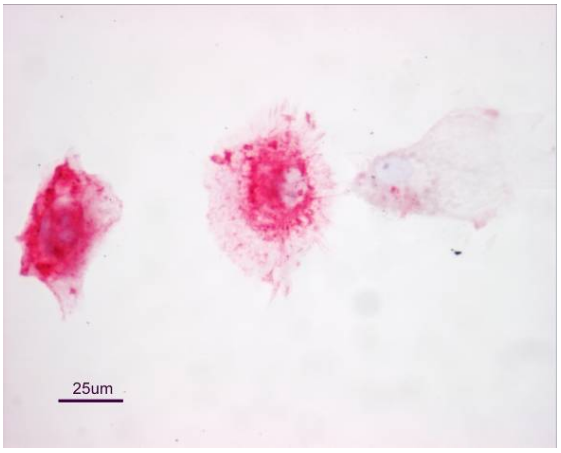

e.

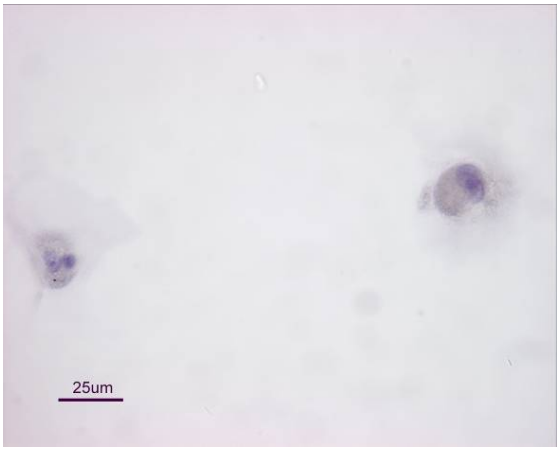

Figure 19. Primary explant tissue in DMEM. Primary explant tissue from DMEM from dog 3, showing staining characteristics for (a) H&E, (b) pancytokeratin, (c) vimentin, (d) E-cadherin, and (e) negative control. Original magnification of 40x.

a.

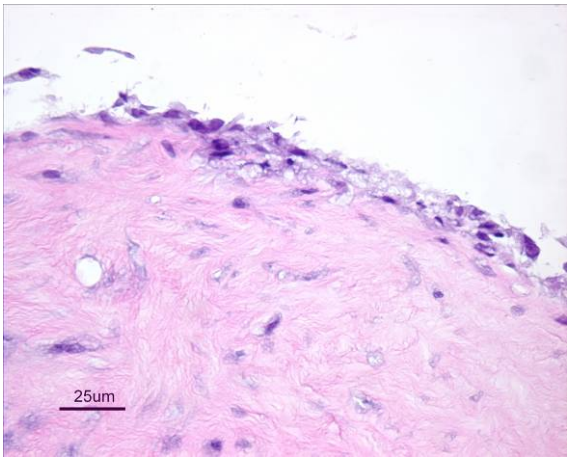

b.

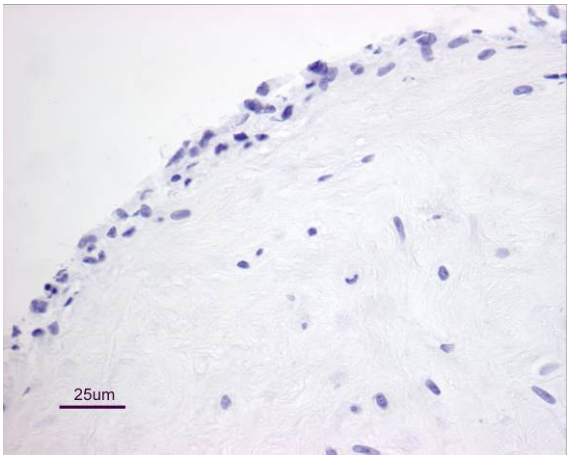

c.

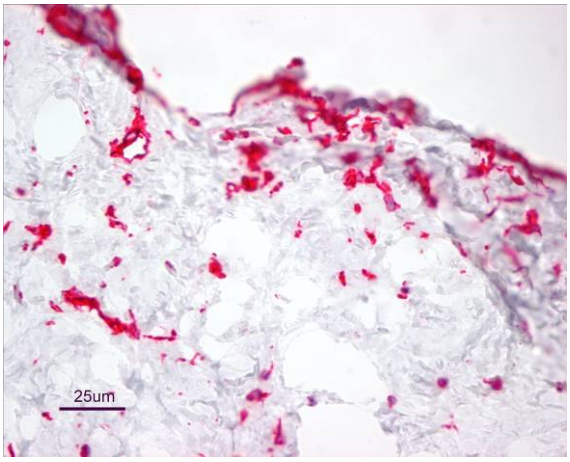

d.

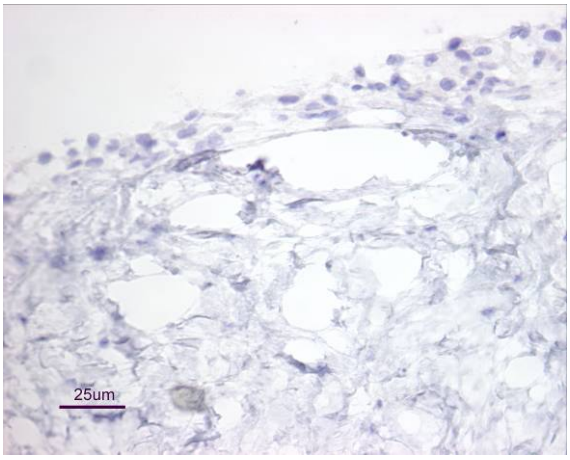

e.

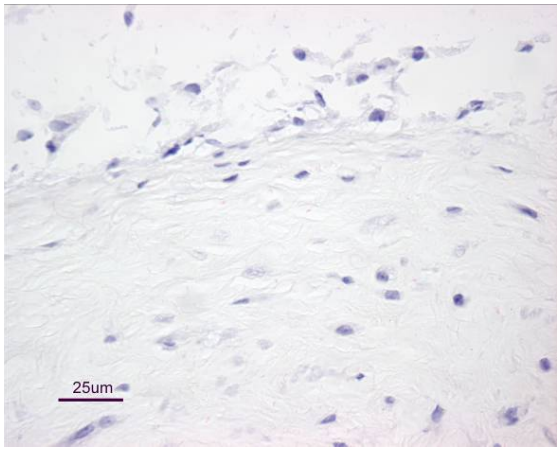

Figure 20. First passage explant cells in DMEM. First passage explant cells from DMEM for dog 3, showing staining for (a) H&E, (b) pancytokeratin, (c) vimentin, (d) E-cadherin, and (e) negative control. Original magnification of 40x.

a.

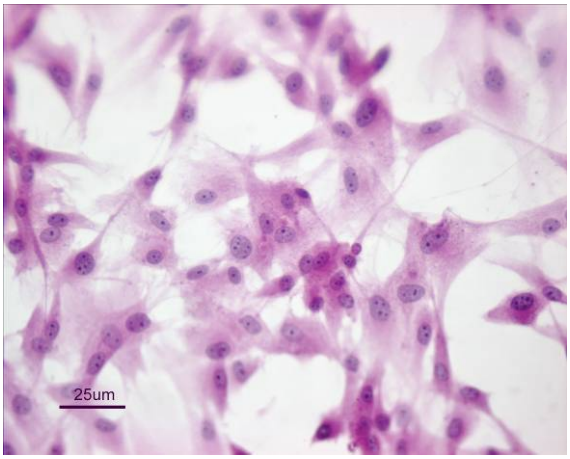

b.

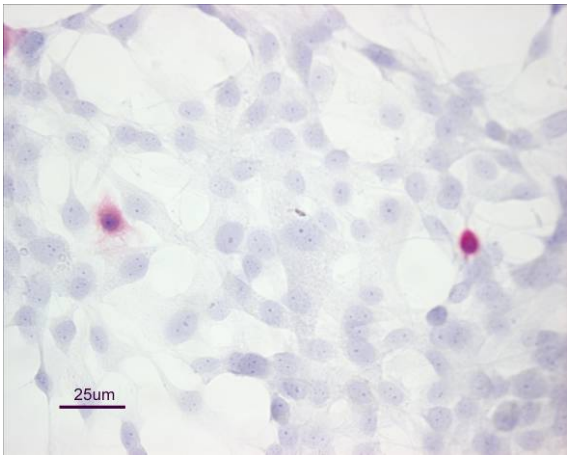

c.

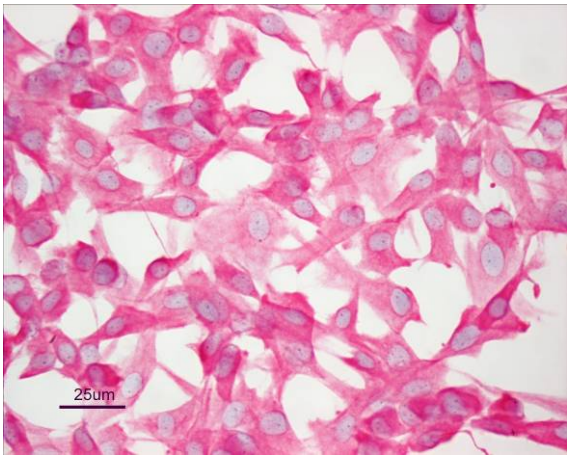

d.

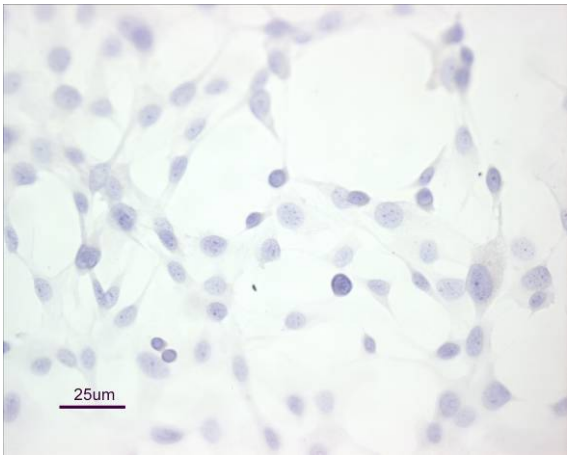

e.

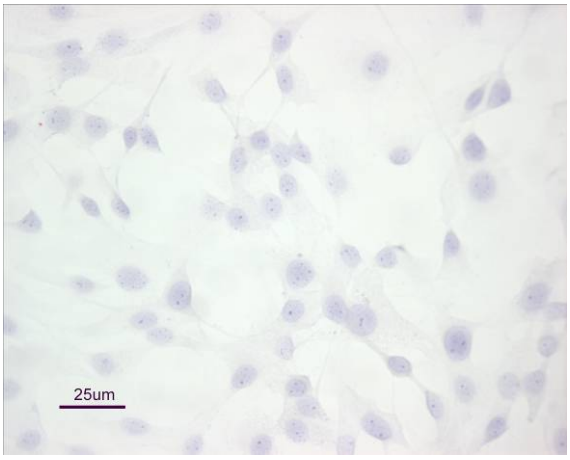

Figure 21. Primary explant tissue in Epilife. Primary explant tissue pieces in Epilife from dog 1, showing staining characteristics for (a) H&E, (b) pancytokeratin, (c) vimentin, (d) E-cadherin, and (e) negative control. Original magnification of 40x.

a.

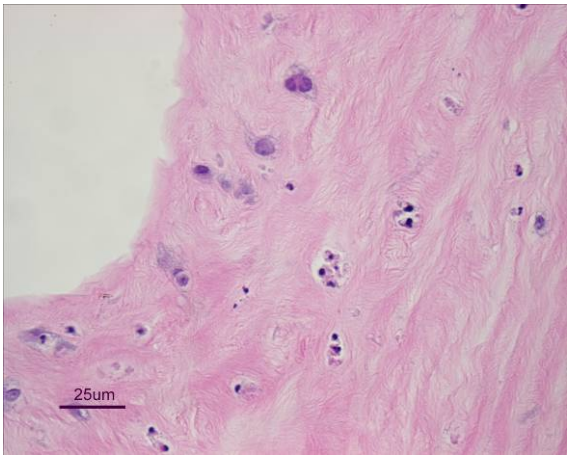

b.

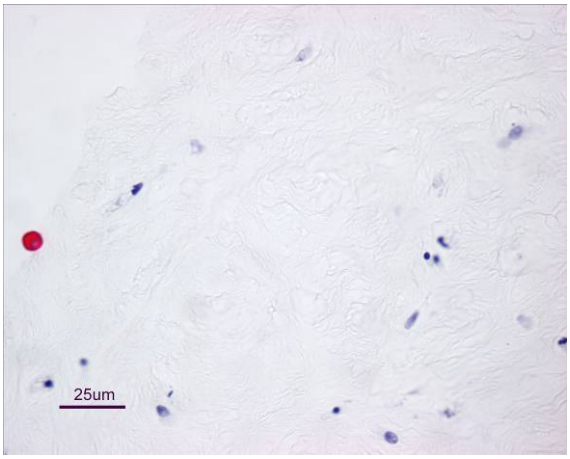

c.

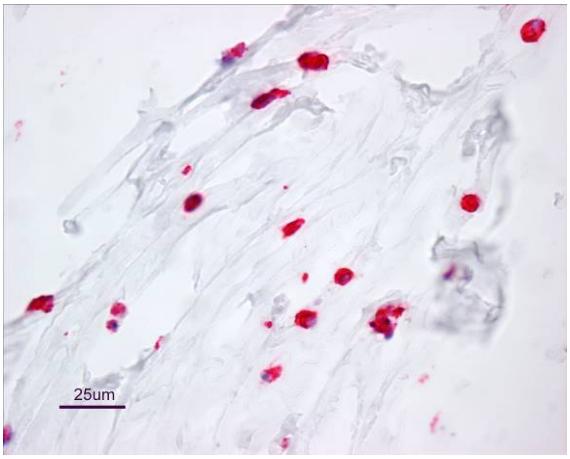

d.

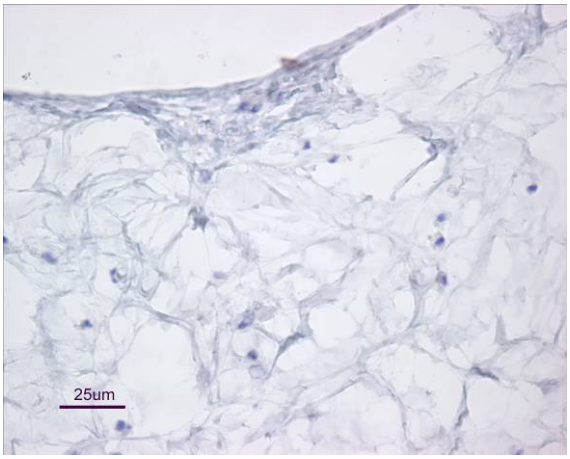

e.

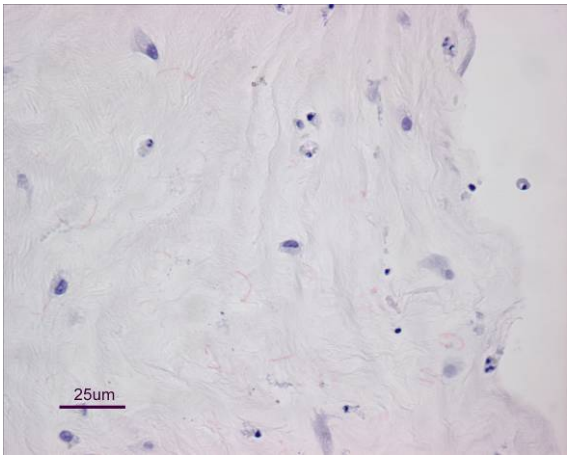

Figure 22. MDCK immunofluorescence. MDCK cells after staining with FITC-conjugated anti-ZO-1. (A) demonstrates the nuclear stain, and (b) shows a similar nuclear fluorescence and lack of cytoplasmic fluorescence with FITC illumination. The immunofluorescent staining technique was unsuccessful in identifying ZO-1 at the cell junctions. The bottom image merges the colors in (a) and (b).

a. b.

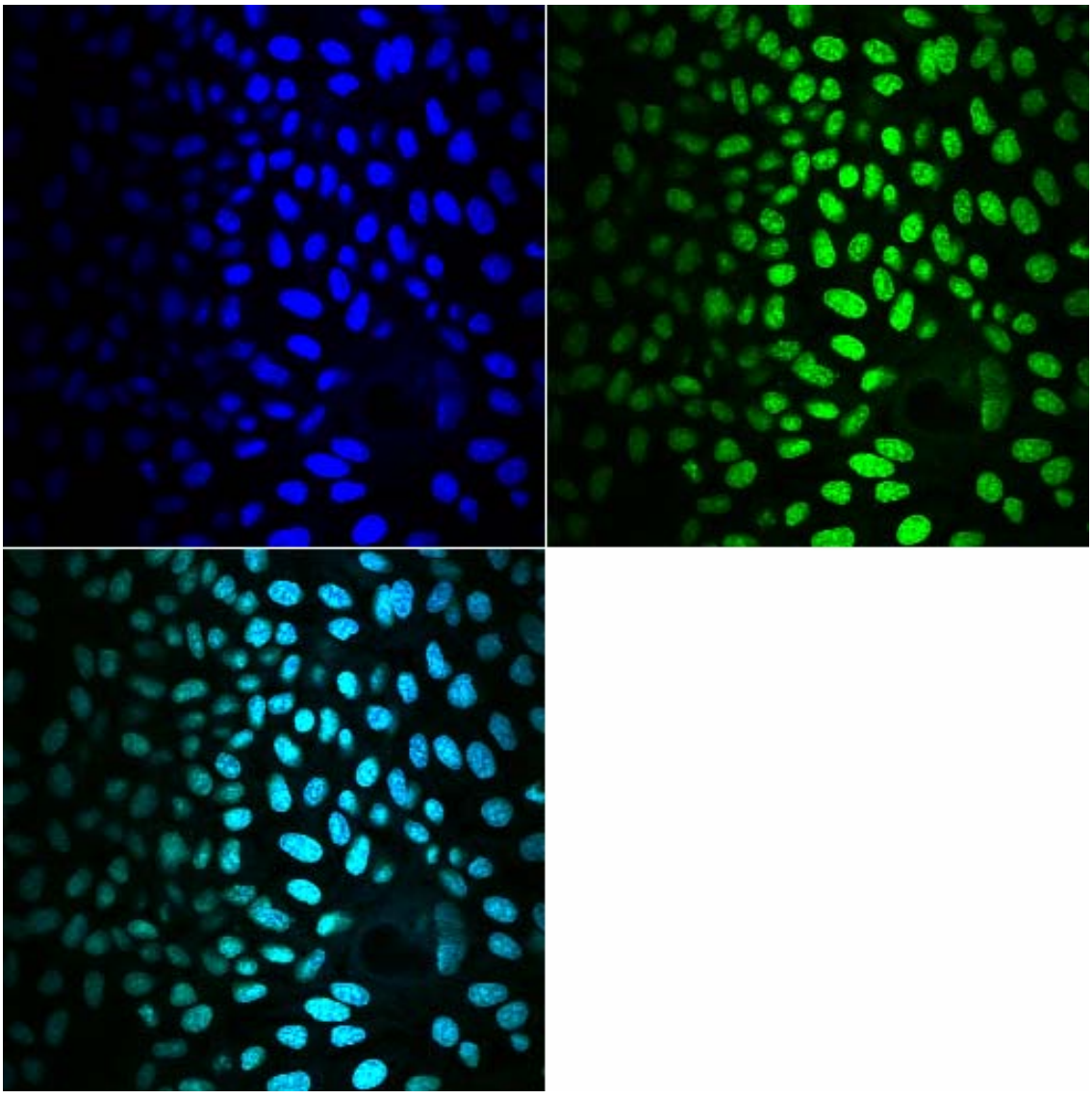

Figure 23. PCR gel electrophoresis from CK5 mRNA amplification. Bands produced from eletrophoresis of PCR amplification products of CK5 mRNA from cDNA of 3EE, 2SD, and MDCK samples. The lanes are labeled, the molecular weights of some of the markers are provided for reference, and the arrow indicates the bands of interest. The migration of the bands from 3EE and 2SD is similar, while that of the band from MDCK appears more rapid, suggestive of a smaller DNA fragment.

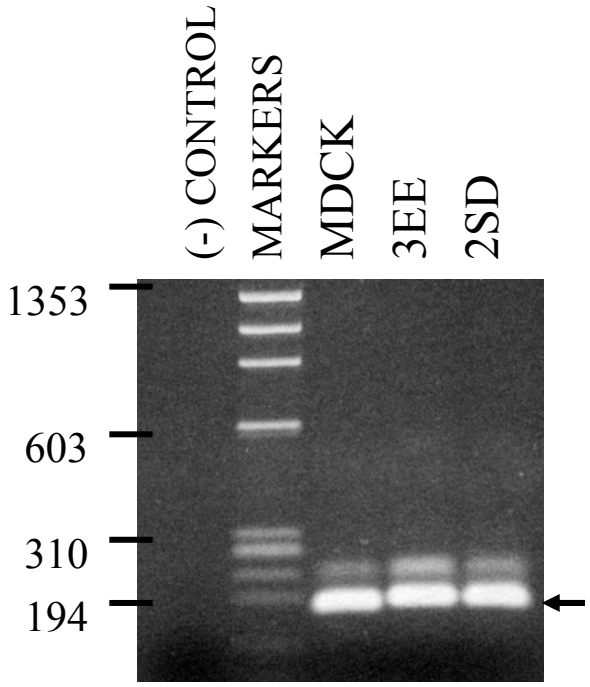

Table 1. Culture timeline.

Dog #	Treatment group	Label	Days to attachment	Days to passage	Days in culture until RNA lysis	Days in culture until Immunocytochemistry
1	Presumed epithelial in Epilife	1EE	1	11	14	14
1	Presumed epithelial in DMEM	1ED	1	10	14	14
1	Presumed epithelial in DMEM → Epilife	1ED→E (Day 14 start)	N/A	N/A	4	N/A
1	Explant in Epilife	1SE	No attachment	N/A	N/A	21
1	Explant in Epilife → DMEM	1SE→D (Day 21 start)	No attachment	N/A	N/A	N/A
1	Explant in DMEM	1SD	6	21	22	22
1	Explant in DMEM → Epilife	1SD→E (Day 22 start)	N/A	N/A	4	N/A
2	Presumed epithelial in Epilife	2EE	1	11	14	14
2	Presumed epithelial in DMEM	2ED	1	7	10	10
2	Presumed epithelial in DMEM → Epilife	2ED→E (Day 10 start)	N/A	N/A	4	N/A
2	Explant in Epilife	2SE	No attachment	N/A	N/A	19
2	Explant in Epilife → DMEM	2SE→D (Day 19 start)	8	N/A	N/A	N/A
2	Explant in DMEM	2SD	6	19	21	21
2	Explant in DMEM → Epilife	2SD→E (Day 21 start)	N/A	N/A	4	N/A
3	Presumed epithelial in Epilife	3EE	1	11	14	14
3	Presumed epithelial in DMEM	3ED	1	10	14	14
3	Presumed epithelial in DMEM → Epilife	3ED→E (Day 14 start)	N/A	N/A	4	N/A
3	Explant in Epilife	3SE	No attachment	N/A	N/A	21
3	Explant in Epilife → DMEM	3SE→D (Day 21 start)	No attachment	N/A	N/A	N/A
3	Explant in DMEM	3SD	6	21	22	22
3	Explant in DMEM → Epilife	3SD→E (Day 22 start)	N/A	N/A	4	N/A

Table 2. RNA concentrations.

ID	A260/ A280 ratio	[RNA] ug/ul	Total µg RNA recovered	ug RNA to cDNA
1EE	1.4502	0.045	3.6	0.36
2EE	1.6453	0.043	3.44	0.34
3EE	1.8102	0.053	4.24	0.43
1ED	1.4852	0.080	6.4	0.64
2ED	1.8788	0.177	14.16	1.00
3ED	1.7755	0.096	7.68	0.77
1SD	1.5354	0.324	25.92	1.00
2SD	1.5778	0.481	38.48	1.00
3SD	1.6022	0.453	36.24	1.00
1EDE	1.3792	0.017	1.36	0.13
2EDE	1.4660	0.084	6.72	0.68
3EDE	1.5652	0.033	2.64	0.27
1SDE	1.7354	0.158	12.64	1.00
2SDE	1.5356	0.419	33.52	1.00
3SDE	1.5569	0.414	33.12	1.00
MDCK	1.5913	0.660	52.8	1.00

Table 3. Comparative C_T analysis concentrations.

Canine corneal sample	Mean C_T CK5 mRNA	Mean C_T 18S rRNA	ΔCt	Mean ΔCt
1EE	16.43	19.24	-2.81	
2EE	16.18	19.08	-2.90	-3.01
3EE	16.19	19.50	-3.31	
1ED	18.29	18.50	-0.21	
2ED	17.13	18.39	-1.26	-1.02
3ED	16.87	18.45	-1.58	
1EDE	21.30	21.00	0.30	
2EDE	17.67	18.51	-0.84	
3EDE	19.38	20.11	-0.73	
1SD	28.15	18.81	9.34	
2SD	19.47	18.53	0.95	3.87
3SD	19.70	18.36	1.33	
1SDE	29.31	18.62	10.68	
2SDE	21.22	18.29	2.92	
3SDE	23.13	18.99	4.14	

Table 4. Associations between cell type with growth media and CK5 mRNA expression.

CK5 mRNA was up regulated by a factor of 3.97 when EE was compared with ED. However, when EE was compared with SD, the results were not reliable due to a very wide CI for the Relative Expression Ratio.

Growth Media Compared	Target Gene	House Keeping Gene	Relative expression Ratio (95% CI)	P-Value
EE vs ED	CK5 mRNA	18S rRNA	3.97 (2.85 to 7.29)	0.033
EE vs SD	CK5 mRNA	18S rRNA	118 (16 to 6538)	0.064

Chart 1. CK5 mRNA PCR amplification of serial dilutions cDNA from canine corneal sample 3EE. The x-axis represents the cycle, and the y-axis provides the amplification values. The threshold cycle is represented by the bold horizontal line.

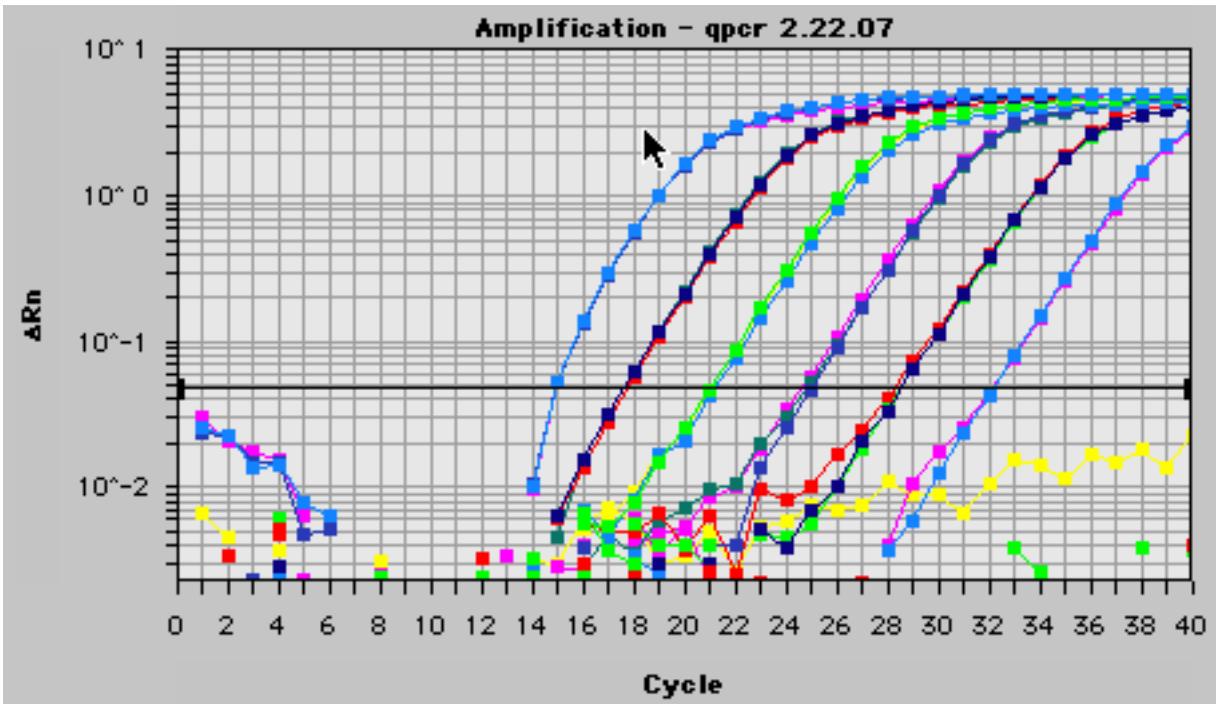

Chart 2. Amplification efficiency of CK5 mRNA from canine cornea.

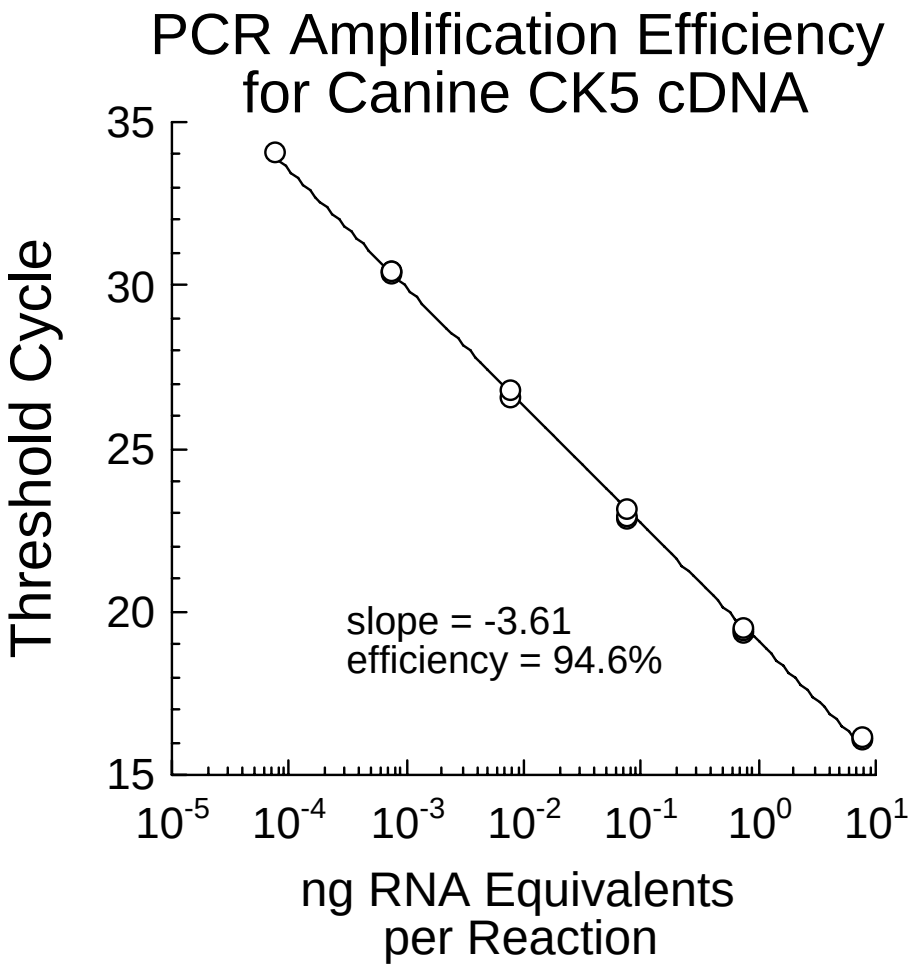

Chart 3. CK5 mRNA PCR amplification from canine corneal samples. The x-axis represents the cycle, and the y-axis provides the amplification values. The threshold cycle is represented by the bold horizontal line.

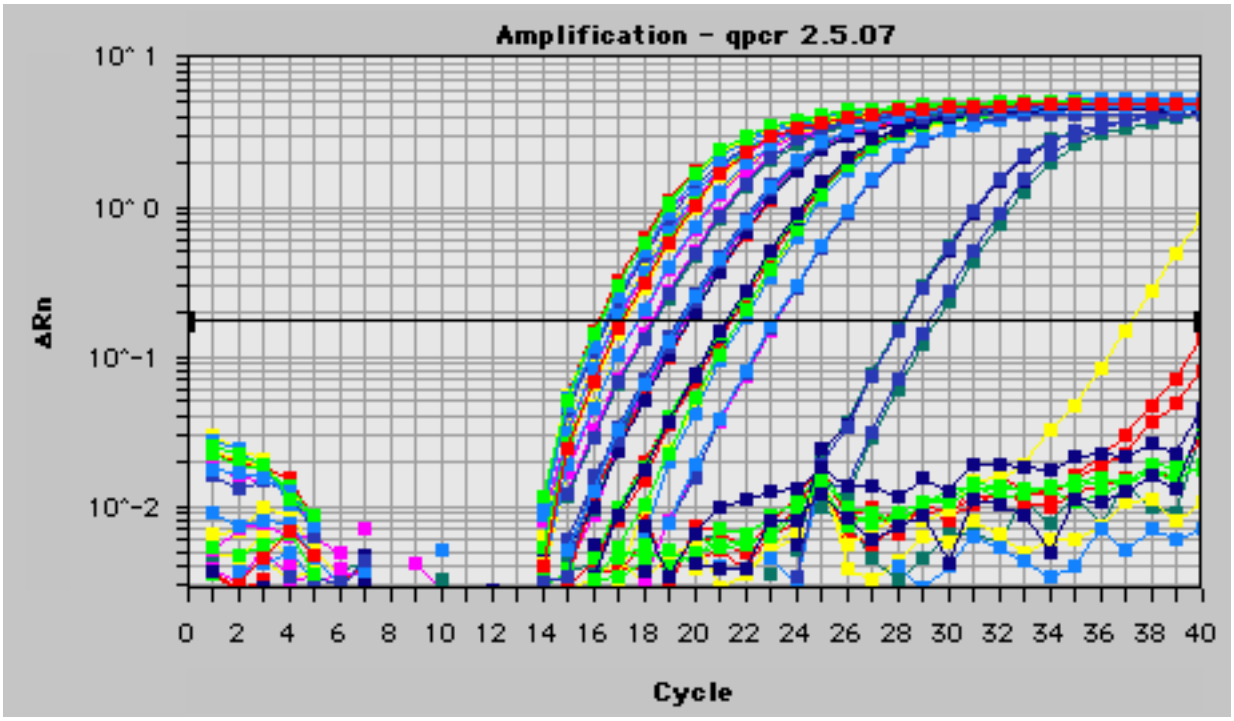

Chart 4. Mean C_T values for CK5 mRNA amplification from canine cornea. The mean C_T values for CK5 mRNA amplification from the three replicates of each of the corneal samples are shown here.

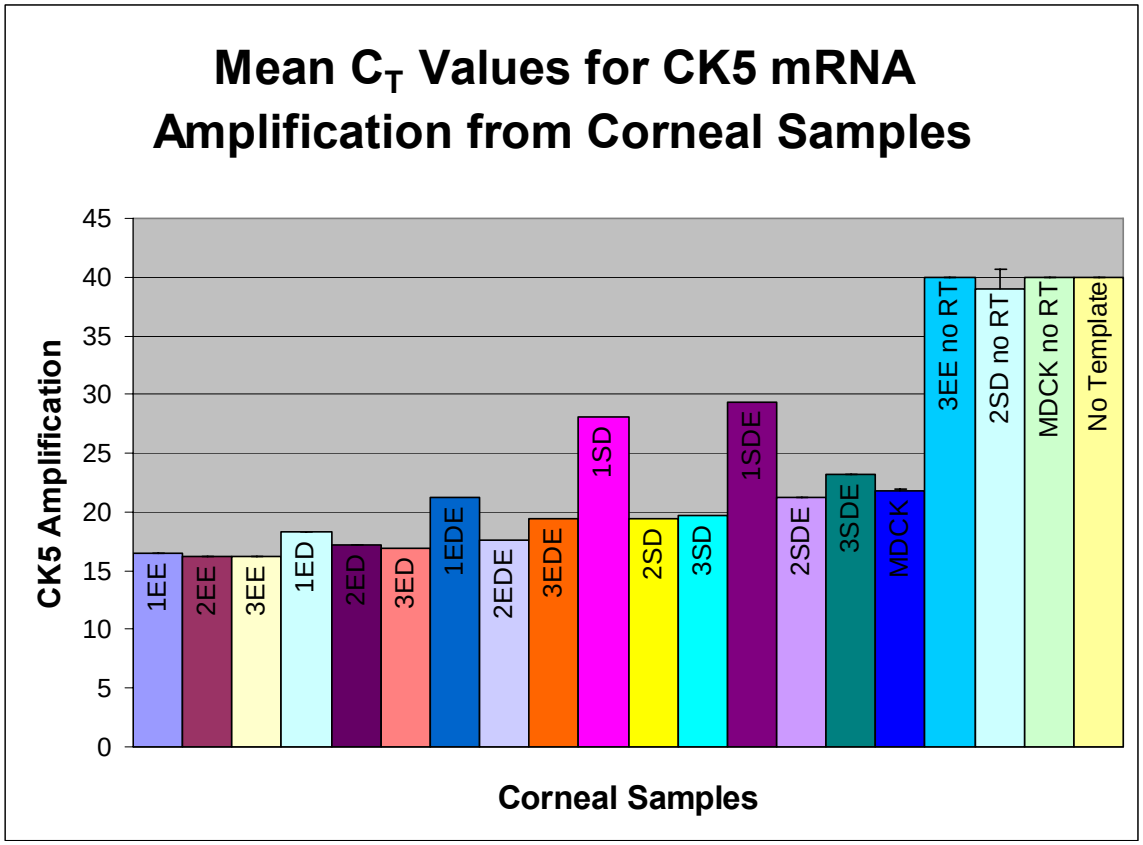

Chart 5. Dissociation curves of PCR products from canine corneal samples. Dissociation curves from PCR amplification products from (a) the 3EE amplification efficiency sample, and (b) the routine corneal samples. Temperature is on the x-axis and the slope of the dissociation curve is on the y-axis. The melting temperature is 85ºC.

a.

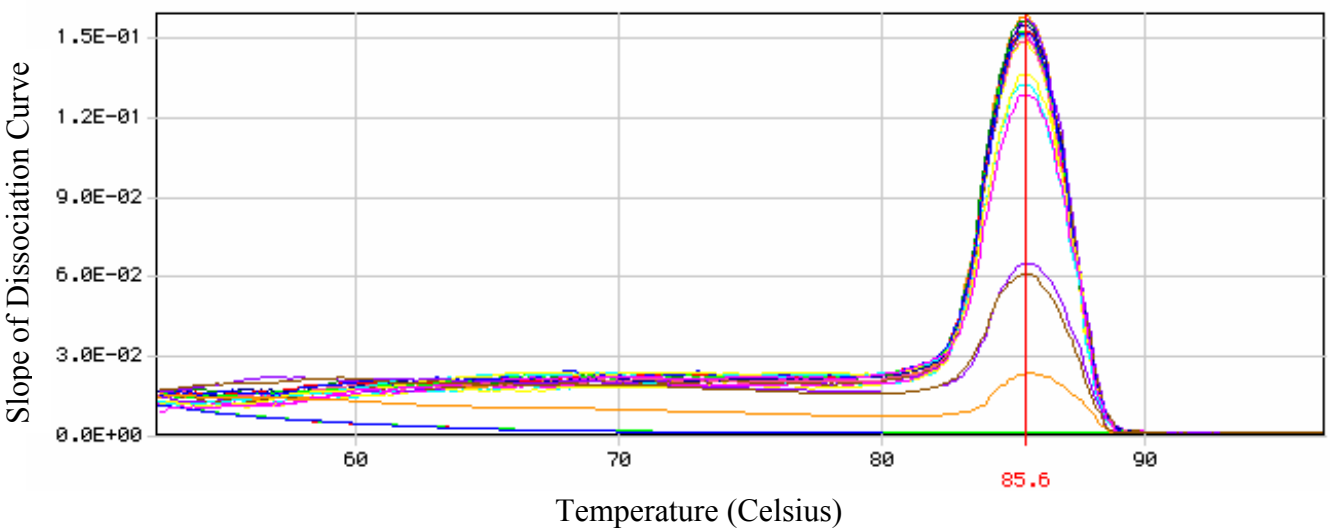

b.

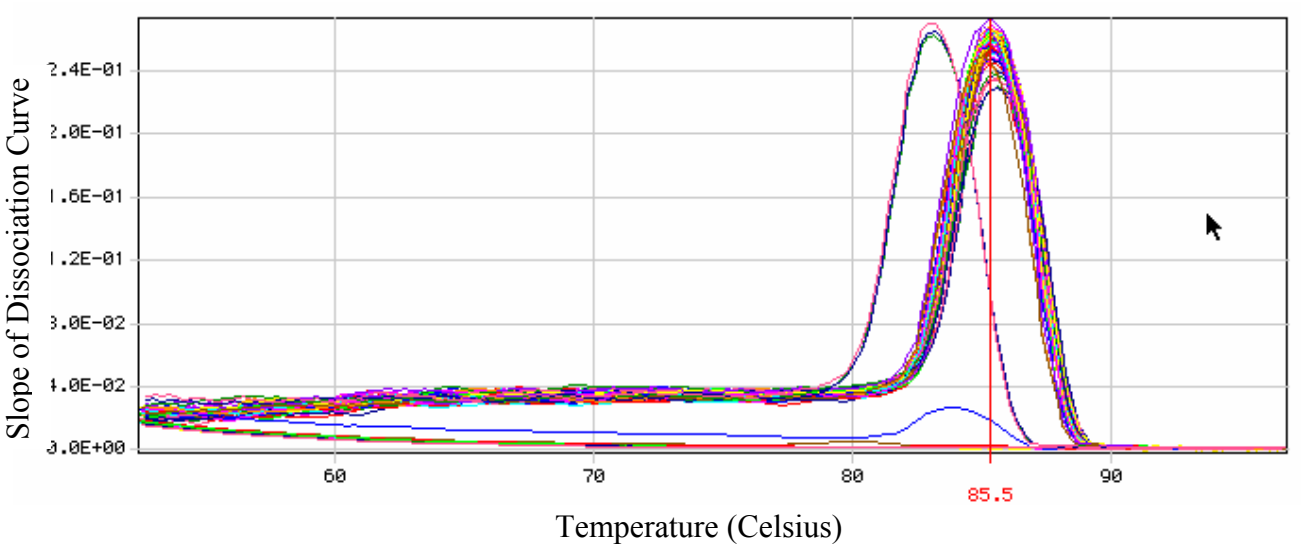

Chart 6. Dissociation curve of PCR product from MDCK cells.

Dissociation curve from the products of PCR amplification of the MDCK cells. Temperature is on the x-axis and the slope of the dissociation curve is on the y-axis. The melting temperature is 83ºC.

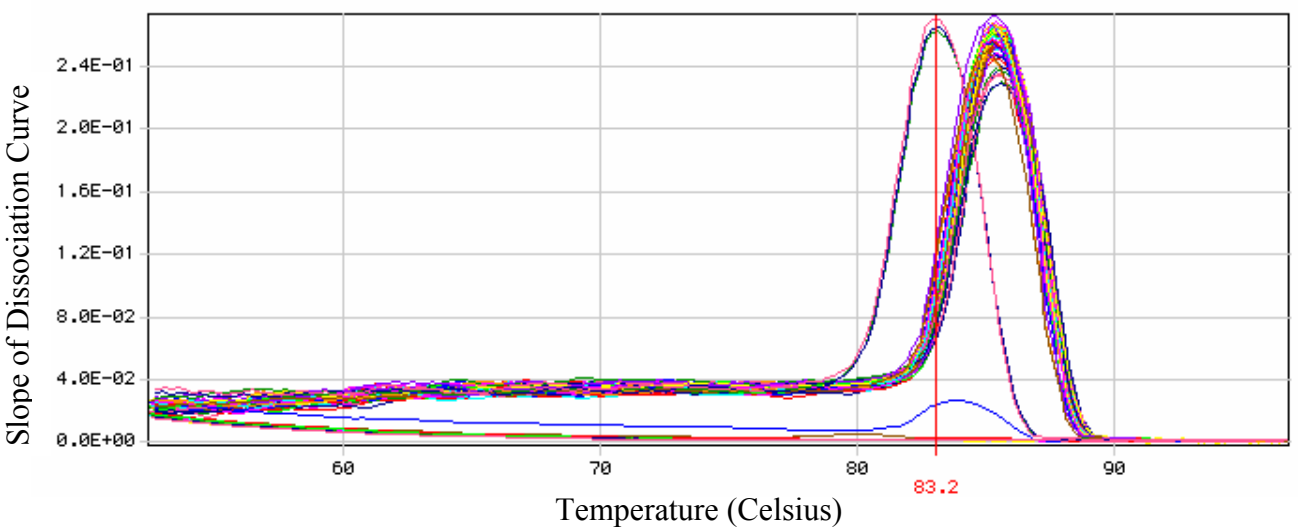

Chart 7. ΔC_T values from canine cornea. The chart shows the ΔC_T values for the corneal samples, demonstrating the differences between amplification of CK5 mRNA and 18S rRNA.

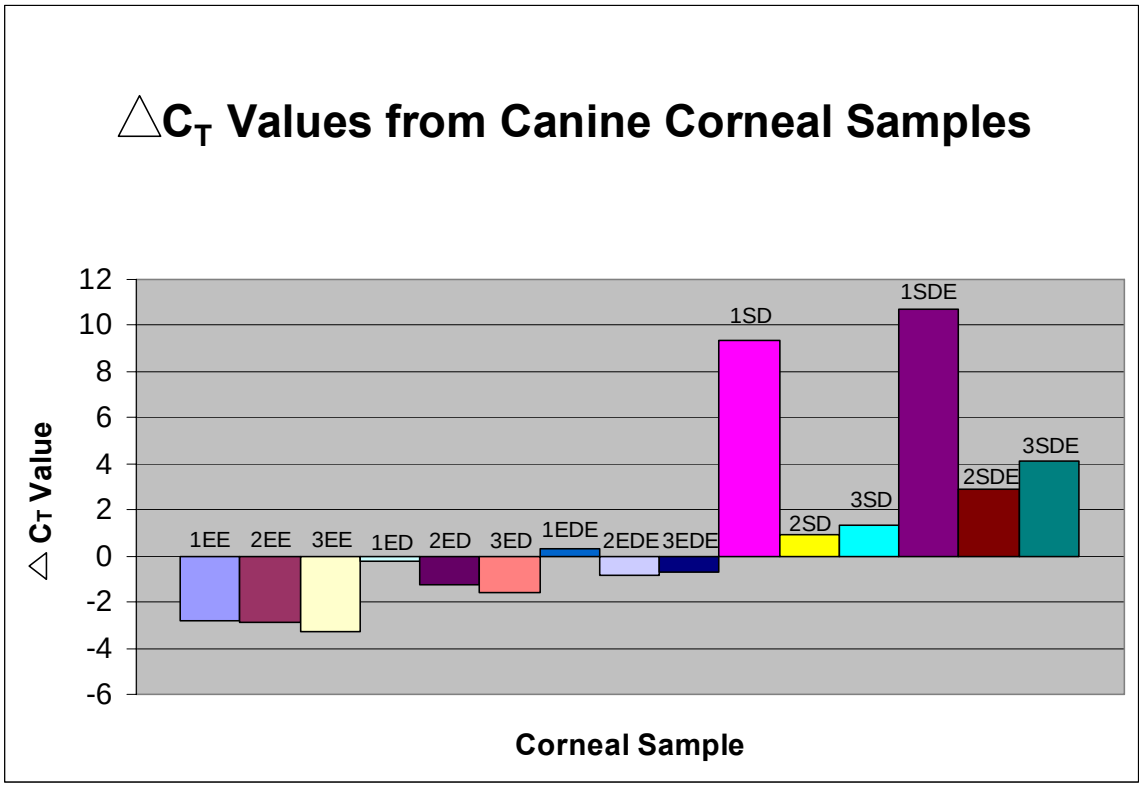

Chart 8. Relative expression of CK5 mRNA from canine corneal samples. The chart demonstrates that the relative expression of CK5 mRNA in EE group is up-regulated by a factor of 3.97 over the ED group.

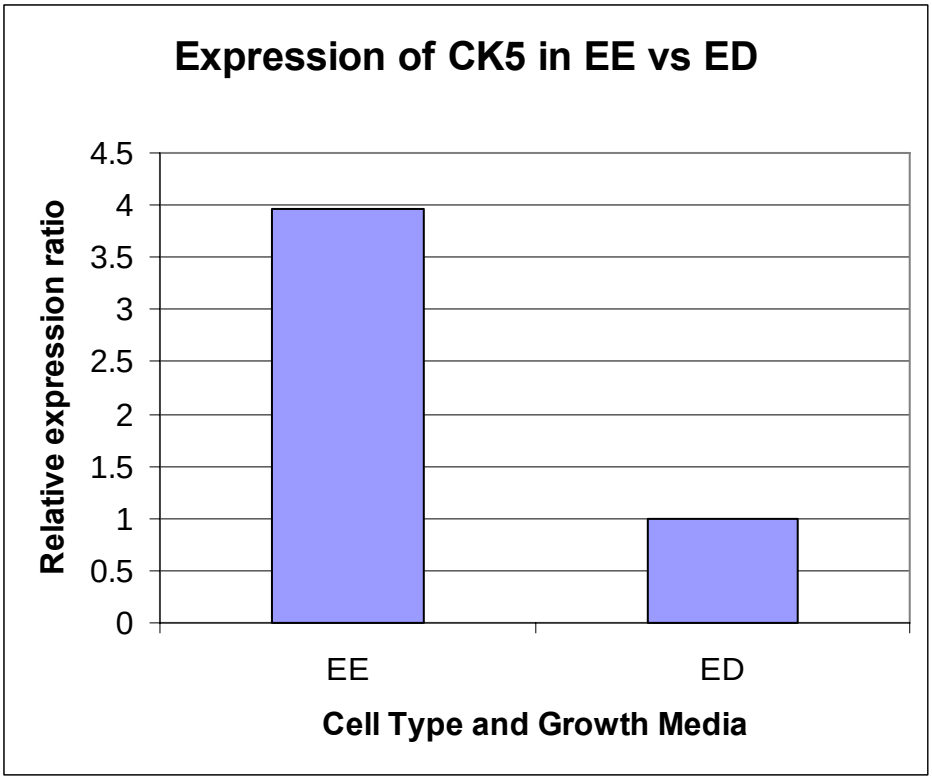

CHAPTER IV. DISCUSSION

Routine H&E of primary corneal samples obtained by superficial keratectomies revealed the expected appearance of stratified squamous epithelium overlying corneal stroma. Pancytokeratin and E-cadherin staining occurred in the stratified squamous epithelial layers, but not in the stromal cells, while vimentin stain uptake only occurred in stromal cells. Post-trypsinization, immunohistochemistry of the corneal tissues revealed that most of the epithelial cells had been released from the underlying stroma. The stromal cells stained positively for vimentin, and rare detached epithelial cells stained positively for pancytokeratin and E-cadherin. The observed staining characteristics were expected, based on previous reports of the staining characteristics of these antibodies in corneal tissues.[13,26,66,68,70]

Starting one week after culture commencement, primary corneal samples cultured from dog 2 consistently demonstrated a more rapid rate of growth when compared to cultures from dogs 1 and 3. There was no obvious explanation for this since ophthalmic examinations were normal in all three dogs, the eyes were treated the same at the time of sampling, and the culture environments were similar. Post-mortem physical examination on all three dogs revealed no evidence of systemic disease, and all three dogs were young adult male intact pit bull terrier mixes. However, it is possible that dog 2 was healthier than the other two animals, which may have influenced initial cell growth rates in culture.

Initially suspended cells, presumed and determined to be predominantly epithelial, began adhering to the culture plates within 24 hours of culture commencement, regardless of the medium. Cell morphologies in both media included polyhedral, fusiform, stellate, and round cells. These primary presumed epithelial cells approached confluence and were therefore passaged a mean of 2 days earlier when cultured in DMEM with FBS as compared to Epilife®. Additionally, while first passage cells in DMEM with FBS approached confluence within a few days, first passage cells in Epilife® failed to reach confluence prior to processing. There were no distinctive differences among cell morphologies observed for the presumed epithelial cells during primary or first passage

cultures in either medium (Figures 5-11). The decision to process the first passage cells in Epilife®, despite marked subconfluence, was made based on preliminary studies in which canine corneal epithelial cells did not thrive beyond two weeks in culture. For the cultures in which DMEM with FBS was changed to Epilife®, cell numbers progressively declined during the four days after the medium change was made. Since the cells were nearly two weeks of age and approaching confluence when the medium change was made, it is likely that the cells were undergoing apoptotic cell death despite the medium change, rather than in response to it. Another possibility is that Epilife® does not provide adequate nutrients and growth factors to support an aging cell culture population.

In contrast to the rapid attachment of the presumed epithelial cells, the tissue pieces that contained predominantly stromal cells required at least 6 days to successfully adhere to the plates when cultured in DMEM with FBS. Thereafter, densely packed fusiform cells, with occasional polyhedral and stellate morphologies, were observed progressively explanting from the tissues (Figure 10). After passaging, cells remained fusiform to stellate, consistent with the morphologies of keratocytes and fibroblasts.

Throughout the time in culture, the tissue pieces containing predominantly stromal cells cultured in Epilife® medium failed to adhere to the plates. As demonstrated in Figure 21, viable cells were still present in the tissues, with positive vimentin staining and predominantly negative pancytokeratin and E-cadherin staining. The immunocytochemical staining properties support the prediction that these post-trypsinized tissues contained predominantly stromal cells. Epilife® medium may have inhibited initial attachment of the corneal tissues to the culture plates, or the medium may have inhibited migration, growth, and proliferation of the stromal cells. In the explant culture from dog 2, in which the Epilife® medium was changed to DMEM with FBS, the tissue eventually attached to the culture plate, and cells were observed explanting from the tissue. This supports the idea that Epilife® medium may not provide adequate nutrients or growth factors to facilitate attachment of non-epithelial tissues and/or proliferation of non-epithelial cells.

Madin-Darby canine kidney cells were used as a reference for the immunocytochemical staining characteristics of the culture cells. These cells were weakly pancytokeratin and E-cadherin positive, and they were strongly vimentin positive. Though vimentin staining typically occurs in cells of mesenchymal cell origin *in vivo*, several *in vitro* investigations have documented the presence of positive vimentin staining in cells of epithelial origin.[25,33,86,90] MDCK cells and rabbit corneal epithelial cells have been recognized as cells of epithelial origin that express vimentin *in vitro*.[25,33,86,90] Investigators speculate that the transition from an epithelial to a myoepithelial phenotype *in vitro* results in altered expression of proteins.[15] Due to the prolonged existence of MDCK cells *in vitro*, it is also possible that these cells have undergone mutations that resulted in the staining qualities observed in this study.[86,90] For example, certain phenotypes of dedifferentiated MDCK cells have been recognized to demonstrate decreased cytokeratin and E-cadherin expression with increased vimentin expression *in vitro*.[86,90]

The immunocytochemical staining characteristics were similar for the first passage presumed epithelial cells, regardless of medium. Cells stained positively for pancytokeratin, vimentin, and E-cadherin, as shown in Figures 16-17. Figure 18 shows that few cells (<5% confluence) were present on the immunocytochemical slides of the epithelial cells in DMEM with FBS from dogs 1 and 3 (1ED and 3ED). This likely resulted from improper fixation or processing, as 30% confluence of cells was observed prior to fixation for both dogs, and cultures were fixed simultaneously. For all three dogs, the positive staining for pancytokeratin and E-cadherin indicated that these initially suspended cells in DMEM with FBS and Epilife® were predominantly epithelial, as expected. Since epithelial cells from the tissue sections were negative for vimentin staining and the stromal cells were positive, it is possible that a presence of stromal cells in these predominantly epithelial cultures was the cause of positive vimentin staining in these cultures. However, since nearly all cells stained positively for all three antibodies, a more likely conclusion is that canine corneal epithelial cells in culture express certain mesenchymal proteins, including vimentin, which is similar to the observations in MDCK cells and rabbit corneal epithelial cells previously described.[25,33,86,90]

Immunohistochemistry of the tissue pieces containing predominantly stromal cells from DMEM with FBS and Epilife® revealed the expected staining characteristics. Vimentin staining was positive, and pancytokeratin and E-cadherin staining were negative. Rare epithelial cells in these tissues demonstrated positive pancytokeratin staining. Immunocytochemistry of the first passage explanted cells from DMEM cultures showed positive vimentin staining and negative pancytokeratin and E-cadherin staining. Since tissues in Epilife® did not adhere to the culture plates and no cells explanted, immunocytochemistry was not performed on these cultures.

Immunofluorescence for ZO-1 was unsuccessful. Fluorescence near epithelial cell junctions was the expected result, but this was not observed in either MDCK or canine corneal cells. For the cultured canine corneal epithelial cells, it is also possible that cells failed to develop the appropriate intercellular desmosomal junctions for stimulation of expression of ZO-1.[69] Additionally, corneal research in rats has identified that ZO-1 expression is concentrated in the superficial corneal layers.[69] If the corneal epithelial cells cultured from dogs in this study were predominantly basal or wing cells, then ZO-1 expression may not have been recognized with immunofluorescence.[69] However, based on the lack of observation of fluorescence in both the MDCK cells and the corneal cells, it is more likely that there was a flaw in technique rather than an actual lack of expression of ZO-1. The fixation technique may have masked expression of ZO-1, the length of time between fixation and immunofluorescence may have altered the results, the FITC-conjugated ZO-1 antibody may have been defective, or the equipment may not have been operating properly.[101] The study design allowed only one attempt for detection of immunofluorescence to ZO-1, so the failure of fluorescence was not further investigated.

To further characterize the biochemical qualities of the cells cultured, quantitative real time RT-PCR was performed to amplify expression of CK5 mRNA. Cytokeratin 5 is known to be expressed in basal corneal epithelial cells of other species as well as other non-corneal tissues in dogs.[6,26] Results of PCR of the predominantly epithelial cultures revealed that cells grown in Epilife® expressed more CK5 mRNA than similar cells grown in DMEM with FBS. Expression of CK5 mRNA in epithelial cells cultured in

Epilife® medium was up-regulated by a factor of 3.97 when compared to epithelial cells cultured in DMEM with FBS. Epilife® medium may promote cells to retain the epithelial characteristic of CK5 mRNA expression better than DMEM with FBS. Alternatively, there may have been less selection for epithelial cells in the DMEM cultures, allowing for increased growth of stromal cells and fibroblasts. Since stromal cells and fibroblasts are not of epithelial origin, they should not express CK5, which could explain the relative decreased expression of CK5 mRNA in the DMEM cultures. However, some expression of CK5 mRNA was observed in the predominantly stromal cultures from DMEM with FBS. Either epithelial contamination of these cultures was sufficient to allow for detection and amplification of CK5 mRNA, or cultured canine corneal stromal cells express CK5 mRNA. When the expression of CK5 mRNA in epithelial cells in Epilife® was compared to stromal cells in DMEM with FBS, the results were not reliable due to a very large confidence interval for the relative expression ratio. It is likely that the relatively large variation in ΔC_T values for the stromal cells in DMEM (9.34, 0.95, 1.33) caused the wide confidence interval for the ratio. The value of 9.34, observed from sample 1SD reflected decreased expression of CK5 mRNA compared to 2SD and 3SD. Possible reasons include a relative lack of epithelial cells in the 1SD culture compared to the others, poor cell viability at the time of RNA crude cell lysate, or an error in processing for PCR. The latter two possibilities are less likely, since the mean ΔC_T value for 18S rRNA expression from sample 1SD was similar to the other samples, and all corneal samples were handled in concert.

To assess whether the products amplified by PCR for CK5 mRNA maintained the expected sequence predicted for canine CK5, DNA sequencing was performed. While the product from the corneal samples matched perfectly with the predicted sequence for canine CK5, the product from the MDCK cells matched the predicted sequence for CK8. Since the sequences and sizes of these cytokeratins are similar, there may have been reasonable opportunity for inadvertent amplification of CK8 using primers for CK5. Additionally, due to their prolonged *in vitro* existence, MDCK cells may have undergone certain mutations resulting in altered expression of various factors.[86,90] Specifically,

dedifferentiated MDCK cells reportedly show decreased or abolished expression of various cytokeratins, including CK5, when compared to differentiated MDCK cells.[86]

CHAPTER V. CONCLUSIONS

The purpose of this study was to investigate whether Epilife® provides a superior culture environment for canine corneal epithelial cells when compared to DMEM with FBS, and to document the cytochemical expression of cultured canine corneal cells. Based on the results of the study, epithelial cells proliferate and reach confluence more rapidly in DMEM with FBS than in Epilife®. No differences were observed among the staining characteristics of epithelial cells for pancytokeratin, vimentin, and E-cadherin, regardless of which medium was used. Positive vimentin staining of cultured corneal epithelial cells was an important finding in this study. Based upon this result, researchers should not use vimentin as a means of distinguishing cells of mesenchymal versus epithelial origin for canine corneal cultures. Based on the PCR for CK5 mRNA expression, Epilife® medium promotes canine corneal epithelial cells to retain their epithelial characteristic of CK5 mRNA expression better than DMEM with FBS. Additionally, Epilife® did not support attachment or growth of canine corneal stromal tissue pieces, which may be of benefit in minimizing stromal cell and fibroblast contamination of canine corneal epithelial cultures. While Epilife® is reportedly selective for epithelial cell growth, there is no specific indication that it would inhibit adherence of tissues and expansion of stromal cells.[24,70,79] Nonetheless, it is possible that the chemical composition of Epilife® does in fact inhibit stromal tissue attachment and cellular proliferation by failing to provide adequate nutrients, enzymes, and growth factors required to support these events. Perhaps the explant cultures would have attached and expanded better if serum had been added to the Epilife® medium.

Limitations of the study include the small number of dogs sampled and the comparison of only two culture media. Increasing the number of dogs may have allowed for more intensive statistical analyses of the results of cell growth rates in culture, immunocytochemical staining intensities, and PCR. Additionally, comparing cell growth in Epilife® with FBS to DMEM without FBS may have allowed for better interpretation of the effects of serum on canine corneal cell growth *in vitro*. Further investigations on

the effect that Epilife® culture medium, with and without the addition of serum, has on individual epithelial and stromal cells in suspension or explant cultures may be warranted. In addition to the assessments of pancytokeratin, vimentin, and E-cadherin, evaluations for other markers of canine corneal epithelial and stromal cells should be performed to promote a better understanding of the *in vitro* and *in vivo* biochemical and immunocytochemical characteristics of these cells. Research characterizing canine corneal cultures is in its relative infancy compared to that of numerous other species. Further studies are required to allow for the establishment of well-characterized cell lines, toxicology studies, and eventual tissue bioengineering for functional reconstruction of canine corneal layers.

LITERATURE CITED

1. Samuelson DA. Ophthalmic Anatomy In: Gelatt KN, ed. *Vet Ophthalmol*. Third Edition ed. Baltimore: Lippincott Williams and Wilkins, 1999;45-61.

2. Gum GG, Gelatt KN, Ofri R. Physiology of the Eye In: Gelatt KN, ed. *Vet Ophthalmol*. Third ed. Baltimore: Lippincott Williams and Wilkins, 1999.

3. Kumar A, Zhang J, Yu FS. Innate immune response of corneal epithelial cells to Staphylococcus aureus infection: role of peptidoglycan in stimulating proinflammatory cytokine secretion. *Invest Ophthalmol Vis Sci* 2004;45:3513-3522.

4. Peiffer RL, Wilcock BP, Dubielzig RR, et al. Fundamentals of Veterinary Ophthalmic Pathology In: Gelatt KN, ed. *Vet Ophthalmol*. Third Edition ed. Baltimore: Lippincott Williams and Wilkins, 1999;381-392.

5. Whitley RD, Gilger BC. Diseases of the Canine Cornea and Sclera In: Gelatt KN, ed. *Vet Ophthalmol*. Third Edition ed. Baltimore: Lippincott Williams and Wilkins, 1999;635-673.

6. Lu H, Zimek A, Chen J, et al. Keratin 5 knockout mice reveal plasticity of keratin expression in the corneal epithelium. *Eur J Cell Biol* 2006;85:803-811.

7. Marfurt CF, Murphy CJ, Florczak JL. Morphology and neurochemistry of canine corneal innervation. *Invest Ophthalmol Vis Sci* 2001;42:2242-2251.

8. Gilger BC, Whitley RD, McLaughlin SA, et al. Canine corneal thickness measured by ultrasonic pachymetry. *Am J Vet Res* 1991;52:1570-1572.

9. Du Y, Chen J, Funderburgh JL, et al. Functional reconstruction of rabbit corneal epithelium by human limbal cells cultured on amniotic membrane. *Mol Vis* 2003;9:635-643.

10. Audus KL, Bartel RL, Hidalgo IJ, et al. The use of cultured epithelial and endothelial cells for drug transport and metabolism studies. *Pharm Res* 1990;7:435-451.

11. Toropainen E, Ranta VP, Talvitie A, et al. Culture model of human corneal epithelium for prediction of ocular drug absorption. *Invest Ophthalmol Vis Sci* 2001;42:2942-2948.

12. Hardarson T, Hanson C, Claesson M, et al. Time-lapse recordings of human corneal epithelial healing. *Acta Ophthalmol Scand* 2004;82:184-188.

13. Yoshida S, Shimmura S, Shimazaki J, et al. Serum-free spheroid culture of mouse corneal keratocytes. *Invest Ophthalmol Vis Sci* 2005;46:1653-1658.
14. Wu KY, Wang HZ, Hong SJ. Effect of latanoprost on cultured porcine corneal stromal cells. *Curr Eye Res* 2005;30:871-879.
15. Berryhill BL, Kader R, Kane B, et al. Partial restoration of the keratocyte phenotype to bovine keratocytes made fibroblastic by serum. *Invest Ophthalmol Vis Sci* 2002;43:3416-3421.
16. Jester JV, Huang J, Fisher S, et al. Myofibroblast differentiation of normal human keratocytes and hTERT, extended-life human corneal fibroblasts. *Invest Ophthalmol Vis Sci* 2003;44:1850-1858.
17. Bednarz J, Teifel M, Friedl P, et al. Immortalization of human corneal endothelial cells using electroporation protocol optimized for human corneal endothelial and human retinal pigment epithelial cells. *Acta Ophthalmol Scand* 2000;78:130-136.
18. Alaminos M, Del Carmen Sanchez-Quevedo M, Munoz-Avila JI, et al. Construction of a complete rabbit cornea substitute using a fibrin-agarose scaffold. *Invest Ophthalmol Vis Sci* 2006;47:3311-3317.
19. Kang SS, Wang L, Kao WW, et al. Control of SV-40 transformed RCE cell proliferation by growth-factor-induced cell cycle progression. *Curr Eye Res* 2001;23:397-405.
20. Schwab IR. Cultured corneal epithelia for ocular surface disease. *Trans Am Ophthalmol Soc* 1999;97:891-986.
21. Sharif NA, Wiernas TK, Howe WE, et al. Human corneal epithelial cell functional responses to inflammatory agents and their antagonists. *Invest Ophthalmol Vis Sci* 1998;39:2562-2571.
22. Yanoff M. In vitro biology of corneal epithelium and endothelium. *Trans Am Ophthalmol Soc* 1975;73:571-620.
23. Nishida K, Yamato M, Hayashida Y, et al. Functional bioengineered corneal epithelial sheet grafts from corneal stem cells expanded ex vivo on a temperature-responsive cell culture surface. *Transplantation* 2004;77:379-385.

24. Teixeira AI, McKie GA, Foley JD, et al. The effect of environmental factors on the response of human corneal epithelial cells to nanoscale substrate topography. *Biomaterials* 2006;27:3945-3954.
25. Grieco V, Patton V, Romussi S, et al. Cytokeratin and vimentin expression in normal and neoplastic canine prostate. *J Comp Pathol* 2003;129:78-84.
26. Ramalho LN, Ribeiro-Silva A, Cassali GD, et al. The expression of p63 and cytokeratin 5 in mixed tumors of the canine mammary gland provides new insights into the histogenesis of these neoplasms. *Vet Pathol* 2006;43:424-429.
27. Song J, Izumi K, Lanigan T, et al. Development and characterization of a canine oral mucosa equivalent in a serum-free environment. *J Biomed Mater Res A* 2004;71:143-153.
28. Araki K, Ohashi Y, Sasabe T, et al. Immortalization of rabbit corneal epithelial cells by a recombinant SV40-adenovirus vector. *Invest Ophthalmol Vis Sci* 1993;34:2665-2671.
29. Halenda RM, Grevan VL, Hook RR, et al. An immortalized hamster corneal epithelial cell line for studies of the pathogenesis of Acanthamoeba keratitis. *Curr Eye Res* 1998;17:225-230.
30. Hendrix DV, Ward DA, Barnhill MA. Effects of anti-inflammatory drugs and preservatives on morphologic characteristics and migration of canine corneal epithelial cells in tissue culture. *Vet Ophthalmol* 2002;5:127-135.
31. Huang SC, Hsiao LD, Chien CS, et al. Characterization of bradykinin receptors in canine cultured corneal epithelial cells: pharmacological and functional studies. *J Biomed Sci* 2002;9:213-222.
32. Sandmeyer LS, Keller CB, Bienzle D. Culture of feline corneal epithelial cells and infection with feline herpesvirus-1 as an investigative tool. *Am J Vet Res* 2005;66:205-209.
33. SundarRaj N, Rizzo JD, Anderson SC, et al. Expression of vimentin by rabbit corneal epithelial cells during wound repair. *Cell Tissue Res* 1992;267:347-356.
34. Zito-Abbad E, Borderie VM, Baudrimont M, et al. Corneal epithelial cultures generated from organ-cultured limbal tissue: factors influencing epithelial cell growth. *Curr Eye Res* 2006;31:391-399.

35. Zhang X, Sun H, Tang X, et al. Comparison of cell-suspension and explant culture of rabbit limbal epithelial cells. *Exp Eye Res* 2005;80:227-233.
36. Chen CC, Chang JH, Lee JB, et al. Human corneal epithelial cell viability and morphology after dilute alcohol exposure. *Invest Ophthalmol Vis Sci* 2002;43:2593-2602.
37. Koizumi N, Cooper LJ, Fullwood NJ, et al. An evaluation of cultivated corneal limbal epithelial cells, using cell-suspension culture. *Invest Ophthalmol Vis Sci* 2002;43:2114-2121.
38. Kedjarune U, Pongprerachok S, Arpornmaeklong P, et al. Culturing primary human gingival epithelial cells: comparison of two isolation techniques. *J Craniomaxillofac Surg* 2001;29:224-231.
39. Bednarz J, Doubilei V, Wollnik PC, et al. Effect of three different media on serum free culture of donor corneas and isolated human corneal endothelial cells. *Br J Ophthalmol* 2001;85:1416-1420.
40. Jang IK, Ahn JI, Shin JS, et al. Transplantation of reconstructed corneal layer composed of corneal epithelium and fibroblasts on a lyophilized amniotic membrane to severely alkali-burned cornea. *Artif Organs* 2006;30:424-431.
41. Tezel TH, Del Priore LV. Serum-free media for culturing and serial-passaging of adult human retinal pigment epithelium. *Exp Eye Res* 1998;66:807-815.
42. Huhtala A, Mannerstrom M, Alajuuma P, et al. Comparison of an immortalized human corneal epithelial cell line and rabbit corneal epithelial cell culture in cytotoxicity testing. *J Ocul Pharmacol Ther* 2002;18:163-175.
43. Thuret G, Manissolle C, Campos-Guyotat L, et al. Animal compound-free medium and poloxamer for human corneal organ culture and deswelling. *Invest Ophthalmol Vis Sci* 2005;46:816-822.
44. Haber M, Cao Z, Panjwani N, et al. Effects of growth factors (EGF, PDGF-BB and TGF-beta 1) on cultured equine epithelial cells and keratocytes: implications for wound healing. *Vet Ophthalmol* 2003;6:211-217.
45. Hirano S, Sagara T, Suzuki K, et al. Inhibitory effects of anti-glaucoma drugs on corneal epithelial migration in a rabbit organ culture system. *J Glaucoma* 2004;13:196-199.

46. Robertson DM, Li L, Fisher S, et al. Characterization of growth and differentiation in a telomerase-immortalized human corneal epithelial cell line. *Invest Ophthalmol Vis Sci* 2005;46:470-478.
47. Hendrix DV, Ward DA, Barnhill MA. Effects of antibiotics on morphologic characteristics and migration of canine corneal epithelial cells in tissue culture. *Am J Vet Res* 2001;62:1664-1669.
48. Huang SC, Chien C, Hsiao L, et al. Mechanisms of bradykinin-mediated Ca(2+) signalling in canine cultured corneal epithelial cells. *Cell Signal* 2001;13:565-574.
49. Garcia-Hirschfeld J, Lopez-Briones LG, Belmonte C. Neurotrophic influences on corneal epithelial cells. *Exp Eye Res* 1994;59:597-605.
50. Nishida T, Nakagawa S, Awata T, et al. Fibronectin promotes epithelial migration of cultured rabbit cornea in situ. *J Cell Biol* 1983;97:1653-1657.
51. Nishida T, Nakamura M, Ofuji K, et al. Synergistic effects of substance P with insulin-like growth factor-1 on epithelial migration of the cornea. *J Cell Physiol* 1996;169:159-166.
52. Gelatt KN, Gum GG, Brooks DE, et al. Dose response of topical pilocarpine-epinephrine combinations in normotensive and glaucomatous Beagles. *Am J Vet Res* 1983;44:2018-2027.
53. Gelatt KN, Gum GG, Wolf ED, et al. Dose response of topical carbamylcholine chloride (carbachol) in normotensive and early glaucomatous beagles. *Am J Vet Res* 1984;45:547-554.
54. Gelatt KN, Larocca RD, Gelatt JK, et al. Evaluation of multiple doses of 4 and 6% timolol, and timolol combined with 2% pilocarpine in clinically normal beagles and beagles with glaucoma. *Am J Vet Res* 1995;56:1325-1331.
55. Gelatt KN, Mackay EO. The ocular hypertensive effects of topical 0.1% dexamethasone in beagles with inherited glaucoma. *J Ocul Pharmacol Ther* 1998;14:57-66.
56. Gelatt KN, Mackay EO. Effect of different dose schedules of bimatoprost on intraocular pressure and pupil size in the glaucomatous Beagle. *J Ocul Pharmacol Ther* 2002;18:525-534.

57. Gum GG, Gelatt KN, Gelatt JK, et al. Effect of topically applied demecarium bromide and echothiophate iodide on intraocular pressure and pupil size in beagles with normotensive eyes and beagles with inherited glaucoma. *Am J Vet Res* 1993;54:287-293.
58. Gum GG, Kingsbury S, Whitley RD, et al. Effect of topical prostaglandin PGA2, PGA2 isopropyl ester, and PGF2 alpha isopropyl ester on intraocular pressure in normotensive and glaucomatous canine eyes. *J Ocul Pharmacol* 1991;7:107-116.
59. Mathis GA, Regnier A, Hendrix DV, et al. Clinical Ophthalmic Pharmacology and Therapeutics In: Gelatt KN, ed. *Vet Ophthalmol*. Third Edition ed. Baltimore: Lippincott Williams and Wilkins, 1999;291-354`.
60. Whitley RD, Gilger BC. Surgery of the Canine Cornea and Sclera In: Gelatt KN, ed. *Vet Ophthalmol*. Third Edition ed. Baltimore: Lippincott Williams and Wilkins, 1999;675-700.
61. Sandmeyer LS, Keller CB, Bienzle D. Effects of cidofovir on cell death and replication of feline herpesvirus-1 in cultured feline corneal epithelial cells. *Am J Vet Res* 2005;66:217-222.
62. Sandmeyer LS, Keller CB, Bienzle D. Effects of interferon-alpha on cytopathic changes and titers for feline herpesvirus-1 in primary cultures of feline corneal epithelial cells. *Am J Vet Res* 2005;66:210-216.
63. Liu JJ, Kao WW, Wilson SE. Corneal epithelium-specific mouse keratin K12 promoter. *Exp Eye Res* 1999;68:295-301.
64. Shi Y, Tabesh M, Sugrue SP. Role of cell adhesion-associated protein, pinin (DRS/memA), in corneal epithelial migration. *Invest Ophthalmol Vis Sci* 2000;41:1337-1345.
65. Daniels JT, Khaw PT. Temporal stimulation of corneal fibroblast wound healing activity by differentiating epithelium in vitro. *Invest Ophthalmol Vis Sci* 2000;41:3754-3762.
66. Chen Z, de Paiva CS, Luo L, et al. Characterization of putative stem cell phenotype in human limbal epithelia. *Stem Cells* 2004;22:355-366.
67. Joseph A, Powell-Richards AO, Shanmuganathan VA, et al. Epithelial cell characteristics of cultured human limbal explants. *Br J Ophthalmol* 2004;88:393-398.

68. Kiritoshi A, SundarRaj N, Thoft RA. Differentiation in cultured limbal epithelium as defined by keratin expression. *Invest Ophthalmol Vis Sci* 1991;32:3073-3077.
69. Yi X, Wang Y, Yu FS. Corneal epithelial tight junctions and their response to lipopolysaccharide challenge. *Invest Ophthalmol Vis Sci* 2000;41:4093-4100.
70. Papini S, Rosellini A, Nardi M, et al. Selective growth and expansion of human corneal epithelial basal stem cells in a three-dimensional-organ culture. *Differentiation* 2005;73:61-68.
71. Liu S, Li J, Wang C, et al. Human limbal progenitor cell characteristics are maintained in tissue culture. *Ann Acad Med Singapore* 2006;35:80-86.
72. Petridou S, Masur SK. Immunodetection of connexins and cadherins in corneal fibroblasts and myofibroblasts. *Invest Ophthalmol Vis Sci* 1996;37:1740-1748.
73. Kawakita T, Espana EM, He H, et al. Calcium-induced abnormal epidermal-like differentiation in cultures of mouse corneal-limbal epithelial cells. *Invest Ophthalmol Vis Sci* 2004;45:3507-3512.
74. Zbytek B, Pikula M, Slominski RM, et al. Corticotropin-releasing hormone triggers differentiation in HaCaT keratinocytes. *Br J Dermatol* 2005;152:474-480.
75. Joo JH, Alpatov R, Munguba GC, et al. Reduction of Pnn by RNAi induces loss of cell-cell adhesion between human corneal epithelial cells. *Mol Vis* 2005;11:133-142.
76. Barnard Z, Apel AJ, Harkin DG. Phenotypic analyses of limbal epithelial cell cultures derived from donor corneoscleral rims. *Clin Experiment Ophthalmol* 2001;29:138-142.
77. Gordon YJ, Huang LC, Romanowski EG, et al. Human cathelicidin (LL-37), a multifunctional peptide, is expressed by ocular surface epithelia and has potent antibacterial and antiviral activity. *Curr Eye Res* 2005;30:385-394.
78. McDermott AM, Redfern RL, Zhang B, et al. Defensin expression by the cornea: multiple signalling pathways mediate IL-1beta stimulation of hBD-2 expression by human corneal epithelial cells. *Invest Ophthalmol Vis Sci* 2003;44:1859-1865.
79. Teixeira AI, Abrams GA, Bertics PJ, et al. Epithelial contact guidance on well-defined micro- and nanostructured substrates. *J Cell Sci* 2003;116:1881-1892.
80. Ueta M, Nochi T, Jang MH, et al. Intracellularly expressed TLR2s and TLR4s contribution to an immunosilent environment at the ocular mucosal epithelium. *J Immunol* 2004;173:3337-3347.

81. Taylor CR, Shi SR, Barr NJ, et al. Techniques of Immunohistochemistry: Principles, Pitfalls, and Standardization In: Dabbs DJ, ed. *Diagnostics Immunohistochemistry*. Philadelphia: Churchill Livingstone, 2002;3-43.
82. Chaloin-Dufau C, Pavitt I, Delorme P, et al. Identification of keratins 3 and 12 in corneal epithelium of vertebrates. *Epithelial Cell Biol* 1993;2:120-125.
83. Nelson WG, Sun TT. The 50- and 58-kdalton keratin classes as molecular markers for stratified squamous epithelia: cell culture studies. *J Cell Biol* 1983;97:244-251.
84. Hunt RC, Davis AA. Altered expression of keratin and vimentin in human retinal pigment epithelial cells in vivo and in vitro. *J Cell Physiol* 1990;145:187-199.
85. Eger A, Stockinger A, Wiche G, et al. Polarisation-dependent association of plectin with desmoplakin and the lateral submembrane skeleton in MDCK cells. *J Cell Sci* 1997;110 (Pt 11):1307-1316.
86. Pollack V, Scheiber K, Pfaller W, et al. Loss of cytokeratin expression and formation of actin stress fibers in dedifferentiated MDCK-C7 cell lines. *Biochem Biophys Res Commun* 1997;241:541-547.
87. Leong AS, Gilham P, Milios J. Cytokeratin and vimentin intermediate filament proteins in benign and neoplastic prostatic epithelium. *Histopathology* 1988;13:435-442.
88. Ramaekers FC, Hukkelhoven MW, Groeneveld A, et al. Changing protein patterns during lens cell aging in vitro. *Biochim Biophys Acta* 1984;799:221-229.
89. Zhu MQ, De Broe ME, Nouwen EJ. Vimentin expression and distal tubular damage in the rat kidney. *Exp Nephrol* 1996;4:172-183.
90. Marschitz I, Lechner J, Mosser I, et al. Differential expression of cell-cell adhesion proteins and cyclin D in MEK1-transdifferentiated MDCK cells. *Am J Physiol Cell Physiol* 2000;279:C1472-1482.
91. Noe V, Fingleton B, Jacobs K, et al. Release of an invasion promoter E-cadherin fragment by matrilysin and stromelysin-1. *J Cell Sci* 2001;114:111-118.
92. Liwosz A, Lei T, Kukuruzinska MA. N-glycosylation affects the molecular organization and stability of E-cadherin junctions. *J Biol Chem* 2006;281:23138-23149.
93. Yamada A, Irie K, Hirota T, et al. Involvement of the annexin II-S100A10 complex in the formation of E-cadherin-based adherens junctions in Madin-Darby canine kidney cells. *J Biol Chem* 2005;280:6016-6027.

94. Araki-Sasaki K, Aizawa S, Hiramoto M, et al. Substance P-induced cadherin expression and its signal transduction in a cloned human corneal epithelial cell line. *J Cell Physiol* 2000;182:189-195.
95. Wang Y, Chen M, Wolosin JM. ZO-1 in corneal epithelium; stratal distribution and synthesis induction by outer cell removal. *Exp Eye Res* 1993;57:283-292.
96. Sugrue SP, Zieske JD. ZO1 in corneal epithelium: association to the zonula occludens and adherens junctions. *Exp Eye Res* 1997;64:11-20.
97. McPherson MJ, Moller SG, Beynon R, et al. *PCR: The Basics from Background to Bench*. New York City: Springer-Verlag Telos, 2000.
98. Hutton E, Paladini RD, Yu QC, et al. Functional differences between keratins of stratified and simple epithelia. *J Cell Biol* 1998;143:487-499.
99. Pfaffl MW. A new mathematical model for relative quantification in real-time RT-PCR. *Nucleic Acids Res* 2001;29:e45.
100. Pfaffl MW, Horgan GW, Dempfle L. Relative expression software tool (REST) for group-wise comparison and statistical analysis of relative expression results in real-time PCR. *Nucleic Acids Res* 2002;30:e36.
101. Polak JM, Van Noorden S. *Introduction to Immunocytochemistry*. Second ed. Oxford: BIOS Scientific Publishers Ltd., 1997.

APPENDIX 1. CK5 SEQUENCE ALIGNMENT

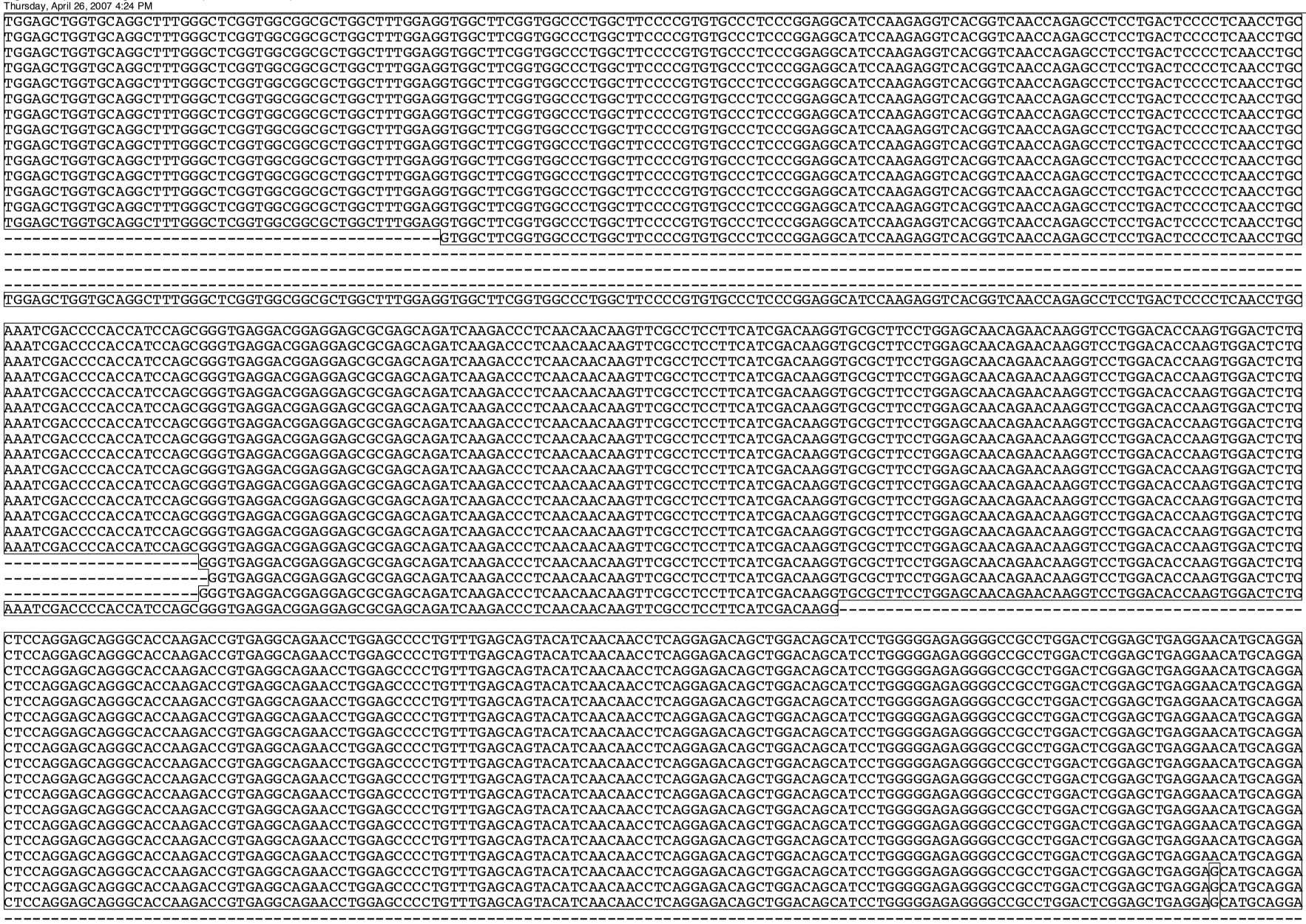

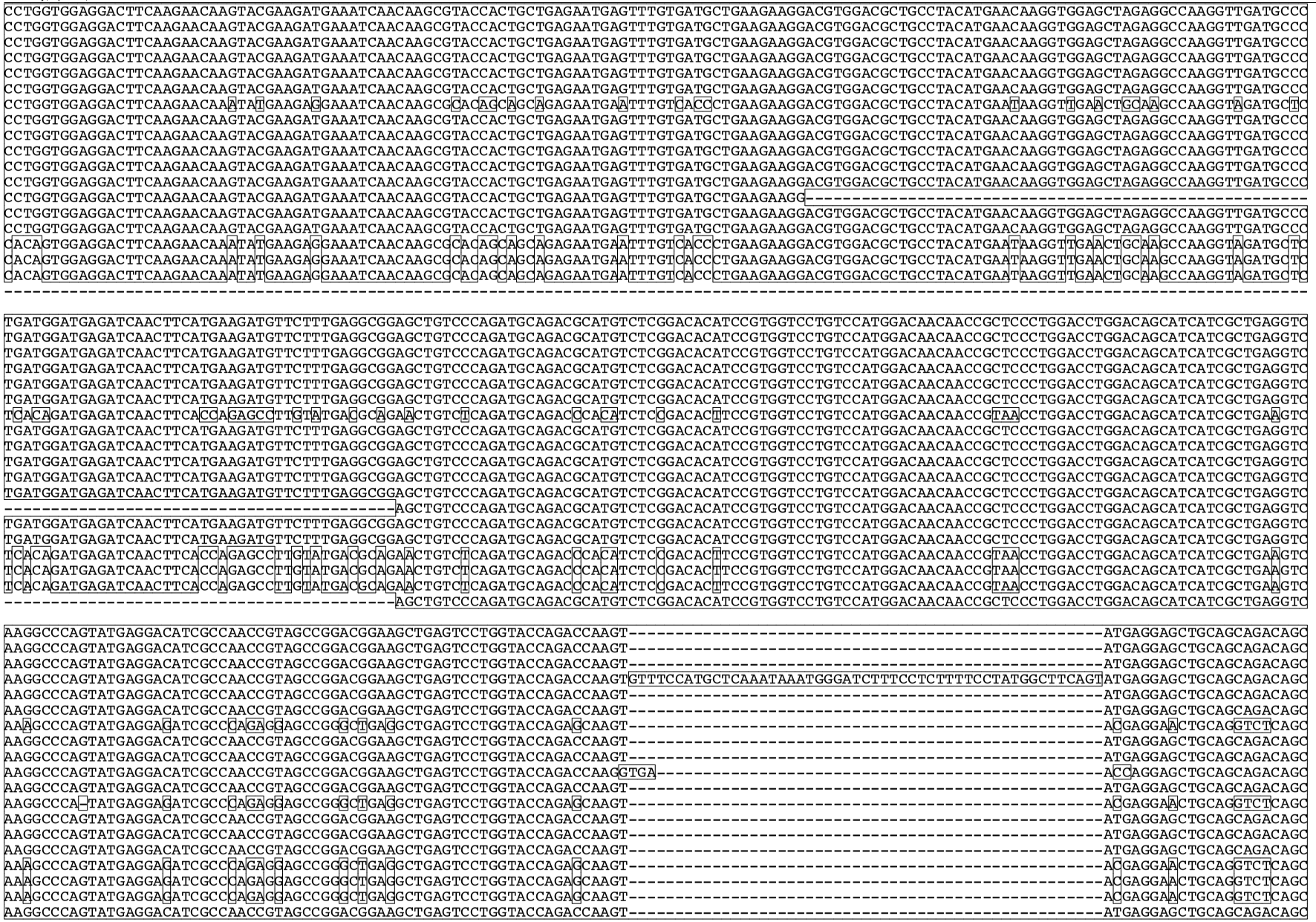
XM_844906.seq
XM_855152.seq
XM_854659.seq
XM_854983.seq
XM_855259.seq
XM_855231.seq
XM_854761.seq
XM_855192.seq
XM_855095.seq
XM_855013.seq
XM_543648.seq
XM_854944.seq
XM_854908.seq
XM_854630.seq
XM_855053.seq
XM_854866.seq
XM_854800.seq
XM_854833.seq
XM_854698.seq

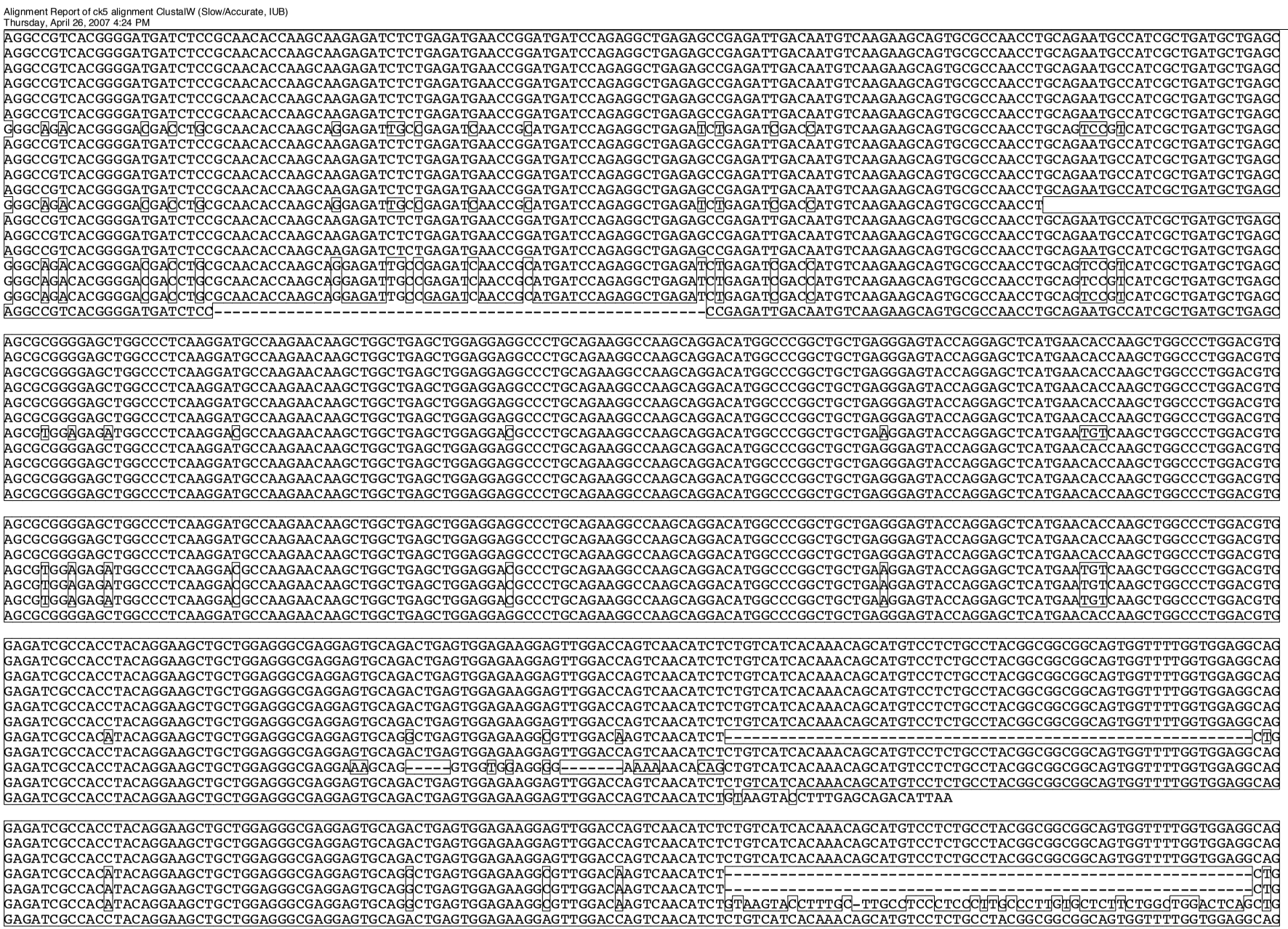
XM_844906.seq
XM_855152.seq
XM_854659.seq
XM_854983.seq
XM_855259.seq
XM_855231.seq
XM_854761.seq
XM_855192.seq
XM_855095.seq
XM_855013.seq
XM_543648.seq
XM_854944.seq
XM_854908.seq
XM_854630.seq
XM_855053.seq
XM_854866.seq
XM_854800.seq
XM_854833.seq
XM_854698.seq

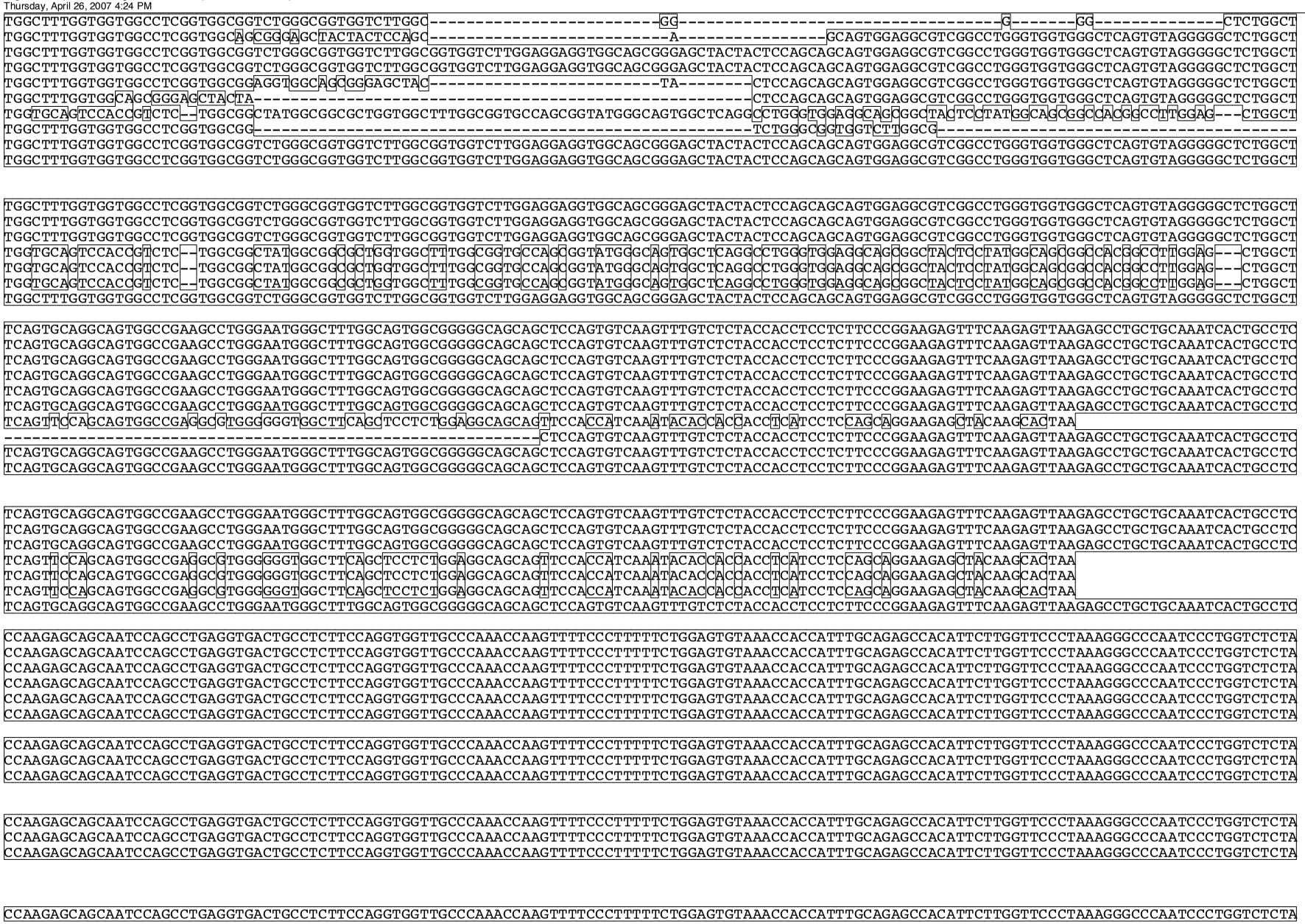

```
GTCTCCCATGTCATGATTCTGTGTTCTGCTTCAAATCAGTCTTTAAGTGTCTATAACATGTTCCTTGATGAGAAAAGAATCCAAAGTTTCTTAATACCTAAACCTTCAGAACAGTGTCCCCATCCCAAACCCAAATTTTG XM_844906.seq
GTCTCCCATGTCATGATTCTGTGTTCTGCTTCAAATCAGTCTTTAAGTGTCTATAACATGTTCCTTGATGAGAAAAGAATCCAAAGTTTCTTAATACCTAAACCTTCAGAACAGTGTCCCCATCCCAAACCCAAATTTTG XM_855152.seq
GTCTCCCATGTCATGATTCTGTGTTCTGCTTCAAATCAGTCTTTAAGTGTCTATAACATGTTCCTTGATGAGAAAAGAATCCAAAGTTTCTTAATACCTAAACCTTCAGAACAGTGTCCCCATCCCAAACCCAAATTTTG XM_854659.seq
GTCTCCCATGTCATGATTCTGTGTTCTGCTTCAAATCAGTCTTTAAGTGTCTATAACATGTTCCTTGATGAGAAAAGAATCCAAAGTTTCTTAATACCTAAACCTTCAGAACAGTGTCCCCATCCCAAACCCAAATTTTG XM_854983.seq
GTCTCCCATGTCATGATTCTGTGTTCTGCTTCAAATCAGTCTTTAAGTGTCTATAACATGTTCCTTGATGAGAAAAGAATCCAAAGTTTCTTAATACCTAAACCTTCAGAACAGTGTCCCCATCCCAAACCCAAATTTTG XM_855259.seq
GTCTCCCATGTCATGATTCTGTGTTCTGCTTCAAATCAGTCTTTAAGTGTCTATAACATGTTCCTTGATGAGAAAAGAATCCAAAGTTTCTTAATACCTAAACCTTCAGAACAGTGTCCCCATCCCAAACCCAAATTTTG XM_855231.seq
                                                                                                                                                  XM_854761.seq
GTCTCCCATGTCATGATTCTGTGTTCTGCTTCAAATCAGTCTTTAAGTGTCTATAACATGTTCCTTGATGAGAAAAGAATCCAAAGTTTCTTAATACCTAAACCTTCAGAACAGTGTCCCCATCCCAAACCCAAATTTTG XM_855192.seq
GTCTCCCATGTCATGATTCTGTGTTCTGCTTCAAATCAGTCTTTAAGTGTCTATAACATGTTCCTTGATGAGAAAAGAATCCAAAGTTTCTTAATACCTAAACCTTCAGAACAGTGTCCCCATCCCAAACCCAAATTTTG XM_855095.seq
GTCTCCCATGTCATGATTCTGTGTTCTGCTTCAAATCAGTCTTTAAGTGTCTATAACATGTTCCTTGATGAGAAAAGAATCCAAAGTTTCTTAATACCTAAACCTTCAGAACAGTGTCCCCATCCCAAACCCAAATTTTG XM_855013.seq
                                                                                                                                                  XM_543648.seq
                                                                                                                                                  XM_854944.seq
GTCTCCCATGTCATGATTCTGTGTTCTGCTTCAAATCAGTCTTTAAGTGTCTATAACATGTTCCTTGATGAGAAAAGAATCCAAAGTTTCTTAATACCTAAACCTTCAGAACAGTGTCCCCATCCCAAACCCAAATTTTG XM_854908.seq
GTCTCCCATGTCATGATTCTGTGTTCTGCTTCAAATCAGTCTTTAAGTGTCTATAACATGTTCCTTGATGAGAAAAGAATCCAAAGTTTCTTAATACCTAAACCTTCAGAACAGTGTCCCCATCCCAAACCCAAATTTTG XM_854630.seq
GTCTCCCATGTCATGATTCTGTGTTCTGCTTCAAATCAGTCTTTAAGTGTCTATAACATGTTCCTTGATGAGAAAAGAATCCAAAGTTTCTTAATACCTAAACCTTCAGAACAGTGTCCCCATCCCAAACCCAAATTTTG XM_855053.seq
                                                                                                                                                  XM_854866.seq
                                                                                                                                                  XM_854800.seq
                                                                                                                                                  XM_854833.seq
GTCTCCCATGTCATGATTCTGTGTTCTGCTTCAAATCAGTCTTTAAGTGTCTATAACATGTTCCTTGATGAGAAAAGAATCCAAAGTTTCTTAATACCTAAACCTTCAGAACAGTGTCCCCATCCCAAACCCAAATTTTG XM_854698.seq

TTCTGGTTCTGACTACCTCCAGAATGTGTTCAATAAAATGCTTTTATA                                                                                                  XM_844906.seq
TTCTGGTTCTGACTACCTCCAGAATGTGTTCAATAAAATGCTTTTATA                                                                                                  XM_855152.seq
TTCTGGTTCTGACTACCTCCAGAATGTGTTCAATAAAATGCTTTTATA                                                                                                  XM_854659.seq
TTCTGGTTCTGACTACCTCCAGAATGTGTTCAATAAAATGCTTTTATA                                                                                                  XM_854983.seq
TTCTGGTTCTGACTACCTCCAGAATGTGTTCAATAAAATGCTTTTATA                                                                                                  XM_855259.seq
TTCTGGTTCTGACTACCTCCAGAATGTGTTCAATAAAATGCTTTTATA                                                                                                  XM_855231.seq
                                                                                                                                                  XM_854761.seq
TTCTGGTTCTGACTACCTCCAGAATGTGTTCAATAAAATGCTTTTAT                                                                                                   XM_855192.seq
TTCTGGTTCTGACTACCTCCAGAATGTGTTCAATAAAATGCTTTTATA                                                                                                  XM_855095.seq
TTCTGGTTCTGACTACCTCCAGAATGTGTTCAATAAAATGCTTTTATA                                                                                                  XM_855013.seq
                                                                                                                                                  XM_543648.seq
                                                                                                                                                  XM_854944.seq
TTCTGGTTCTGACTACCTCCAGAATGTGTTCAATAAAATGCTTTTATA                                                                                                  XM_854908.seq
TTCTGGTTCTGACTACCTCCAGAATGTGTTCAATAAAATGCTTTTATA                                                                                                  XM_854630.seq
TTCTGGTTCTGACTACCTCCAGAATGTGTTCAATAAAATGCTTTTATA                                                                                                  XM_855053.seq
                                                                                                                                                  XM_854866.seq
                                                                                                                                                  XM_854800.seq
                                                                                                                                                  XM_854833.seq
TTCTGGTTCTGACTACCTCCAGAATGTGTTCAATAAAATGCTTTTATA                                                                                                  XM_854698.seq
```

Decoration 'Decoration #1': Box residues that match the Consensus exactly.

APPENDIX 2. PCR AMPLIFICATION PRODUCTS FROM CORNEAL CELLS AND MDCK CELLS

GAGCGCGAGCAGATCAAGA → BH-520
GAGCGCGAGCAGATCAAGACCCTCAACAACAAGTTCGCCTCCTTCATCGACAAGGTGCGCTTCCTGGAGCAACAGAACAAGGTCCTGGACACCAAGTG

GACTCTGCTCCAGGAGCAGGGCACCAAGACCGTGAGGCAGAACCTGGAGCCCCTGTTTGAGCAGTACATCAACAACCTCAGGAGACAGCTG
BH-521 (R/C) ← CAACAACCTCAGGAGACAGCTG

Observed sequence of CK5 amplified from corneal cDNA (189 bp)

GAGCGCGAGCAGATCAAGA → BH-520
GAGAAGGAGCAGATCAAGAGCCTCAACAACAAGTTTGCCTCCTTCATCGACAAGGTCAGACACCTGGAGCAGCAGAACAAAATCCTGGAGACCAAGTG

GAGCCTCCTGCAGCAGCAGAAAACCTCTCGGAGCAACATAGACAACATGTTTGAGAGCTACATCAACAACCTCCGGAGGCAGCTG
BH-521 (R/C) ← CAACAACCTCAGGAGACAGCTG

Observed sequence of CK8 amplified from MDCK cDNA (183 bp)

VITA

Jamie was born on August 30, 1978, in Metairie, Louisiana. She grew up in Metairie, attending and graduating from high school in 1996.

Jamie then attended Louisiana State University and earned her Bachelor of Science degree in Wildlife and Fisheries with a minor in Zoology. She was accepted into the Louisiana State University School of Veterinary Medicine and graduated as a Doctor of Veterinary Medicine in 2003.

After graduation, Jamie completed a 1-year rotating internship at Angell Animal Medical Center of Boston. She was then accepted into the combined Residency & Masters program at the Virginia-Maryland Regional College of Veterinary Medicine, pursuing a Residency in Ophthalmology, and a Master of Science in Biomedical and Veterinary Sciences.